

Hamid Reza Riyahi Bakhtyari

**Evaluation of the Capability of QuickBird Data
for Automatic Delineation of Individual Tree
Crowns in Sparse Deciduous Forests
Case-Study in the Zagros Region of Iran**



Cuvillier Verlag Göttingen
Internationaler wissenschaftlicher Fachverlag

GEORG-AUGUST-UNIVERSITY GÖTTINGEN
FACULTY OF FOREST SCIENCE AND FOREST ECOLOGY

BURCKHARDT-INSTITUTE
Chair of Forest Inventory and Remote Sensing



**EVALUATION OF THE CAPABILITY OF QUICKBIRD DATA FOR
AUTOMATIC DELINEATION OF INDIVIDUAL TREE CROWNS
IN SPARSE DECIDUOUS FORESTS.
CASE-STUDY IN THE ZAGROS REGION OF IRAN**

A dissertation to obtain the degree of Doctor at the Faculty of the Forest Science and Forest Ecology of
Georg-August-University Göttingen

By

Hamid Reza Riyahi Bakhtyari

Göttingen 2010

Abstract

This work represents first attempts at delineating individual tree crowns in Zagros area using QuickBird data. The Zagros forest zone is the second important forest region of Iran with high ecological and socio-economic values and provides services to a significant parts of Iran's human population. These forests are experiencing rapid degradation due to environmental and human impact at local scale. To efficiently manage these forests for conservation and other ecological purposes forest managers demand to have detailed information on forest composition and structure. Because of the wide extent as well as spatial structure of these forests, extracting the required information by means of traditional field based methods is time-consuming and costly, whilst application of low-medium resolution satellite imagery will not yield accurate and reliable results. It is, therefore, critically important to investigate the new advanced spaceborne remote sensing technologies that permit to extract detail information. Very high spatial resolution satellite imagery can supply forest management planning with individual tree based information, which was unfeasible to accomplish with the same efficiency and precision with moderate-resolution satellite imagery. Application to the Zagros forests face to the unique technical challenges including high variability in crown shape and size, strong effects of the background reflectance, and varying age and health condition.

The capabilities of QuickBird imagery examined with the data acquired over the Oak forest site on the South West of Iran. Different image fusion techniques were applied to exploit optimal spatial and spectral information of this imagery. The core technical objective was selecting a fusion method with high fidelity of spectral and spatial information. Quality assessment of fused images showed that the PCA method performs better than the others in this study.

Individual tree crowns were delineated using Marker Controlled Watershed and LoG methods. Marker Controlled Watershed method starts with detecting the significant edges, after that obtaining a relevant marker set, representing the locations of the individual tree crowns, then according to a certain rules delineate the Watersheds from the combination of markers and edges. The LoG method starts from converting image to the binary using Out's method and then extracts significant edges using the Laplacian of Gaussian filter. It

was then important to portray the overall effectiveness of the performed delineation methods. To evaluate the delineation results crown by crown accuracy assessment was performed. This accuracy considers the degree of correspondence between Computer-Generated Segments (CGS) and the actual Ground Reference Segments (GRS). Apparent quality measures and conditions for determining the delineation accuracy is defined and used.

The accuracy assessment showed in this study that about 50% of crowns can be delineated with high accuracy (perfect match) in both methods. The LoG method seems well suited and approximately 58.1% of crowns were delineated with high accuracy (perfect match). The total rate of good matches for this method was 9.8%. There were few omissions errors. Commission errors, i.e., CGS not associated with GRS did not occur. Automated tree crown delineation in deciduous sparse forests with variable crown shape and size is a complicated procedure.

In this study QuickBird imagery showed wide capabilities for individual tree crown delineation in sparse forests of Zagros region. Further investigations are also needed to document the potential of QuickBird imagery in different acquisition and forest types, such as more heterogeneous stands and complex topography.

In memory of my father

...A never-ending source of inspiration

To my mother

With love and eternal appreciation

Acknowledgements

I would like to express my deep and sincere gratitude to my supervisor, Professor Christoph Kleinn, Head of the Chair of Forest Inventory and Remote Sensing, Georg-August-University of Göttingen. His wide knowledge and his logical way of thinking have been of great value for me. His understanding, encouraging and personal guidance have provide a good basis for the present thesis.

I warmly thank Dr. Hans Fuchs for his assistance in answering critical scientific questions and friendly help. His extensive discussions around my work and interesting ideas have been very helpful for this study.

I owe my most sincere gratitude to Dr. František Vilčko who developed the DELIN program and gave me help during my difficult moments.

I would like to thank to Ministry of Science, Research and Technology of Iran (MSRT) for providing financial support and for foresight in creating and developing the PhD scholarship program.

My appreciation extends to the commitment of Chair of Forest Inventory and Remote Sensing of Georg-August-University of Göttingen in paying for QuickBird image acquisition in the Fars province. Undertaking such a commitment is not easy, considering the high costs involved! Without this image, my story could not have been solid.

I extend my gratitude to the Fars Natural Resources Head Organization (FNRHO) for providing all the necessary supports and excellent field logistics. I also extend my sincere thanks to a number of FNRHO staff who contributed valuable field assistance, technical support or managerial backing to this study.

I would like to thank my colleagues, Ulrike Docktor, Hendrik Heydecke, Reinhard Schlote for technical and administrative matters in the Chair of Forest Inventory and Remote Sensing at the University of Göttingen. Special thanks go to my fellows, Axel Buschmann, Paul Magdon, Haijun Yang, Ali Darvishi for their help in visual inspection of fusion results, scientific discussions and support.

The Iranian colleagues in Göttingen thank you for the support. Payam Fayyaz made me feel at home in Germany. Hossein Hosseinkhani, thank you for your parental support and advice. I would like to thank Dr. Ali Nouri, Dr. Iraj Gholami, Dr. Lutz Fehrmann, Ali Reza Moshki, as friend and colleague for their steadfast support and critical reviewing parts of my thesis. Ali Ghorbani, my brother, friend, thanks for the support and encouragement that you have always given me.

I wish to give gratitude to my father, mother and sisters, who went through a lot during the years I was abroad. They have given to me continuous support and deserve so much more than a simple 'thank you'. I owe them a lot and will be grateful to them all my life.

TABLE OF CONTENTS

Table of contents	viii
List of tables	xi
List of figures	xii
List of Abbreviations	xiv
INTRODUCTION.....	1
1.1 An overview on the Zagros forests.....	1
1.2 General motivation.....	2
1.3 Potential applications of the very high resolution imagery in precision forestry...	6
1.4 Goals and Objectives.....	8
1.5 Outline of the study	9
BACKGROUND	11
2.1 Common definitions.....	11
2.2 Automated individual tree crown delineation	12
2.2.1 Forestry applications	14
2.2.1.1 Forest inventory.....	14
2.2.1.2 Species classification	16
2.3 Very high spatial resolution imagery.....	17
2.3.1. Fusion in automated tree crown delineation	18
2.3.2 QuickBird imagery	19
2.4 Parameters affecting delineation procedure	20
2.4.1 Internal factors.....	20
2.4.1.1 Crown texture.....	20
2.4.1.2 Crown morphology	21
2.4.1.3 Crown spatial arrangement.....	22
2.4.1.4 Tree density	22
2.4.2 External factors	23
2.4.2.1 Spatial and spectral characteristics.....	23
2.4.2.2 Image acquisition geometry and sun angle	23
2.5 Categorization of automatic individual tree crown delineation techniques	24
2.5.1 Tree delineation ‘bottom-up’ algorithms.....	26
2.5.1.1 Directional texture.....	26
2.5.1.2 Valley following	27
2.5.1.3 Template matching	27
2.5.2 Tree identification and delineation ‘top-down’ algorithms	29
2.5.2.1 Threshold-based spatial clustering method	29
2.5.2.2 Multiple scale edge segments.....	29
2.5.2.3 The Vision Expert System.....	31
2.5.2.4 Double-aspect method.....	31
2.5.3 Combined methods.....	32

MATERIAL AND METHODS	38
3.1 Study area	38
3.2 Data acquisition.....	41
3.3 Survey design and field data collection.....	43
3.3.1 Plot establishment	43
3.3.2 Individual tree survey.....	44
3.3.3 Crown survey	45
3.3.4 Height survey	46
3.3.5 Geodatabase establishment	46
3.4 Regression analysis	47
3.5 Image processing.....	48
3.5.1 Pre-processing	48
3.5.1.1 Conversion to top-of-atmosphere spectral radiance.....	48
3.5.1.2 Precise image co-registration	48
3.5.2 Image fusion.....	49
3.5.2.1 Concept of image fusion	49
3.5.2.2 Brovey fusion method.....	50
3.5.2.3 IHS fusion method	51
3.5.2.4 PCA fusion method	52
3.5.2.5 Gram-Schmidt fusion method.....	52
3.5.2.6 Ehlers fusion method.....	54
3.5.2.7 PC + Wavelet fusion method.....	55
3.5.3 Image fusion quality assessment.....	57
3.5.3.1 Protocol for quality assessment.....	57
3.5.3.2 Quality metrics	58
3.5.3.3 Visual quality assessment.....	62
3.5.4 Image segmentation.....	63
3.5.4.1 Definition of image segmentation	63
3.5.4.2 Image segmentation techniques	63
3.5.4.2.1 Thresholding segmentation	64
3.5.4.2.2 Edge based segmentation methods.....	65
3.5.4.2.3 Watershed segmentation method.....	69
3.5.5 Automated tree crown delineation.....	73
3.5.5.1 Initial image preparation	73
3.5.5.2 Mask generation	74
3.5.5.3 Tree crown delineation using the LoG edge detector.....	74
3.5.5.4 Tree crown delineation using marker-controlled Watershed segmentation ...	75
3.6 Crown delineation quality assessment	78
3.7 Crown detection assessment.....	83
RESULTS.....	84
4.1 Regression analysis	84
4.2 Image fusion evaluation	85
4.2.1 Results of visual quality assessment	85
4.2.2 Results of statistical quality assessment.....	89
4.3 Tree crown delineation results.....	93

4.3.1 Delineation evaluation of LoG method.....	98
4.3.2 Delineation evaluation of the Watershed method.....	99
4.4 Tree crown detection results.....	99
DISCUSSION.....	101
5.1 The delineation algorithms.....	101
5.2 Comparing the applied methods.....	105
5.3 The image fusion methods	107
5.4 Regression analysis	108
5.5 Comparison with other research.....	109
5.6 Wider application of the delineation algorithms	115
SUMMARY	118
APPENDIX 1 CATEGORIES OF CGS – GRS OVERLAP	122
REFERENCES.....	127

LIST OF TABELS

Table 1.1 A selection of important references for individual tree crown delineation	4
Table 1.2 Examples of applications of high resolution data in precision forestry.	7
Table 1.3 Very high spatial resolution satellites.....	20
Table 3.1 Acquisition configuration parameters of the QuickBird images.....	42
Table 4.1 Some statistics on the difference between the original and synthesized images (in radiance or relative value) for band 1.....	90
Table 4.2 Some statistics on the difference between the original and synthesized images (in radiance or relative value) for band 2.	90
Table 4.3 Some statistics on the difference between the original and synthesized images (in radiance or relative value) for band 3.....	91
Table 4.4 Some statistics on the difference between the original and synthesized images (in radiance or relative value) for band 4.....	91
Table 4.5 The global errors of the compared methods.....	93
Table 4.6 Results of the delineation evaluation of LoG method.....	98
Table 4.7 Tree crown detection error and accuracy.....	100
Table 4.8 Results of the delineation evaluation of the Watershed method.....	100

LIST OF FIGURES

Figure 2.1 A schematic diagram of individual and grouped trees.....	12
Figure 2.2 Categorization of automated tree crown delineation techniques.....	25
Figure 3.1 The location of study area in Iran.....	38
Figure 3.2 The selected study site overlaid on the shaded relief DTM.....	39
Figure 3.3 A test site of QuickBird imagery.....	42
Figure 3.4 Illustration of sample plots on the DEM and plot design	43
Figure 3.5 One plot of the sample crown map.....	47
Figure 3.6 Flow chart of the IHS fusion method.....	51
Figure 3.7 Flow chart of the PCA fusion method.....	52
Figure 3.8 Flow chart of the Gram-Schmidt fusion method.....	53
Figure 3.9 Flow chart of the Ehlers fusion method.....	55
Figure 3.10 Flow chart of the PC + Wavelet fusion method.....	56
Figure 3.11 Sobel edge detector masks.....	66
Figure 3.12 Laplacian edge detector masks.....	67
Figure 3.13 (a) 3D plot of LoG function, (b) cross section showing zero crossing	68
Figure 3.14 Topographic representation of a gray scale image.....	69
Figure 3.15 Illustration of the flooding of the relief and dam building	70
Figure 3.16 Illustration of (rain-falling) process of Watershed transform	71
Figure 3.17 Morphological paradigm for image segmentation	72
Figure 3.18 Illustration of the resultant image after Sobel edge detection.....	75
Figure 3.19 Three typical cases of closed contours after edge detection.....	76
Figure 3.20 An example of distance image and its correspondent 3D view.....	77
Figure 3.21 Minima imposition technique.....	77
Figure 3.22 The 12 categories of GRS and CGS configurations	81
Figure 3.23 User interface of DELIN program.....	82
Figure 3.24 A sample output of DELIN software.....	83
Figure 4.1 Scatterplot with fitted regression line.....	84
Figure 4.2 Results of QuickBird fused sub images.....	89

Figure 4.3 (a) Initial image. (b) Crown mask image. (c) Histogram of the initial image. (d) Histogram of the crown mask image.....	94
Figure 4.4 An example of automatically delineated tree crowns by the LoG method...	95
Figure 4.5 An example of automatically delineated tree crowns by marker controlled Watershed segmentation.....	95
Figure 4.6 An example of crown delineation results of the initial image shown in Figure 4.3 following raster to vector conversion.....	96
Figure 4.7 An example of crown delineation results of the initial image shown in Figure 4.3 following raster to vector conversion.....	97

List of Abbreviations

Symbol	Definition
APM	Automatic Point Matching
CASI	Compact Airborne Spectrographic Imager
CC	Correlation Coefficient
CCD	Charge-Coupled Device
CGS	Computer-Generated Segments
DGPS	Differential Global Positioning System
DIV	Difference In Variances
DN	Digital Number
DSM	Digital Surface Model
DWT	Discrete Wavelet Transform
EDM	Euclidean Distance Map
ERGAS	Erreur Relative Globale Adimensionnelle de Synthèse
FAO	Food & Agricultural Organization of United Nations
FFT	Fast Fourier Transformation
FNRHO	Fars Natural Resources Head Organization
FRWO	Forest Rangeland and Watershed Management Organization
GCP	Ground Control Point
GPS	Global Positioning System
GRS	Ground Reference Segments
GS	Gram-Schmidt
GSD	Ground Sample Distance

HP	High Pass
HVS	Human Visual System
IDWT	Inverse Discrete Wavelet Transform
IHS	Intensity- Hue-Saturation
ITC	Individual Tree Crown
LM	Local Maxima
LMSR	Local Maxima Smoothing Relation
LoG	Laplacian of Gaussian
LP	Low Pass
LSRP	Lower Spatial Resolution Panchromatic
MCS	Marker-Controlled Segmentation
MEIS	Multi-detector Electro-optical Imaging Sensor
MHSP	Modified High Spatial resolution Pan
MS	Multispectral
NDVI	Normalized Difference Vegetation Index
NIR	Near Infrared
PAN	Panchromatic
PC	Principal Component
PCA	Principal Component Analysis
PDOP	Positional Dilution of Precision
RASE	Relative Average Spectral Error
SDD	Standard Deviation of the Difference image
SLRP	Simulated Low Resolution Pan
STCI	Synthetic Tree Crown Image
TIDA	Tree Identification and Delineation Algorithm
TOA	Top Of Atmosphere
TROF	Tree Resources Outside Forests
UNCCD	UN Convention to Combat Desertification
VBA	Visual Basic for Applications

VES

Vision Expert System

VHR

Very High Spatial Resolution

Chapter 1

Introduction

1.1 An overview on the Zagros forests

Iran is located in one of the world's driest region. With about 12 million hectare of forests (i.e. 7.3 percent of total area of the country), it is considered to be amongst the low forest cover countries (FAO, 2002). The forests of Iran can be classified into five zones: Caspian, Zagrosian, Arasbaran, Irano-Touranian, Khalijoomanian, which include varied forest types and are rich in terms of the biological diversity. The Zagros forest zone is the second most important forest region that includes more than 180 tree and shrub species, predominantly of the oak genus (*Quercus* spp). Western oak forests cover an area about 5.5 million hectares (about 3.3% of Iran's territory) of a topographically complex and extensive system of mountains, extending from North-west to the South-east of the country. Regarding water balance, the role of Zagros forests is indispensable, while the region collects around 30% of the annual precipitation and includes some of the most important rivers of the country. Beyond ecological functions, these forests play an important role in safeguarding the livelihood system for around 30% of the country's population and their livestock (more than 50 % of the livestock population of Iran). In fact, the western oak forests have multiple socio-economic and ecological functions that are important at the global, national and local scales. They also play vital roles in improving landscape aesthetics, water supply, reducing runoff, and preventing soil erosion. According to such a high ecological and socio-economic values of the Zagros forests, forest managers have to balance conservation, economy and other aspects of these forests. So far, the conversion of forested lands to agriculture, illegal logging, fuel wood collection and charcoal production have been considered as the most important reasons of forest degradation in this region. During past decades, Zagros forests have been under drastic anthropogenic pressures, which threatened their future existence and

Government activities failed to halt forest degradation. Since 1961, most of the forest management plans have never been implemented or could not achieve their goals, because of the lack of detail information as well as weak stakeholders participation between the relevant sectors (Fattahi, 2003). Therefore, investigation on the present status and changes of Zagros forests is essential to find more reliable and sustainable solutions for the both forest managers and decision makers.

In 1996, Iran joined to the United Nations Convention on Biological Diversity and protection of the Zagros Biodiversity received a high priority in the Biodiversity's National Action Plan. Since 2000 a new long-term program for conservation of the Zagros forests has been developed by the Forest Rangeland and Watershed Management Organization (FRWO).

1.2 General motivation

With growing concerns about sustainability in forest management practices, the request for accurate and reliable information on forest attributes on both tree and stand levels such as crown area, tree height, volume and percent cover are becoming more and more demanding. The traditional labor intensive and field based forest inventory is normally expensive and time-consuming. The high expenses are due to the large amount of human labor used in data acquisition and processing (Hyypä *et al.*, 2005). Remote sensing as an alternative approach offers the potential for more efficient assessment of various forest attributes especially for situations where site access is limited. For many years traditional medium spatial resolution remote sensing imagery has been used to describe and predicting forest parameters using classification and regression methods (De Wulf *et al.*, 1990; Trotter *et al.*, 1997; Franklin & Turner, 1992; Franklin & McDermid, 1993). In Iran, many efforts have been done to generate forest density maps in Zagros area using low to medium resolution satellite imagery (Saroe, 1996; Riyahi, 2001; Darvishsefat & Saroe, 2003; Ahmadi Sani *et al.* 2006). The results of these approaches often are too inaccurate to be used in any modeling or management scenarios. These studies revealed that the special structure of the Zagros forests, i.e. low crown cover and effects of background reflectance restricted the application of low resolution satellite imagery for estimation of

the forest parameters accurately. On the other hand, rapid decline of the Zagros forests necessitates the development of more accurate and sustainable management regimes. In recent years the availability of high resolution airborne (i.e. CASI, MEIS-II) and space borne (i.e. IKONOS, QuickBird) imagery, present an opportunity to shift from extracting average values of stands toward the single tree scale (Gougeon 1995a, Gougeon *et al.*, 2003). Potential improvement of the utility of remote sensing may be achieved through the application of very high resolution imagery that allows improving the estimation of stand density, volume, basal area, and canopy closure compared to the lower resolution data. In fact, automatic individual tree crown delineation can provide detail and reliable information to improve forest planning and decision making for forest conservation in the Zagros area. Therefore, a shift in image analysis paradigm is also needed in order to automatically extract tree based attributes. Simple pixel based classifiers can hardly be used to delineate individual objects in high resolution imagery and consequently it is essential to develop new image segmentation techniques and examine them under different forest type and acquisition conditions. The interaction between forest canopy and incident sunlight can result in a variety of spectral and spatial characteristics which are highly dependent on sun, sensor and target configuration (Lamar *et al.*, 2005). Coniferous trees have rather distinct tree crowns especially species which have conical crown shapes which cause bordering shadows that are particularly useful in delineation process. Moreover, in coniferous stands, the tops of the trees are typically the brightest pixels in high spatial resolution images (Gougeon, 1997) which make it feasible to find the tree location and the crown projection line. In contrast, deciduous trees typically have broad elliptical spreading crowns with specific self-shadowing foliage and multi crown crests. Also in natural forest stands deciduous trees tend to interwine and form mixed groups. These particular spatial arrangements of trees as well as inherent crown surface heterogeneity make individual tree crown delineation a highly demanding challenge in deciduous forests. Most of the current automated tree crown delineation algorithms have been applied in high density planted conifer forests and developed for symmetrical and circular crowns which have one bright point at the center Table (1.1).

Table 1.1 A selection of important references for individual tree crown delineation.

Reference study	Data type	Resolution (m)	Forest type	Location
Wang <i>et al.</i> (2004)	CASI	0.6	conifer	Canada
Dralle & Rudemo (1997)	Aerial photo	0.15	conifer	Denmark
Maltamo <i>et al.</i> (2003)	Digital video	1	conifer	Finland
Wulder <i>et al.</i> (2000)	MEIS II	1	conifer	Canada
Zagalikis <i>et al.</i> (2005)	Aerial photo	0.32	conifer	Scotland
Brandtberg (1999a)	Aerial photo	0.1	conifer	Sweden
Erikson (2004)	Aerial photo	0.03	conifer	Sweden
Pouliot <i>et al.</i> (2002)	Aerial photo	0.05-0.15	conifer	Canada
Leckie <i>et al.</i> (1999)	CASI	0.7	conifer	Canada
Bai <i>et al.</i> (2005)	Aerial photo	0.5	conifer	Canada
Haara & Haarala (2002)	Aerial photo	0.25	mixed	Finland
Korpela <i>et al.</i> (2006)	Aerial photo	0.1	conifer	Finland
Utterer <i>et al.</i> (1998)	Aerial photo	0.25	conifer	Finland
Erikson (2003)	Aerial photo	0.1	conifer	Sweden
Pitkänen (2001)	Aerial photo	0.5	conifer	Finland
Fuchs (2003)	Aerial photo	0.25	Con./ Dec.	Germany
Bunting & Lucas (2006)	CASI	1	Mixed	Australia
Warner <i>et al.</i> (1998)	Aerial photo	0.06	Deciduous	USA
Pollock (1998)	CASI & MEIS II	0.6,0.36	conifer	Canada
Wulder <i>et al.</i> (2004)	IKONOS& MEIS II	1	conifer	Canada

While developments of algorithms for conifer forests attract significant attention, relatively fewer efforts have been spent on the natural deciduous forests which accommodate trees with variable crown size and shape. Moreover, comparative studies among the existing methods are rare so far. In order to make multitude methods more operational, it would be desirable to characterize them according to their strength and weakness for example methods that can better handle sparse deciduous forests and which that can better handle dense conifer forests.

In spite of disadvantages of aerial photos and airborne imagery, these data were the main sources for the bulk of earlier investigations (Table 1.1). Some disadvantages of these data include inherent geometric artifacts that are a function of the camera or sensor optics

and the relatively small area of the ground they typically cover (Wulder *et al.*, 2004). With the advent of new very high resolution satellite imagery, another chapter was opened in the individual crown detection era. Very high-resolution satellite imagery (<1m) with multi-spectral high-revisit frequency and large area coverage has the potential to overcome some of the common problems of airborne data. The commercially available high resolution satellite imagery with competitive cost relative to existing aerial photos can deliver unprecedented high quality georeferenced data with spatial resolution suitable for individual tree crown detection. The rapid increase in the number of high resolution satellite imagery that will be available in the near future motivates further studies about their application, advantages and limitations. The primary objective of this study is to apply image fusion techniques available in commercial image processing softwares on QuickBird data and evaluate the objective and subjective quality of synthesized images. The results and outcomes help understanding advantages and disadvantages of such fusion methods for QuickBird imagery. Fundamental studies are needed to clarify how much a crown delineation method is reliable with respect to the different forest conditions and satellite imagery. The main objective of this study is to apply relevant crown delineation methods on QuickBird imagery and assess the accuracy of the results qualitatively and quantitatively. This knowledge is supposed to provide an opportunity to find a suitable combination of image processing and image segmentation methods to be used in open forests of Iran and elsewhere.

Individual tree delineation appears to be a reasonable starting point for additional efforts to estimate tree sizes and volume. The delineation approaches developed in this study provide tree positions and the immediate neighborhood constellation for each tree that were laborious and hardly available before. Such datasets are sufficiently accurate for evaluating spatial patterns of tree populations and examining the degree of aggregation in the distribution of tree species. This information is a basis for distance-dependent individual tree growth models (Gadow & Hui, 1999). Tree delineation has the potential to model tree structural variables such as tree height and stem diameter (Pouliot *et al.*, 2002). Variables such as DBH, tree height and crown length were the best to estimate biomass of all above- and belowground compartments (Xiao & Ceulemans, 2004). Forest structural

features (e.g., snags, stem density, species composition) have been proposed as indicators in sustainable forestry programs.

1.3 Potential applications of the very high resolution imagery in precision forestry

Precision forestry deals with the possibilities of obtaining relevant information for forest management and forest planning precisely and linking this information to the locations (coordinates) using advanced methods of information technology to improve operations and processes (Becker, 2001). Precision forestry employs high technology sensing and analytical tools to support site-specific, economic, environmental, and sustainable decision-making for the forest sector (Bill Dyck, 2003). Very high resolution imagery in conjunction with the global positioning system (GPS), and geographic information systems (GIS), play a key role in precision forestry approaches. Very high resolution remote sensing can deliver data at a scale which individual tree crowns can be detected, and capability of up scaling to stand and forest level. Gougeon & Leckie (2001) contend that high resolution imagery encourage and facilitate precision forestry. Many argue that high resolution imagery would allow capturing a range of multi-resource management information such as stem density, crown closure, snag locations, forest gap size and distribution, more rapidly, objectively and cost effectively than current ground based survey or manual interpretation of aerial photographs (Gougeon *et al.*, 2003, Zagalikis *et al.*, 2005, Maltamo *et al.*, 2003).

As could be expected, high spatial resolution imagery has a wide spectrum of applications ranging from individual stem counting to more advanced biomass estimation (Table 1.2). Successful delineation of individual crowns using automated processes, provide an opportunity to generate a range of spectral and spatial information of each crown. This information can be combined with field-measured values and environmental datasets for modeling and mapping tree attributes across the whole landscape. The number of stems is one of the first attributes of interest which may be used in modeling tree interactions e.g. growth modeling (Pitkänen, 2001). Detail information concerning the natural variation in the spatial distribution of trees between and within the stands could improve the management planning in terms of robust growth prediction (Pukkala,

1990). Moreover, tree species composition, size distribution and spatial distribution of trees affect processes, such as regeneration, growth, competition and mortality of trees (Utterera *et al.*, 1998).

Table 1.2 Examples of applications of high resolution data in precision forestry applications for a wide range of attributes.

Topic	Related studies
Tree species classification	Brandtberg, 1999a ; Erikson, 2004; Pollock, 1998; Gougeon, 1995a; Gougeon <i>et al.</i> , 1999; Bunting & Lucas, 2006; Larsen, 2007; Olofsson <i>et al.</i> , 2006; Brandtberg, 2002; Leckie <i>et al.</i> , 1999b; Pinz, 1999; Leckie & Gougeon, 1999
Damage assessment	Leckie <i>et al.</i> , 1992 ; Murtha & Fournier, 1992 ; Haara & Nevalainen, 2002
Crown closure and forest gap	Leckie <i>et al.</i> , 1999b
Growth and change detection	Bai <i>et al.</i> , 2005
Stem diameter and basal area estimation	Wulder <i>et al.</i> , 2000; Zagalakis <i>et al.</i> , 2005
Spatial pattern analysis and tree position	Dralle, 1997; Utterera <i>et al.</i> , 1998; Korpela <i>et al.</i> , 2006
Crown area and diameter distribution	Maltamo <i>et al.</i> , 2003 ; Pouliot <i>et al.</i> , 2002 ; Gougeon, 1995a
Tree volume	Zagalakis <i>et al.</i> , 2005
Stem counting	Gougeon, 1995b; Dralle & Rudemo, 1996; Leckie & Gougeon, 1999
Canopy height	Zagalakis <i>et al.</i> , 2005
Biomass estimation	Zagalakis <i>et al.</i> , 2005

Multitemporal very high resolution data provide the capability for monitoring and assessing the mortality of individual trees over time. A great change in the reflectance of tree crowns subject to stress and pest infestation can be detected using high resolution imagery, especially in the near infrared spectral range. It is feasible to identify the

stressed and damaged individual crowns as well as resistance individuals which survived after disease or insect/pest outbreak. Very high resolution data has a valuable role to play in forest health monitoring programs. This data offers an alternative for estimating the location and extent of pest attacks (Coops *et al.*, 2006), for example, Leckie *et al.* (1992) outlined the capabilities of high resolution imagery for operational use in damage assessment and found a close relationship between spectral features extracted from MEIS imagery and tree defoliation caused by the spruce budworm. Haara and Nevalainen (2002) argued that segmentation of very high spatial resolution imagery can provide satisfactory results with adequate accuracy for detecting dead or heavily defoliated trees.

Tree species identification is crucial in many forest studies, forest inventories, forest management and other applications. Extracting spectral properties of delineated tree crowns provides an opportunity to identify individual trees species. Numerous studies have demonstrated the suitability of very high resolution imagery for individual tree based species identification including Erikson (2004), Pollock (1998), Gougeon (1995a), Gougeon *et al.* (1999), Bunting & Lucas (2006), Larsen (2007), Olofsson *et al.* (2006), Brandtberg (2002), Leckie *et al.* (1999a).

Maltamo *et al.*, 2003 suggested that not only possible to separate tree species most precisely by stable geometric characteristics of digital images, but also it is doable to construct diameter distribution and tree models for each species.

The correlation between crown characteristics and tree diameter has been found to vary and to be dependent on the tree species (Maltamo *et al.*, 2003). After the tree crown size has been detected and measured, it is possible to utilize the correlation between crown and diameter at breast height to estimate tree and stand-wise forest characteristics (Zagalikis *et al.*, 2005). But that relation is frequently weak.

1.4 Goals and Objectives

The overall objective of this thesis research was to improve forest planning and decision making for conservation by providing detailed and reliable information. The specific objective was to evaluate the potential of QuickBird data to automatically delineate

individual tree crowns in deciduous forests. To achieve the overall objective, the following technical objectives have been formulated:

- To increase the spatial resolution of multispectral data using different image fusion techniques.
- To evaluate the visual and statistical quality of different fused images acquired from QuickBird Panchromatic and multispectral images.
- To analyse the relationship between crown area and tree height.
- To adapt an appropriate individual tree crown delineation algorithm for Zagros forests.
- To evaluate the accuracy of the delineation results.

1.5 Outline of the study

This thesis analyses and evaluates the potential of QuickBird data to delineate individual tree crowns in deciduous sparse forests.

Chapter 1 provides a general introduction to the thesis and it emphasizes the importance of the Zagros forests and motivates the necessity of reliable and accurate individual tree based information for planning and managing this region. Forestry potential of high resolution technology as well as QuickBird imagery is described. Also the research objectives are listed.

Chapter 2 explores the challenges and possibilities of high resolution data for automated individual tree crown delineation approach through literature review. The existing methods for individual tree crown delineation are categorized. Practical applications of individual tree delineation in the forestry domain are described.

Chapter 3 describes the location of the study forest site as well as the field measurement protocol. The general approach of this research is introduced. Individual tree crown delineation is consisting of three main parts: pre-processing, image fusion and image segmentation.

Chapter 4 presents the results of both visual and statistical quality assessment of fused images. Results of the crown by crown accuracy assessment of two crown delineation methods are presented.

Chapter 5 concludes this thesis with a summary and discussion of the main findings and directions for future works.

Appendix 1 presents categories of Computer Generated Segments (CGS) – Ground Reference Segments (GRS) overlap.

Chapter 2

Background

2.1 Common definitions

Since the individual trees are the core elements of any delineation program, a clear definition of the tree-related terms is essential. International definitions (FAO, 2004; IPCC, 2006), specify tree as a woody perennial with a single main stem, or in the case of coppice with several stems, having a more or less definitive crown. According to these definitions a shrub is a woody perennial plant, generally more than 0.5 meters and less than 5 meters in height at maturity and without definite crown. Height limits for trees and shrubs should be interpreted with flexibility, particularly the minimum tree and maximum shrub height, which may vary between 5 and 7 meters. It can be seen that, still no clear criteria for the distinction of tree and shrub is available. Tree crown, can be defined as part of a tree, which supports the photosynthesizing tissue absorbing and employing radiant energy in the living processes (Kleinn, 2007). According to Gschwantner *et al.* (2009) the crown consists of the living branches and their foliage. Tree crown is the only visible and measurable part of a tree on the high resolution optical imagery. Individual tree crown delineation aims at finding the outermost perimeter of each crown. In the natural deciduous forests tree crowns tend to intertwine and often making mixed groups that appear as single crowns on high resolution imagery. In developing the procedure for automated crown delineation in such forests it is important to define the end products. The out put is a vector polygon layer delineating either the crown of a single tree, or the combined crowns of grouped trees. Figure 2.1 illustrates a schematic diagram of typical examples of various individual crowns view from above and side.

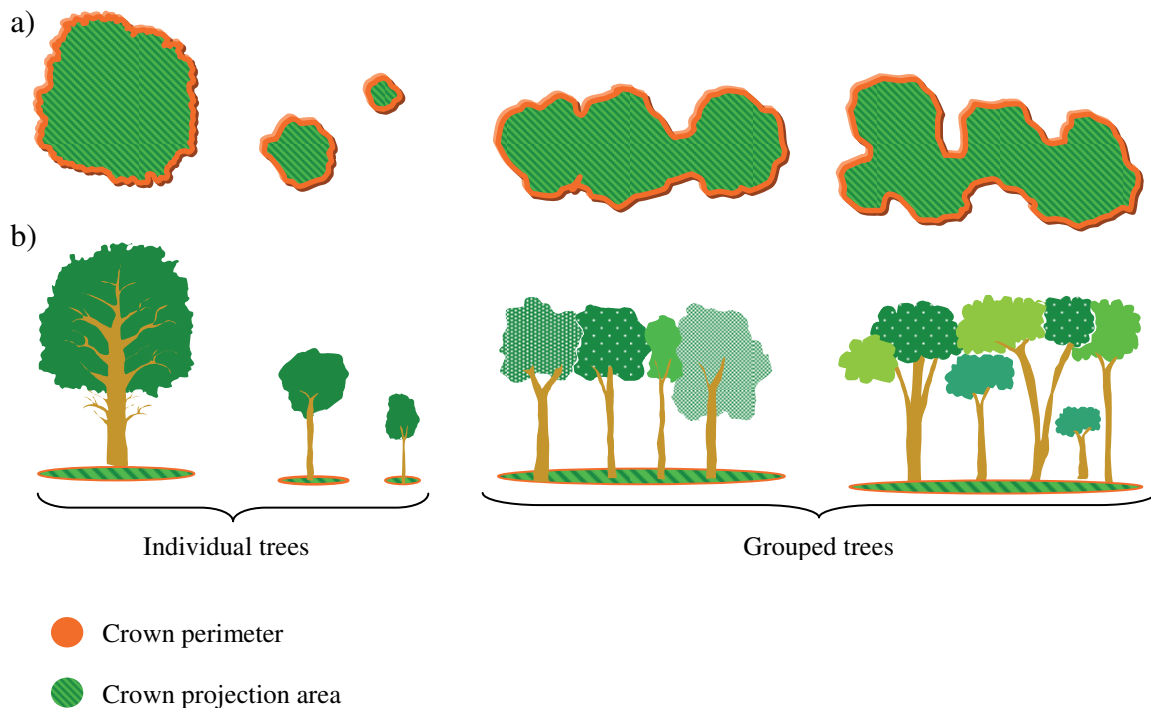


Figure 2.1 A schematic diagram of individual and grouped trees, illustrating the crowns view from above (a) and associated sideview (b).

2.2 Automated individual tree crown delineation

Traditionally individual tree crowns are extracted through manual tracing of aerial photos (Pitt & Glover, 1993). This procedure requires highly qualified remote sensing experts, making this information source expensive for large area mapping. However it is feasible to manually produce a crown map for entire forest, but extremely time-consuming, costly and large discrepancies may occur among different interpreters (Brandtberg & Walter, 1998; Zagalikis *et al.*, 2005). The fact that high resolution imagery can be collected in digital format and is multispectral offers automatic interpretation capability (Gougeon & Leckie 2003). Automatic tree crown delineation, as an alternative approach has been developed to recognize and isolate single trees (Leckie *et al.*, 2002). The concept is fully or partly replacing the human image interpreter by a seeing and recognizing computer, capable of making many decisions on its own, with a minimum of human intervention during the image processing and analysis (Brandtberg, 1999c). Computer-assisted interpretation of digital imagery presents a possible solution to acquiring more reliable

information, reducing time and costs, and increasing the consistency. Teaching a computer to recognize individual trees successfully is not an easy endeavor. At finer scales, all branches are visible and it is a complicated task to group them correctly together to a single tree crown. While at coarser levels of scales, a tree crown may have merged together with its neighbors (Brandtberg & Walter, 1998). For decades, remote sensing experts (Gougeon, 1995 a, b; Pollock, 1998; Wulder *et al.*, 2000; Erikson, 2003) have been focused on developing reliable processing and analyzing techniques to delineate individual trees as precisely as possible. Valley following method follows local minima reflectance values in between crowns and applies a rule based approach to determine the crown boundaries proposed by Gougeon (1995b). The STCI (Synthetic Tree Crown Image) algorithm, developed by Pollock (1994) and Larsen & Rudemo (1998), applies a model of trees under different view and illumination geometry and tries to find optimal matches of these models with local radiometric values. The local maximum detection method first detects local maxima reflectance values which are essential to represent the tops of upper canopy trees and then uses these as reference points for crown delineation (Culvenor, 2002; Pinz, 1991; Pouliot *et al.*, 2002). The edge detection method was applied by Brandtberg & Walther (1998) this method uses the abrupt changes in intensity values to determine the crown boundary. Probabilistic methods based on Markov Random Field modeling or random ellipses models applied by Descombes and Pechersky (2006) and Perrin *et al.* (2006).

The majority of the tree delineation algorithms assume the brightness values of the image in the vertical dimension, resulting in a radiometric ‘topography’. The analogy of a tree crown being radiometrically equivalent to a mountain peak is common among most of delineation algorithms, but the difference among techniques for processing individual trees is due to the diverse image spatial structure. It emerges from the complex relationship between image spatial resolution the arrangement of trees, and crowns spatial and spectral characteristics. In general, as the image spatial resolution decreases, the most appropriate delineation techniques appears to change from valley following, to radiance peak filtering, to texture, to geometrical optical modeling (Wulder *et al.*, 2000).

A wide variety of high resolution data with different spectral and spatial resolution from different forest types has been examined to evaluate the robustness of individual tree crown delineation techniques. Still it is very hard to determine the best method without considering these complex conditions. In some cases a combination of two or three methods should be applied to get good results. In the scientific remote sensing image processing literature the task of tree crown delineation is also referred to as:

- individual tree identification (Culvenor 2002);
- individual tree detection (Pitkänen *et al.*, 2004; and Wulder *et al.*, 2000);
- automatic tree extraction (Straub, 2003 a, b; Straub, 2004);
- crown segmentation (Erikson, 2003 and Lamar *et al.*, 2005);
- individual tree crown (ITC) delineation (Gougeon & Leckie, 2001, Gougeon *et al.*, 2003).

2.2.1 Forestry applications

2.2.1.1 Forest inventory

Automated tree crown delineation offers detailed, precise, accurate and timely tree maps (Gougeon & Leckie, 2001). By using the individual tree approach numerous forestry attributes such as stem density, crown closure, crown size, forest gaps, gap distribution, etc. can be extracted automatically using high resolution imagery (Gougeon & Leckie, 2001). In tree based forest sampling, by measuring major individual tree characteristics (e.g. crown area, crown diameter, tree height, and species) it is possible to model other valuable tree attributes, such as basal area, stem volume for the same tree. This information can be used to estimate standwise forest information such as mean height, stem volume and tree species proportions (Suárez *et al.*, 2003, Maltamo, 2003, Hyypä 2005, Korpela *et al.*, 2006). Stand level stem number estimation, crown cover and crown spacing are important attributes in forest inventory and forest planning and can improve the accuracy of standwise growth model predictions.

To estimate stem number per hectare Dralle & Rudemo (1996) applied kernel smoothing on aerial photos of pure even aged Norway spruce stand in Copenhagen (Denmark). Their approach, as they confirmed by cross validation, performed satisfactorily for all thinning grades except the unthinned control.

In southern Finland, Korpela *et al.* (2006) explored the performance of the local maxima method for detecting the image position of individual tree tops by using digitized aerial photos. A novel 3D approach was developed to assess accuracy. The best and most reliable results were obtained in the central part of images in their study.

Understanding the spatial distribution of trees is an essential key for forest management planning. To determine the spatial pattern of trees from digital aerial photographs Uuttera *et al.* (1998), applied point-process and region growing combined with active surface representation approaches to segment individual trees. Due to the large amount of misclassified clustered spatial patterns as regular patterns, and regular patterns as random patterns, the usability of digital aerial photographs seems to be limited for point-process based determination of the spatial pattern of trees.

Utilizing photogrammetry in combination with crown delineation techniques, Zagalikis *et al.* (2005) estimated tree and stand characteristics in plantation forests in Scotland. Estimation success varied, depending on the illumination conditions during the acquisition of aerial photos. In the best condition the estimates of stand top height, basal area, volume, biomass and density were similar to the ground-measured stand characteristics ($\pm 10\%$). The authors concluded that this combined method can be used as alternative for the derivation of stand attributes such as stand height, stand basal area, stand volume and stand biomass for Sitka spruce plantation in Great Britain.

In British Columbia, Leckie *et al.*, 1999 employed CASI multispectral imagery to fulfill forest management information needs. Crown closure and forest gaps were estimated by thresholds, various band ratio filter techniques and tree delineation algorithms. An algorithm was developed to extract gaps and gap statistics from the masks produced through the closure estimation methods. Tailored threshold methods produced the best results.

2.2.1.2 Species classification

High resolution imagery offers the capability of exploiting spectral statistical parameters such as maximum, minimum, mean, range, distribution at individual tree basis. Each tree species has a unique and inherent spectral characteristic. This property may be used to separate it from other tree species if the algorithm used is capable of differentiating between these different spectral characteristics. Tree species is not only important in itself in forest management, but also needed to estimate timber volume.

Gougeon (1995a) examined various types of multispectral signatures to discriminate five coniferous species using digitized aerial photographs. He also addressed the need for new multispectral classification approaches to consider individual tree crowns rather than the pixels as the object to classify.

On the west coast of Canada, Leckie *et al.* (2005) examined the capability of individual tree analysis with CASI imagery over a hemlock, amabilis fir, and cedar dominated old growth site. Tree delineation performed by the valley following approach of (ITC) suite¹ software. There were difficulties to perform species classification at tree level caused by variability of the spectral signatures within the same species, tree health and trees partly or fully shaded by other trees. To overcome these problems several signatures were developed to represent each species. Trees were classified according to species (hemlock, amabilis fir, and cedar) using object-based spectral classification however, species could not be determined for unhealthy and shaded trees. Therefore, two combined classes including “shaded class” and “unhealthy class” for all species were used for further analysis. To evaluate how well each automated isolated tree was classified a tree-for-tree isolation and species classification accuracy assessment procedure was developed. The accuracy of individual tree species classification proved adequate to form the prevalent forest composition at stand level. Moreover spatial information like crown shape, size, pattern, and texture can be used to improve individual tree species identification.

¹ ITC Suite software developed by Dr. F. A. Gougeon. It runs under the EASI/PACE Image Analysis System of PCI Geomatics Inc. (yet, not sold by PCI Geomatics).

Brandtberg (2002) presented an application of fuzzy set theory for the classification of individual tree crowns into species groups in color infrared aerial photographs of central Sweden. Erikson (2003) suggested a decision function both in the spatial and in the spectral domain to segment individual crowns as well as classify their species using aerial color infrared images. In Sweden, Erikson (2004) proposed a method to automatically classify segmented tree crowns using scanned color infrared aerial photographs of naturally regenerated and mature forest. It used different image measures based on radiometric (color) information and the morphometric (shape) attributes of the segmented tree crowns to classify four different species. For 3 cm spatial resolution images and a total 791 crown segments the overall classification accuracy was 77%. If only distinction of conifer and deciduous is considered the accuracy was 91%.

Leckie *et al.* (2003) demonstrated a data processing stream for automated stand delineation and species composition estimation in forests on the west coast of Canada using high resolution multispectral airborne imagery. In order to delineate tree crowns or clusters of crowns automated tree isolation algorithms were applied. An object-oriented single tree classification was conducted. Forest stands are mainly defined by similar species composition, density, closure, height, and age. In this study, the classified single trees were regrouped into forest stands using stem density, crown closure, and species composition. Species classification accuracy was determined by comparing the average stand composition from the automated technique to that derived from ground transects or plots. Traditional forest inventory and management planning in Canada is based on stand maps at a scale of 1:10000. The authors argued that these maps can be successfully achieved by automated analysis operate at the individual crown level. Moreover for the young fairly uniform stands, both stand delineation and species composition estimation were of a quality suitable for operational use in inventory and forest management.

2.3 Very high spatial resolution imagery

The specification “Very High Spatial Resolution” (VHR) is not well-defined but commonly used for a geometric resolution of multispectral sensors with a ground sampling distance (GSD) of up to 4m (Kleinschmit, 2007). Aerial images and digitized

aerial photographs of very high spatial resolution (10-100 cm per pixel) have been used for initial research on individual tree crown delineation for many years (Gougeon, 2000). In spite of the limitation of airborne systems (e.g. geocoding, spectral and radiometric problems, and bidirectional reflectance effects) significant results were obtained (Dralle & Rudemo, 1997; Korpela *et al.*, 2006). While airborne imagery was still in its primary stages of development to employ for single tree crown mapping the launch of the new generation of high-resolution (up to 0.60 m) commercial satellites started a new era for forest mapping research at tree level (Gougeon and Leckie, 2006; Chubey *et al.*, 2006). These new generation of satellites can provide both panchromatic (Pan) and multispectral fine resolution imagery of large area coverage.

2.3.1 Fusion in automated tree crown delineation

Automated individual tree crown delineation and tree species identification requires high spatial and high spectral resolution. The high-resolution panchromatic image has better spatial details (sharp edges, small objects) as well as fine texture. Image fusion, can be used to integrate the geometric detail of a Pan image and the color information of a low-resolution multispectral images (MS) to produce high-resolution MS data (Zhang, 2004). Image fusion can therefore provide a wealth of spatial and spectral information beyond the single Pan and MS bands. The challenge in extracting tree crowns in sparse forests lies in eliminating the background reflectance effects. These high resolution multispectral data can provide the opportunity of creating a mask image to guarantee that the next processing and analysis steps concentrate only on the trees. Furthermore, it would be possible to utilize various synthetic and ratio bands to improve the delineation process. Since the wavelength range of the new satellites is extended from the visible into the near infrared the traditional fusion methods useful for fusing low resolution satellite data cannot achieve quality fusion results for new generations of high-resolution satellite imagery (Zhang, 2004; Tu *et al.*, 2001). The major problem of the traditional image fusion techniques is the color distortion of the fused images. Moreover, the type of landscape or objects presented within the image has strong influence upon the quality of synthesized images (Wald, 2002).

2.3.2 QuickBird imagery

The QuickBird satellite owned by Digital Globe was launched on October 18, 2001, and provides the highest resolution imagery among available commercial satellites. QuickBird is a pushbroom system with four multispectral bands, Blue (450-520 nm), Green (520-600 nm), Red (630-690 nm) and Near Infrared (NIR) (760-900 nm) with the resolution of 2.4 meters Ground Sample Distance (GSD) at nadir. The panchromatic channel (450-900 nm) has a resolution of 0.6 meters GSD at nadir. This satellite operates at an altitude of 450 km in a sun-synchronous orbit. Depending on the latitude of the site, revisit times vary between 1-3.5 days because of side-looking capability. QuickBird imagery products are distributed in several processing and accuracy levels which support a wide range of applications. The standard imagery products are well suited for image classification and analysis. These types of products are radiometrically as well as geometrically corrected and mapped to a cartographic projection. The radiometric corrections comprise relative radiometric response between detectors, non-responsive detector fill, and a conversion for absolute radiometry. Geometric corrections are done using the satellite attitude and ephemeris information. These corrections account for the spacecraft orbit position, earth rotation and curvature as well as panoramic distortions. The topographic relief was normalized with respect to the reference ellipsoid using a coarse digital elevation model (DEM) (Digital Globe Inc., 2007).

However QuickBird is one of the first commercial satellites that offer high quality (spatial and spectral) imagery (Table 1.3) the final products may contain some inherent distortions.

Based on Kleinschmit *et al.* (2007) the slant and inclination effects occur for view angles greater than 15° which may influence on the classification or interpretation process. Reflective materials like metal or glass can induce an over-charge in the sensor's CCDs resulting in white cones on the image. Along objects with high contrast 'rainbow' pixels may occur which is due to the separate processing of single multispectral bands. Errors during the down linking process from sensor to earth can produce high and artificial texturing of areas with low reflection. Employing different kernels in resampling

processes by Digital Globe can result in different standard imagery, though captured on the same day, but processed in later time.

Table 1.3 Very high spatial resolution satellites (Kleinschmit 2007, modified).

System	Country	Lunch date	GSD(m) Pan/MS
IKONOS 2	USA	1999	0.82/3.24
QuickBird	USA	2001	0.61/2.44
Orb View 3	USA	2003	¼
FORMSAT-2	Taiwan	2004	2/8
Cartosat 1	India	2005	2.5 pan
TopSat	UK	2005	2.5/5
ALOS	Japan	2006	2.5/10
ResourceSat DK-1	Russia	2006	1/3
KOMPSAT-2	South Korea	2006	¼
WorldView I	USA	2007	0.46 pan
Orb View 5	USA	2007	0.41/1.64
RapidEye	Germany	2007	6.5
Pleiades	France	2008	0.7/2.8
WorldView II	USA	2008	0.46/1.84

A wide variety of high resolution (spectral and spatial) remote sensing imagery is available and successful implementation of these data to delineate individual tree crowns requires a good knowledge about its capabilities and limitations. In the next subsections some of the most important of these factors will be presented.

2.4 Parameters affecting delineation procedure

2.4.1 Internal factors

2.4.1.1 Crown texture

Crown texture may be defined by crown apex, margin, and branch pattern (Philipson, 1997). The term texture refers to the spatial distribution of crown reflectance variations and uniformities. Texture indicates measures such as smoothness, coarseness, and

regularity of a tree crown (Navulur, 2006). Crown texture varies in different tree species and within particular tree species by growth stage and health condition. Crown structure has the main influence on crown surface reflectance which generally occurs at different scales, ranging from individual leaves and stems to internal crown structure (Culvenor, 2003). Forked branches or crowns dissected by hardwood branches and shadows cause a spatial separation between crown segments that often leads to the over dissection of an individual crown into multiple parts (Lamar *et al.*, 2005). For example, large branches may have their own shadow within the crown or any self shaded area in the lit side and branches sticking out of the crown make a rough convex surface (Gougeon, 1998). Since most of the current crown delineation algorithms are based on a moving window, consequently using fixed window dimension over the whole image tends to fragment a single rough crown into numerous small isolations. Moreover in template based approaches Pollock (1999) argued that the underestimation of crown area relative to ground measurements is probably because of tree crown intersection and the failure to resolve branches at the outer crown extend that are visible from the ground.

2.4.1.2 Crown morphology

Natural variation of tree crown size, shape, and composition plays an important role in many crown delineation and identification techniques. Li & Strahler (1986, 1992) argued that the pattern of shadow that the crowns cast on the background and on one another is strongly dependent on the three-dimensional geometry of trees. Also the degree to which the shadow would be visible on the image is a function of the crown shape, the shape of shadow and illumination. Gaps between foliage elements within a crown that allows sunlight to pass through the canopy, cause irregularities in crown shape and observed radiance. Li and Strahler (1992) indicate that the shape and density of tree crowns in conjunction with the brightness contrast control the reflected radiance received by the sensor. Successful tree locating using LM filtering depends on the size of trees in relation to the image spatial resolution. In general for a given spatial resolution, bigger trees are easier to locate because they are represented with higher number of pixels than the small trees (Wulder, 2000). For template matching methods, Pollock (1999) found that irregular

crown forms especially for some hardwood trees caused an error in the automatic recognition results.

2.4.1.3 Crown spatial arrangement

Forest vertical and horizontal structure influences the composition of forest surfaces observed by a sensor (Goodwin *et al.*, 2005). In natural forests usually dominant trees have a large crown covering intermediate and suppressed trees. So, only few sub-dominant and suppressed trees are visible on the remote sensing imagery. In this situation, it is impossible to expect any delineation process to precisely isolate individual tree crowns. If the trees cannot be detected by naked eye, the segmentation method cannot provide reliable estimates (Maltamo, 2003). Whereas, an open canopy structure (as apposed to a closed canopy) may increase the difficulties due to more light penetrating the forest canopy and unpredictable nature of the background reflectance (Goodwin *et al.*, 2005). It has been shown that the spatial distribution of trees in natural forests often follows a clumped or contagious pattern. This may result in groups of tightly clustered crowns where it is difficult - even for human interpreters - to distinguish one tree's foliage from another (Culvenor, 2002). The lack of spatial separation between neighboring tree crowns can lead to the over-aggregation of several individual crowns into one segment (Lamar *et al.*, 2005).

2.4.1.4 Tree density

Canopy-light interaction which affects the delineation procedure is a factor of physical arrangement of trees in the forest stands. The number of trees in the stand is a function of age and crown size. Pitkänen (2001) studied the effect of stand density on the accuracy of estimation. He concluded that tree detection worked well in stands where the density was less than 1500 tree/ha; however he mentioned the spatial resolution as another limitation factor. Erikson (2004) investigated the effect of crown density on delineation using three different methods. A very relevant observation was that there is a separation between methods that can well handle dense forests and those which can well handle sparse forests.

2.4.2 External factors

2.4.2.1 Spatial and spectral characteristics

Selection of the optimum spatial resolution and the most appropriate spectral channel for automated tree crown delineation will have a critical influence on the outcome of the tree delineation process, particularly the size and number of trees that can be defined (Culvenor, 2002). In forests with widely varying crown sizes non-optimum spatial resolution is a common problem (Brandtberg & Walter, 1998). Optimum spatial resolution will vary between forest types and individual algorithms; they typically require that the ground resolution cell of the sensor be considerably smaller than the size of the tree crown objects in the scene (Culvenor, 2002). Optimizing the spatial resolution for small trees results in the over-segmentation of large trees while optimization for large trees typically results in the merging or omission of smaller trees (Wulder, 2003).

2.4.2.2 Image acquisition geometry and sun angle

Factors such as view angle, sun elevation, and topography have a significant effect on the radiometric and geometric properties of tree crown as seen by a remote sensor (Pouliot *et al.*, 2005). In a high spatial resolution image, although the base of a tree may be in the correct geographic location, different view angles can cause lay-over, resulting in an appearance that the top of tree is leaning away from its base. The amount and direction of this leaning is dependent on the view angle (Wulder *et al.*, 2008). For the same tree, this can result in a differently shaped and sized crown and different locations of the crown center point. The effect of topography is not widely researched. Surface characteristics (e.g. slope, aspect), in conjunction with illumination and view angle have significant effects on crown reflectance properties. Slope and aspect can affect the area of shadow cast from a single crown onto the sloping background and on the mutual shadowing relations between tree crowns (Gemmell, 1998). Topography also affects pixel size and shape, which in turn can impact crown size estimates, but this effect can be minimized through orthorectification (Pouliot *et al.*, 2005). For different forested imagery, the interaction between forest canopy and incident sunlight can result in a variety of different spectral and spatial characteristics (Lamar, 2005). Culvenor (2002) demonstrated that an

increase in solar zenith angle results in a decrease in the number of clusters delineated. Non vertical viewing angles also resulted in fewer clusters being delineated, with less accurate delineated trees near the edge of an image compared with trees closer to the center. Culvenor *et al.* (1998) simulated variation in sun angle and viewing geometry of a forested landscape to make judgments about the effects of this variation on the automated tree crown delineation. The results indicated solar elevation less than 70 degrees and off-nadir viewing of greater than 40 degrees may yield unreliable results in terms of the number and average area of crowns. Zagalikis *et al.* (2005) observed that lower sun elevation leads not only to an underestimation of the number of trees, but also to the underestimation of crown area because of the effects of the larger shadows on the determination of the crown areas of the neighboring trees. The acquisition of the imagery should be at a time of day and year when the elevation of the sun is high. Based upon the results of their study, image capture before 11:00 or after 13:00 local time will produce unreliable results especially at high latitudes.

2.5 Categorization of automatic individual tree crown delineation techniques

Within the last decade, automatic delineating, positioning or counting single trees in high resolution imagery has been subject of many research studies. Automatic individual tree crown delineation is a high-technological approach in 'vision' and requires expert knowledge. Various efforts have been done to provide consistent and reliable algorithms. In this section, the advantages and disadvantages of the some common approaches are discussed. Gougeon *et al.* (2003) suggested that tree crown delineation techniques can be classified from the information obtained during the delineation process. They divided the approaches into three main streams, including a) tree location, b) tree location and crown dimension parameterization, and c) full crown delineation methods. Tree location can be determined by an appropriate size for local maxima filter in dense forest areas (Dralle and Rudemo, 1996; Pitkänen, 2001). The second group of techniques is either based on finding local maxima and then the edge of the crown (Utterer *et al.*, 1998) or on matching the image features to two-dimensional crown models (Pollock, 1994; Larsen & Rudemo, 1998). Full individual tree crown delineation algorithms comprise valley

following methods which follows the valleys of shade between tree crowns (Gougeon, 1995b) and the edge detection techniques that follows the edges created by gradient operators and analysis of their curvature (Brandtberg, 1999b).

Wulder *et al.*, (2003) suggested a different categorization scheme. Any technique that utilizes the valleys of shadow among the trees or local minima (as a starting point for isolating crown boundaries) is categorized as a ‘bottom-up’ technique. The second category ‘top-down’ includes techniques which initially find the location of tree crowns from their radiometric maxima. Then they find the location of the crown boundary by any decrease in intensity from the crown center to its edges. The final group of algorithms ‘template matching’ is looking for the best match between the templates of gray values (representing the tree crown) and the base in the entire image. Figure 2.2 shows Wulder’s categorization of the automated tree crown delineation techniques.

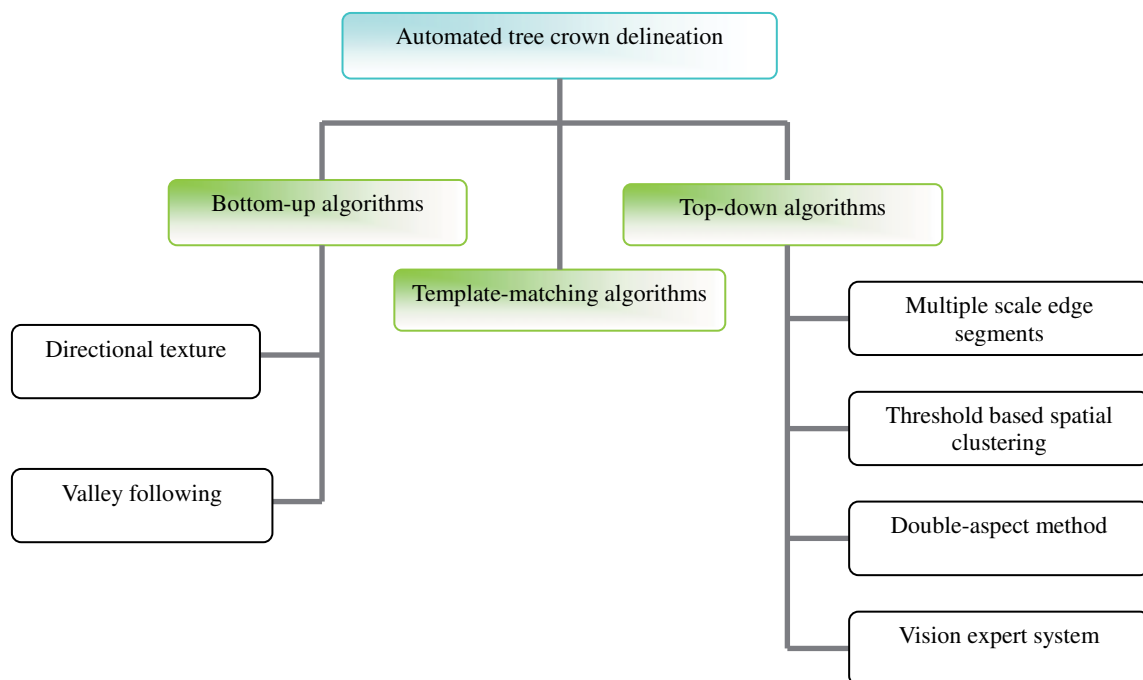


Figure 2.2 Categorization of automated tree crown delineation techniques (adapted from Wulder (2003))

The following sections describe Wulder’s categorization and provide an example of their application.

2.5.1 Tree delineation ‘bottom-up’ algorithms

2.5.1.1 Directional texture

This method was developed by Warner *et al.* (1998) for hardwood forest types. Deciduous forests have a vertical and horizontal structure completely different from conifer forests where the tree crown delineation gave successful results. The main challenges for tree crown delineation in the eastern deciduous forests in North America are various crown shapes, sizes and spacing, complex mosaics of the individual crowns and relatively flat topography of the mature forest canopy. In this type of forests, shadows can not isolate the individual trees and as a consequence, many segments remain open. In this situation orientation information² may help to conjoin these segments. In Warner *et al.* (1998) in the first phase, a new single band illumination/albedo image was built by taking the square root of the sum of the squares of the bands; Because of the high variations in brightness, it was not possible to use a simple threshold to isolate shadows over the scene hence a standard procedure of normalizing pixels was applied to reduce variation. The best window size for normalizing was selected according to the size of single trees, between-tree and between-branch shadows. In the following, to identify many between-tree shadows, with relatively few between-branch shadows a threshold was applied on the image. The result was converted to binary for further processing. Local variance was used as the texture in this study. In the second phase the direction of minimum texture was determined from the comparison of texture in numerous narrow groups of pixels in a square matrix. This matrix was set to value one for angle of interest and zero for those pixels which were not used in texture calculation. The minimum texture was calculated in 20 different directions using an 11 by 11 matrix. The orientation of the texture is aligned with the linear features such as boundaries of individual trees. The texture orientation of shadows provides a link between the isolated shadow segments that can be joined to delineate each tree. Finally, individual tree crowns can be delineated by grouping of bundles of pixels together with similar directional properties. The core of this algorithm is a pre-processing step, specially the size of normalizing matrix. In a few

² The orientation information can be extracted by directional filters. All matrix positions are given a value of zero, except along particular angle which is to be investigated.

cases shadows between larger branches caused incorrect identification of tree boundaries. It would be very hard to subjectively find a normalized window compatible with different crown sizes in a scene. Furthermore, application of this algorithm in sparse forest stands with unpredictable nature of background and variable crown size was problematic.

2.5.1.2 Valley following

Valley following is the first and possibly best known method for automatic tree crown delineation in high spatial resolution imagery developed by Gougeon (1995). The concept of the valley following method is based on three dimensional visualizing a high resolution image of forests. This radiometric 'topography' is obtained by assigning the spatial information in the image to x and y dimensions, while the brightness values of the image are marked to the z dimension. Bright pixels depict the higher region (mountains) whereas dark pixels illustrate the lower regions (valleys). The principal objective of this analogy is to delineate the crowns by joining radiometric valleys. First, valley following algorithm create a local minima network between the crowns. Then, any problem with incomplete minima connection is refined by a rule-based program. This program works by following the crowns outline, finding any small gaps or partially delineated, and then traversing the boundary of crown to fully delineate it.

2.5.1.3 Template matching

In the beginning of the 90's Pollock proposed the first vision system that uses template matching technique for detecting and delineating individual tree crowns in high resolution images for boreal forests. This methodology is the process of determining the location of an object by a spatial cross-correlation process (Choi & Kim, 2002). The image model (template) is characterized by both geometric (i.e., crown envelope shape and the sensing geometry) and radiometric (i.e., scene irradiance, the interaction of the scene irradiance and the tree crown, and the sensor irradiance) properties. In the initial step, the algorithm searches the image for locations where a measure of the match between template and local pattern of image values, is at a local maximum. The matches constitute the initial recognition instances. In the second step the features of each initial

recognition instance are evaluated and the probability of correct recognition is estimated. Initial recognition instances with low correct probability are rejected. During this process some conflicts in interpretation of the same region may occur (i.e., one large crown image versus multiple small crown images). In the final step these conflicts are resolved from physically implausible relationship among the intermediate instances. The results showed that, in highly variable natural forests, the template matching algorithm is unable to cope with irregularities in tree crown form and irradiance that are caused by tight vertical and horizontal spacing of the crowns (Larsen & Rudemo, 1997). An advantage of this procedure is that it is not dependent on the existence of explicit tree crown boundaries (i.e. local minima) or on a clear contrast between the tree crown and the surrounding (Pollock, 1998). Moreover, some improvements in the model allow finding and positioning tree tops from a wide range of viewing angles. Larsen & Rudemo (1997) extend the model in Pollock's former work by including the background. The basic elements that constitute the tree model are single tree crown, a 'ground' plane, light sources and camera. The basic tree crown shape was modeled as a generalized ellipsoid. The interior of the crown is assumed to contain randomly oriented scatters which have different types, optical properties and distributions. The "ground" plane included in the model is a horizontal surface that reflects and absorbs the light, thereby giving a brightness edge at the crown boundary, and allowing the modeled tree to cast a shadow in the ray-traced template. Only the sun and the sky are considered. The diffuse illumination from the ground and from interreflections between trees is ignored. The performance of the algorithm is evaluated by using a variety of off-nadir images from even-aged Norway spruce plantation (Larsen & Rudemo, 1997). This approach provided very good results for the detection of tree peaks. To increase the precision & the rate of top tree detection the effect of optimizing templates & match window were studied by Larsen & Rudemo (1998) and Larsen (1998), respectively. The results showed that this approach can increase the rate of top tree detection.

2.5.2 Tree identification and delineation ‘top-down’ algorithms

2.5.2.1 Threshold-based spatial clustering method

The tree Identification and Delineation Algorithm (TIDA) is a threshold-based spatial clustering method proposed by Culvenor (2002). TIDA was developed to automatically delineate native Eucalypt crowns in Australia. The phrase ‘clustering’ here represents the spatial aggregation of contiguous pixels into spatially unique objects. This algorithm exploits the relationships between the geometric and radiometric crown characteristics for tree delineation. TIDA has three main steps: I) identification of local maxima, II) identification of local minima, and III) clustering of crown pixels. In the first step, the algorithm tries to determine the tree position by calculating the coordinates of the local maxima or ‘seeds’ for each crown. Then, in the second step, spectral minima, or ‘valleys’, are used to construct a continuous network of absolute crown boundaries of one pixel width between all crowns. When spectral maxima and crown boundaries have been identified for the entire image, in the third stage the delineation of each crown is performed using a ‘top-down’, threshold based clustering approach. Only pixels within each ‘enclosure’ defined by the minima may be considered for clustering with the ‘seed’ inside the enclosure. If there is no seed in the enclosure no clustering takes place (Culvenor, 1998).

Evaluation of TIDA has shown that it is the most suited algorithm for forest canopies with dense crowns, as they are more likely to support the assumed relationship between geometric and radiometric crown shape (Wulder, 2003). Simulating variation in sun angle and geometry of a forested landscape by Culvenor (1998) showed that under the current state of development, TIDA cannot provide consistent results under variable illumination and viewing conditions.

2.5.2.2 Multiple scale edge segments

In high resolution images of the forest two texture classes can be distinguished: the internal texture of each tree crown i.e., branches or groups of branches and the internal texture of forest stand i.e., individual tree crowns. These two textures need two relevant

scales to be represented. The topic of employing multiple-scale analysis for identification of most-probable crown boundaries was addressed by Brandtberg & Walter (1998). They developed a novel automatic crown delineation algorithm based on scale-space theory. This theory aims to find a degree of image smoothing or a stable scale at which the studied objects are all presented in the image. The scale-space technique in this algorithm focuses on the tree crown contours, which mainly undergoes rounding-off transformation at higher levels of scale. Therefore, no loss of essential information was expected to occur due to the heuristically chosen and applied scale interval (Brandtberg, & Walter, 1998). The algorithm consists of five main stages, I) image smoothing, II) effective scale notation, III) edge detection, IV) curvature estimation, V) primal sketch. Since crowns are of different size and shapes, smoothing was performed at different scales by means of a family of discrete kernels. A notation of effective scale was adapted to appropriately compare and sum up the primal sketches. In the next step tree crown contours were identified as zero-crossing with convex grey-level curvature, which were computed on the intensity image for each image scale. A threshold ensured that only edge pixels with convex grey-level will be processed. The next stage of algorithm computes a center of curvature at each image scale and for each edge pixel. All center points belonging to the same edge segment made a path or swarm. Based on these points an ellipse was estimated and extended. The values were high in the interior part of the sketch and decreased towards the periphery. Local maxima within the accumulated sketches were used to define the seed points for tree crowns. When all seeds were defined, for each seed a crown segment was grown under the condition that it had no contradict with its neighboring segments or just grow into areas of the image which are brighter than a global minimum threshold. This method was evaluated by comparison with manual delineation and with ground truth. The authors concluded that the performance of the method is almost equivalent to visual interpretation. However, in comparing with ground truth the algorithm had difficulty to discriminate trees standing very close to each other or small trees standing close to large trees. In numerous cases light sun patches on the ground were identified as tree crowns. Although the algorithm was able to capture circular and elongated tree crowns, like other crown delineation methods, it is subject to omission and commission errors in complex forest canopies.

2.5.2.3 The Vision Expert System

In the mid 80's an Austrian forest-condition-inventory program has been developed. The main focus of this program was assessing forest health and vitality, using high resolution color infrared aerial images. To achieve a fully automated forest inventory an image understanding system, the Vision Expert System (VES), was designed by Axel Pinz in the 1980's. The goal of VES was to locate the center of a crown, to estimate the crown radius, and to reliably repeat this processing for all trees in the image. VES will try to resolve conflicts (e.g., trees standing too close) or try to invoke other methods for scene object finding when the result is unsatisfactory (e.g., large region in the image without any interpretation result) (Pinz, 1991). The algorithm starts to search for local brightness maxima in the image. In order to eliminate numerous maxima associated with internal crown structure, a series of low pass kernels with different filter sizes were applied. Each kernel produced its own set of local maxima. Significant maxima from all scales are combined to obtain a set of candidates for blob centers. Verification of blob compactness and significance is performed at image level. By using the original spatial resolution 'radial brightness distributions' is calculated for each blob candidate. After the first verification step the remaining bright blobs may represent the crown of a tree. Further verification at scene level includes reasoning about spatial relations between trees and between trees and other objects. The proposed method by Pinz can not exactly delineate each tree crown but it can find the center of the crown and can provide an area which definitely belongs to the same tree in its surrounding (Pinz, 1999; Pinz *et al.*, 1993).

2.5.2.4 Double-aspect method

Walsworth and King (1999) developed an algorithm to delineate tree crown and identify apexes of Aspen trees. They employed it for modeling of forest structural changes on an acid mine site. The objective was to undertake a preliminary integration of temporal imagery utilizing standard GIS tools, and black and white aerial photography. To achieve this goal, a crown delineation methodology was designed using the variation in aspect (double-aspect) of the radiometric surface. The double aspect tree delineation technique identifies tree centers by determining the intersection of ridge lines. They are calculated

by double application of gray tone surface aspects for each of the four directional pairs (two using the pixel orthogonal direction approximately N-S, E-W, and two diagonally approximately, NW-SE, NE-SW) (Walsworth & King, 1999). When the lines are overlaid, the intersections of ridges represent apexes, while the union of gully lines represents edges. Preliminary testing showed that the union of gullies provided only partial delineation of crown edges and therefore a supplementary crown delineation technique was designed. This process consisted of inverting the gray tone images and employing flooding model and region growing algorithm. The regions are grown from the seeds (tree apex) by adding the similar neighboring pixels outwards and forming a 'cost surface'. A cumulative pixel traversal (cost surface) function was adapted as a technique for delineating illuminated crown perimeters and for merging apexes upon single crowns. The "cost function"³ works by assigning every pixel the minimum cumulative cell traversal sum away from a set of points. In this case the set of point seeds are the tree apex centroids. After removing the gully fence pixels and normalizing the cost surface, a gray-tone weighted proximity surface is produced. The pixels ranked between the central peak and the shadow edge which allowing a means of flexibility defining crown edges. This method was tested for accuracy against a synthetic dataset in which differing noise levels, shadow and texture conditions were applied. The double aspect method attained its best results with random noise values similar to that found within the photography (Walsworth & King, 1998).

2.5.3 Combined methods

Surovy *et al.* (2006) proposed a novel method based on combination of valley-following, template-matching and tree top searching in cork oak forests in central Portugal. In this method a template were defined as a joined knowledge about what can be a tree, regarding the image information and the ground truth information. The templates were formed by the shapes derived from photos using tree-top together with the valley-

³ Cost function is similar to Euclidean distance function, but instead of calculating the actual distance from one point to another, determines the shortest cost distance (or accumulated travel cost) from each cell to the nearest cell in the set of source cells.

More information can be found in http://www.ciat.cgiar.org/access/pdf/ciat_access.pdf

following technique. To evaluate the similarity of found objects two sources of knowledge, the photo itself and the ground truth were used. These areas of knowledge are balanced by assigning the certainty to each point of the crown edge. The certainty is used to decide about the shape or size to be more similar to the known probable crown shape. The method detected approximately 60% of the trees. This approach proved to be helpful for filtering small trees and improving estimation of the form of the crown area.

In Sweden Erikson (2004) employed color infrared aerial photographs and a combination of techniques to classify the individual tree crowns into species. Intensity threshold, distance transform and local maxima filter were applied to find the starting points. For each starting point, the segmentation process was performed by Brownian motion and region growing. A decision rule algorithm was used to classify the segments using color information as well as the shape of the segmented tree crowns. The overall classification result was 77% and 91% for only distinction between conifers and deciduous species. Despite the errors at the tree level, this method can provide a good estimate of the distribution of tree species.

For mixed hardwood/hemlock forest in the United State Lamar *et al.* (2005) developed a novel automated spatial segmentation procedure to delineate individual Eastern Hemlock crowns from temporal large-scale color aerial images. This approach includes five steps identified as (I) shadow thresholding, (II) Euclidean Distance Map (EDM) construction and (III) smoothing, (IV) Watershed segmentation, and small blob joining. By performing a distance transform on spectrally classified binary image, assigning a brightness value to each hemlock pixel corresponding to the pixel's Euclidean distance from its nearest boundary, an EDM was produced. Prior to the Watershed segmentation, to minimize over-segmentation, a Gaussian filter was applied to the EDM. The Watershed transform was performed on the inverted EDM and each minimum as well as its associated catchment basins were segmented. Following the Watershed segmentation a small blob joining was applied to improve overall classification accuracy. A large majority of hemlock blobs (~66-72%) were found to be closely associated with ground reference. Similar overall classification accuracy was found for the multi-temporal image pairs.

Wang *et al.* (2004) applied a two-stage approach with edge detection followed by marker controlled Watershed segmentation for CASI (Compact Airborne Spectrographic Imager) images in British Columbia, Canada. This process uses a Laplacian of Gaussian edge detector to mask out background and generate a series of closed contours. Two sets of treetops were obtained by using a local non-maximum suppression and local maximum-distance method. By integrating the results a marker image was created. This image is used to guide a Watershed segmentation to further differentiate touching and clumping trees and to produce a segmented image of individual tree crowns. Verification with manually delineated crown areas showed that 75.6 percent of all pixels were classified identically. This algorithm performed best for trees viewed from near-nadir. For trees viewed from outside the near-nadir direction, the silhouettes detected from these edge-detection methods are inconsistent with the real tree-crown boundaries.

An automated algorithm was presented by Pouliot *et al.* (2005) to detect and delineate coniferous tree regeneration on clear cut areas in Ontario, (Canada). This algorithm combines strategies of several techniques including optimal image scale determination, initial crown detection, and crown boundary segmentation and refinement. In the preprocessing stage the Near-infrared (NIR) band was selected as the best spectral band via visual examination. Following that conifer vegetation mask created by unsupervised classification of original three spectral bands. Then the NIR image data under the mask were extracted for the detection-delineation processing. In the scale optimization stage, an appropriate scale was selected using adapted visual assessment and the Local Maxima Smoothing Relation (LMSR) procedure. Crown detection and initial segmentation were carried out by an adapted Watershed approach. The results of initial segmentation are highly dependent on the quality of the crown mask; to minimize this dependence the refinement stage was adapted. In the final stage at each local maximum a user-specified number of transects around the candidate crown are extended from the local maximum out to local minimum. Delineation error was assessed comparing to the ground reference data. The individual accuracy index (see section 3.7) was $> 70\%$ for trees larger than 30cm crown diameter.

Straub & Heipke (2007) presented a novel scale-invariant approach to automatically extract trees and to delineate tree crowns from color-infrared aerial imagery and a co-registered Digital Surface Model (DSM). This approach is based on a tree model with three geometric parameters and one radiometric parameter for tree vitality. The image is segmented in a wide range of scales across the linear scale space. The Laplacian of-Gaussian operator is used with different scale parameters. The processing strategy comprises three steps: first, the segmentation of the surface model is performed in a wide range of scales to extract trees from height data. The segmentation is achieved by applying the watershed transformation. Then, the evaluation of derived segments and the selection of the best hypothesis are performed based on tree model parameters (size, circularity, convexity, and vitality). In the last step the outlines of the crowns were refined using active contour models “snakes”⁴. The potential of the approach was investigated using four different data sets. Reference data were generated for all four data sets by manually capturing the position and the crown radius of all visible trees. Two accuracy measures (correctness⁵ and completeness⁶) were introduced based on the three overlapping configurations (True Positive⁷, False Positive⁸, and False Negative⁹). Results showed the completeness range of 41%-81% and the correctness of 66%-100%. Very promising results proved the feasibility of the new approach for automatic tree extraction from remote sensing data.

Maltamo *et al.* (2003) employed digital video imagery to identify tree crowns in Finland coniferous forests by applying tree crown pattern recognition technique. This approach incorporated pre-filtering, seed point extraction and region growing segmentation. A low-pass kernel was performed on the video images to reduce local variation in image

⁴ A snake is an energy-minimizing spline guided by external constraint forces and influenced by image forces that pull it toward features such as lines and edges. For more information see Kass *et al.* (1988).

⁵
$$Corr = \frac{TP}{TP + FP}$$

⁶
$$Com = \frac{TP}{TP + FN}$$

⁷ An extracted tree with a strong overlap to a reference tree.

⁸ An extracted tree with a weak overlap to a reference tree.

⁹ Trees in the reference with a weak overlap to an extracted tree.

intensity. Then the significant local maxima with values greater than a seed threshold are used as seed points for the segmentation process. The region growing segmentation algorithm was run after the seed points have been found. The filtering and segmentation were controlled by four parameters: (I) Cut Ratio (pixel value divided by the local maximum), (II) Difference value (the possible increase between neighboring pixels), (III) Mask size (the size of the operator window for Gaussian filter), and (IV) Seed threshold parameter (defines the minimum tone value for seed points in each channel). This technique was useful especially in mature stands. In dense young stands or in groups of trees, where the single trees can not be recognized some difficulties were expected.

In hemiboreal Swedish forests, Olofsson *et al.* (2006) developed an automatic tree detection and species discrimination scheme, using aerial imagery and template matching techniques. Templates that were generated from a library of three-dimensional virtual model trees are cross-correlated against any potential tree position in the digital image. The tree positions and tree templates with the highest correlations are considered as likely trees. By setting all non-black pixels in the template to TRUE a mask consisting of the sunlit part of the generated template was produced. To extract the color information of an identified tree, the mask is overlaid on the aerial image and pixels within the mask are averaged. The resulting three band triplet (red, green, NIR) for each template hit is saved. Discriminant analysis based on canopy color and equal prior probability for each class was applied. The result showed that at least the two dominating tree species in Swedish forestry, Scots pine and Norway spruce could be well separated. The overall accuracy of discriminating the conifers from the autumn-colored deciduous trees was 88.7%.

Haara & Nevalainen (2002) developed a method to detecting dead and defoliated spruces in aerial CIR photographs in Finland. A robust segmentation method, based on the recognition of tree crown patterns at sub-pixel accuracy, was employed to segment individual trees. First, the images were normalized and smoothed by Gaussian operator. The local maxima above a threshold level were collected into a segment group. Then the segmentation was started from the highest intensity using directional derivatives. The segmentation was restricted by a threshold value and a difference value. The Laplacian-Gaussian operator was used as a collector of the next possible segment pixels. Each

segment was classified to defoliation classes using linear Fisher classification models. The accuracy of the pattern recognition method proved adequate to dead or heavily defoliated stands.

Fuchs (2003, 2005) used digital surface models produced by image modeling in combination with CIR aerial orthophotos to estimate forest and tree variables which are relevant for the European Intensive Monitoring Program (Level 2). He used a hierarchical approach on an experimental observation plot with oak and beech in Germany. First, he separated crown and gaps using a supervised Maximum-Likelihood classification. Then, he delineated individual tree crowns using the Watershed algorithm and the normalized digital surface model. A subsequent object-based discriminant analysis distinguishes tree species and classes of crown condition.

Chapter 3

Material and Methods

3.1 Study area

Location and general description

The study area is located in the southern Zagros Mountains in Western Fars, Iran, with the center of approximately $29^{\circ} 32'$ Northern latitude and $51^{\circ} 53'$ Western longitude (Figure 3.1).



Figure 3.1 The location of study area in Iran.

The Zagros region with an area about 410,000 square kilometers is covered by 5.5 million hectares of forests which contain globally significant biodiversity (Ghazanfari *et al.*, 2004). Zagros is well-known because of its extreme topographical relief and climatic conditions. Large rivers of the country take their sources from this mountain chain and provide essential support to agriculture of the rest of country.

This research was carried out in Iran, Fars province, Dasht-e Barm region in an area about 270 hectares. The altitude was varying from 1250 to 1600 m above the sea level. This area has semi-arid and temperate climate with annual precipitation of approximately 405 mm. Figure 3.2 depicts the selected study area overlaid on the shaded relief DTM. The reasons for selecting this flat area as a study site were the feasibility of field measurements and the goal to minimize the effect of topography and relief displacement. This study area was considered as representative of significant areas within the Western Oak Forests (WOF) in terms of the complexity of the forest structure (i.e. diverse crown shapes, sizes and densities).

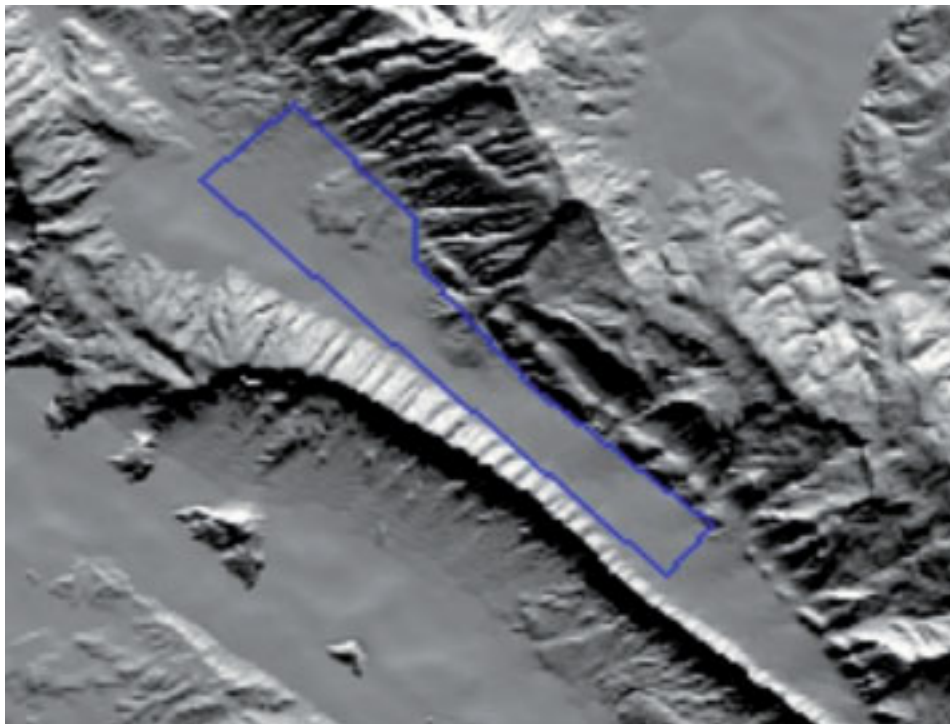


Figure 3.2 The selected study site overlaid on the shaded relief DTM (source 1:25000 topographic maps)

Forest type

Vegetation distribution is influenced by an array of natural factors like soil type, geology, and climate (Stephenson 1990, Hupp & Osterkamp, 1985) and human impacts such as cutting practices, harvesting (Tappeiner *et al.*, 1998, Raich & Tufekcioglu, 2000). The study area is covered by secondary forests that have been cutover repeatedly during many years to supply wood for charcoal production and fodder for livestock. As a result of this process, seedling forests converted to coppice forests which yield no bigger commercial value at industrial scale. In these forests most of trees have multiple trunks that emanate from central root mass. Natural regeneration (from seed) is poor. Based on Ghazanfari *et al.* (2004) the mean diameter growth is approximately 1.78 mm per year which means a tree require an average of 56 years to reach the goal diameter of 20 cm and 84 years to attain a stem diameter of 30 cm (optimal for use as fuelwood). The high shooting capability of oak trees is the main reason for persistence and survival of these forests. Coppice oak trees are generally stunted and have a poor form occupying the flat area and usually reach 5 to 16 m height. Mixed communities occupying the slopes, where tall bushes such as *Amygdalus scoparia*, *Acer cinerascens*, *Pistacia atlantica*, and *Crataegus azoralus* accompany *Quercus persica*. Oak trees are widespread native species in this region. The current forest landscape includes one story stands where Oak (*Quercus persica*) dominates which is made up by stump and/or root sprouts (Sagheb-Talebi, 2004). Unfortunately almost all of oak trees are not of high wood quality.

Forest condition

Nearly thirty percent of the total Zagros forests are located in Fars province. Trees migrated into this region between 10000 and 5500 B.P. (El-Moslimany, 1986). Actually these forests are important as remnants of natural ecosystem offering wildlife habitat and providing services to a significant part of the settled as well as the nomadic population in the region. They are also said to have important influence on water and soil conservation, climate alteration and socio-economical balance of the entire country (Sagheb-Talebi, 2004). The forest resources in this area are known to be degraded and placed under an increasing human and livestock pressure. Over a three month grazing period, the number

of livestock is four times the pasture capacity (Sagheb-Talebi, 2004). Increasing demands of nomadic and settled peoples who rely on wood and non-wood forest products as well as rain-fed farming under the forest canopy are considered as major sources of soil erosion and ecosystem degradation. These have led to the gradual extinction of wildlife due to food supply restrictions, soil degradation and deforestation.

Forestry background

Forests and range lands were nationalized in Iran in the 1960s. Up to now the type of ownership is governmental, which has a strong influence on the management and silvicultural practices in the Zagros forests (Ghazanfari *et al.*, 2004). The Forest, Rangeland and Watershed Organization (FRWO) tried to manage the Zagros forest through different forest management plans for more than 40 years. These plans mostly focused on stopping deforestation, restoring coppice forests and enabling sustainability by products. In 1975, the “Reforestation and Protection” plan was developed which aimed to convert these forests from coppice to seed regenerated forests. Due to the conflict with the needs of local communities all of these plans were failed. Development of collaborative forest management plans with more detailed understanding of the local stakeholders and involving local communities at the level of decision making is being promoted as a solution to alleviate this problem (Ghazanfari *et al.*, 2004). Recently a long term program was developed to conserve Zagros forests based on macroeconomic, macropolitic and local requirements (Pourhashemi *et al.*, 2004).

3.2 Data acquisition

For the present study, digital QuickBird images were purchased by the chair of Forest Inventory and Remote Sensing of Georg-August-University Göttingen. The QuickBird images were acquired on July 01, 2005, at 10:54 local time with the off nadir viewing angle of 13.90°. More acquisition configuration parameters can be found in (Table 3.1). These images were cloud-free over the study area and no visible atmospheric effects were found. The rain-fed wheat crop was harvested at the time of image acquisition so there was no visible biomass. Since the utilized methods for this research do not require

absolute reflectance measurements, atmospheric correction was not applied. A test site of the data set is shown in Figure 3.3.

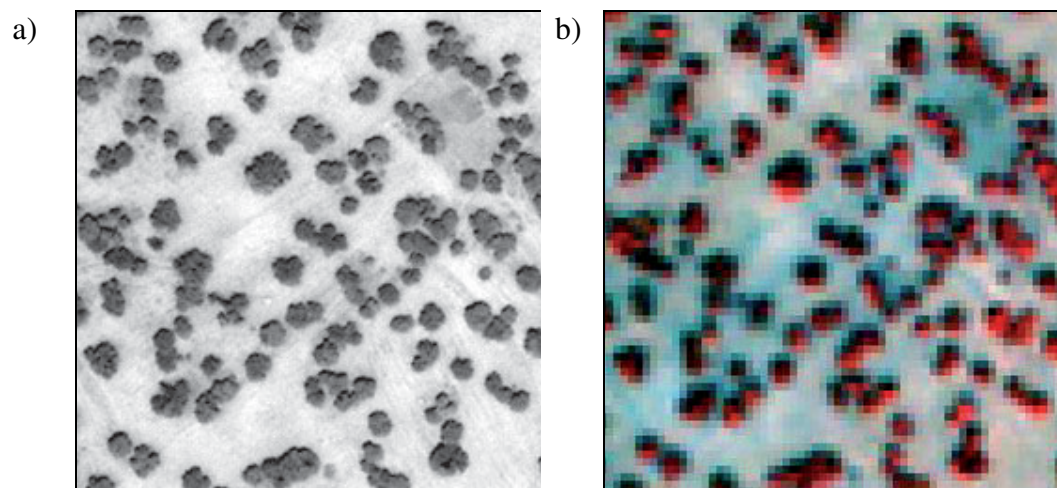


Figure 3.3 A test site of QuickBird imagery a) panchromatic (0.60m) b) multispectral false color composite image (bands 4, 3, 2 in RGB) (2.4m)

Table 3.1 Acquisition configuration parameters of the QuickBird images on July, 01, 2005.

Product level	LV2A
Bits per pixel	16
Off nadir viewing angle	13.90°
Satellite azimuth angle	77.09°
Sun elevation	72.70°
Satellite elevation	75.09°
Time (hh:mm:ss)	10:54:12
Sun azimuth	107.10°

3.3 Survey design and field data collection

3.3.1 Plot establishment

Since it is not feasible to check the whole area, sampling becomes an appropriate means to observe reference objects that will be used for the accuracy assessment. In image segmentation, accuracy assessment measures quantify the extent to which objects in the segmentation match reference objects. The advantage of these measures is that a quantitative index can be generated relative to any set of reference objects. The reference objects can be derived through various sampling schemes and field inspection. To determine the number and spatial location of samples a sample design is required. In this study, based on the need for statistical rigor, constraint of budget and time systematic sampling was applied for the validation plots. Previous studies in Zagros area (Zobeiry, 1979) applied plot size of 1000 m² to provide photo volume table using 1:20000 aerial photos. A sample scheme was designed considering the relations between study area, the size and the number of required individual sample plots Figure 3.4.

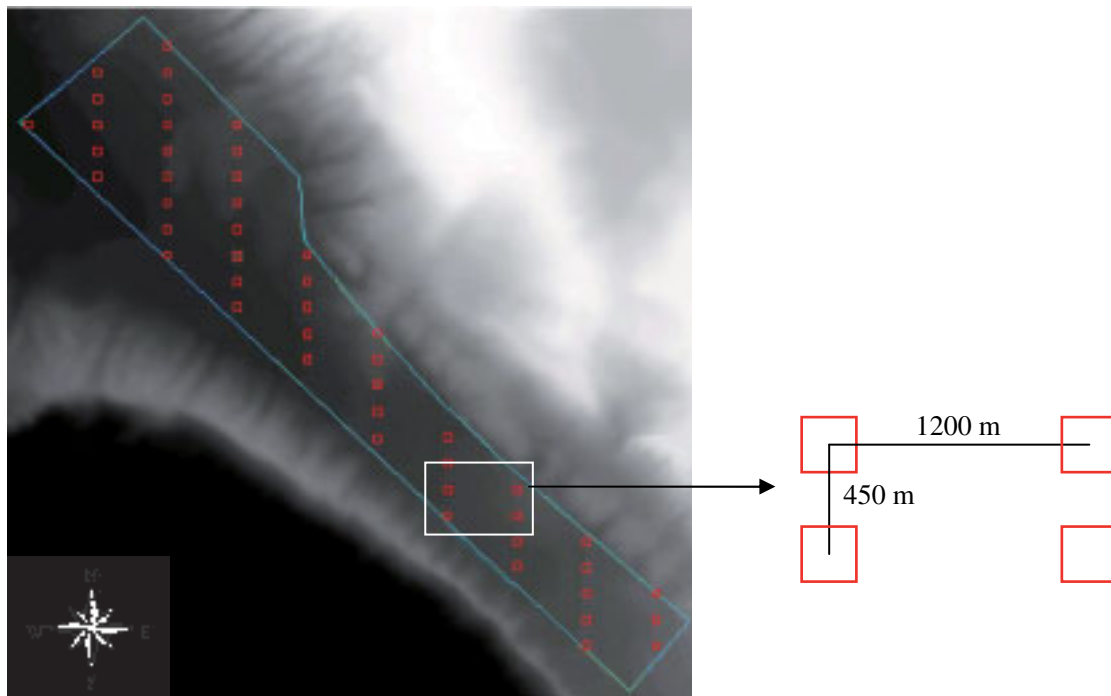


Figure 3.4 Illustration of sample plots on the DEM and plot design used (source: 1:25000 topographic maps, sample plot not to scale).

According to the selected scheme about 2% of the study area was sampled in a rectangular 1200 m by 450 m grid of sampling points with 30 m by 30 m square plots. The position of the first sample was randomly selected and each successive sample was taken at the specified interval thereafter. During the summer 2005 and 2006, 49 plots were measured by the author and a field crew of Fars Natural Resources Head Organization (FNRHO).

3.3.2 Individual tree survey

Successful discrimination of neighboring trees whose crowns are interlaced is a very difficult task both on images and in the field. In the Zagros forests multiple trunk trees and their complex spatial arrangement make this issue more complicated. Moreover the coppice nature of trees blurs the definition of an individual tree crown. A clear definition of individual tree crowns can facilitate and improve the whole process. Hence a tree-element was developed to guide the field crew during field measurements. The tree-element can be defined as a tree with single crown or cluster of trees with intertwined crowns of the same species with height and crown area greater than 5 m and 3 m² respectively see Figure 2.1. The sample plots were overlaid on 1:25000 topographic maps and utilized by the field crews for navigation. The color prints of fused QuickBird imagery (1:500 scale) were utilized as a standard map to identify plots and tree-elements boundaries. The following attributes were recorded for each tree-element within the plot:

- Identification number,
- Position,
- Species,
- Crown area,
- Total height.

Following locating each plot center and finding its boundary in the field the survey team navigated from crown to crown to match each crown in color prints with tree-elements within the plot. Tree-elements were delineated and labeled with the corresponding tree identification number on the color prints. A unique identification number which was

allocated to each tree-element proved useful in ensuring to avoid missing or duplicating tree measurements. Within each plot the coordinate of every tree-element was measured by GPS receiver. In addition for each tree-element the species and the number of stems were recorded. Notes on the nature of the ground vegetation, plowed field and rainfed farming were made.

3.3.3 Crown survey

The necessity to survey tree crowns in the most precise way assumes great importance either in the crown map production or in investigating the crown area-tree height relationship. The main goal of the crown survey was to produce a precise sample-based crown map to evaluate the accuracy of the automatic tree crown delineation results (chapter 4). Moreover, it provides the basis to investigate the relationship between crown area and tree height at stand level. A good GPS receiver is the most proper tool to meet such expectations. In this research the Differential Global Positioning System (DGPS) receiver Leica GS20 has been used for the crown survey. It is a 12-channel L1 code and phase handheld receiver for professional data mapping. With the external antenna it provides the most accurate positions as well as the ability to monitor the quality of coordinates during the collection. The receiver was set to the manufacture recommendations about satellite elevation and Positional Dilution of Precision (PDOP). To survey tree crowns, the approach adapted in this research was walking around or along the crown boundary of every tree-element with the DGPS receiver while looked at the crown perimeter. The crown projection did not use in this study. After delineation, each tree-element received a tree identification number. All boundary trees that occurred at or near the plot boundary were measured. The GS20 receiver accompany with GIS Data PRO office software which enables downloading RTCM corrections through the Internet and offers editing tools and data export functions. GIS Data PRO allows a good integration between GPS and GIS mapping solution (Leica Geosystem). The field measurements were post-processed by incorporating GIS DataPro office software and correction data of the closest GPS reference station (Qatar) which was about 400 km far from the study area. One approach that was not considered for this study is determination

of absolute positional accuracy of DGPS measurements. So it was not feasible to determine the positional accuracy for each crown. However the accuracy of the results was significantly improved after the post processing, in the case of leaning trees, deformed crowns and missing trees it was necessary to perform further edits in the lab. In these conditions what is visible on the image can be accepted as a reference. The positional accuracy of QuickBird standard data was acceptable to be used as the base. To provide the reference for these crowns they were digitized on screen on the QuickBird imagery.

3.3.4 Height survey

Tree height is one of the important tree attributes which can be used to identify site classification (when age is known) and estimating biophysical variables. As tree height survey is a time-consuming and labor intensive process to measure in the field, correlations with other attributes like crown area can help to model this attribute. To investigate the relationship between tree height and crown area, during the field survey, within each plot, the height of every tree or cluster of trees greater than 5 m was measured with a Suunto clinometer (PM-5) and a distance tape.

3.3.5 Geodatabase establishment

During the field crown survey 257 individual or clusters of tree crowns were identified in 49 plots. All these crowns were spatially recorded as polygons in a GIS vector layer. To provide the opportunity of manipulating and retrieving specific information quickly and accurately a geodatabase was created. In this relational database each polygon has a label which shows its plot number and its location in the plot. Other ground based information (e.g. tree height, crown height, and number of stems) were assigned to each polygon as an attribute table. By joining the individual sample plot polygons, the sample-crown map was produced for the whole study area. This map provides an excellent reference for evaluating the accuracy of the automated crown delineation results. Figure 3.5 illustrates one plot of the final sample crown map as measured in the field.

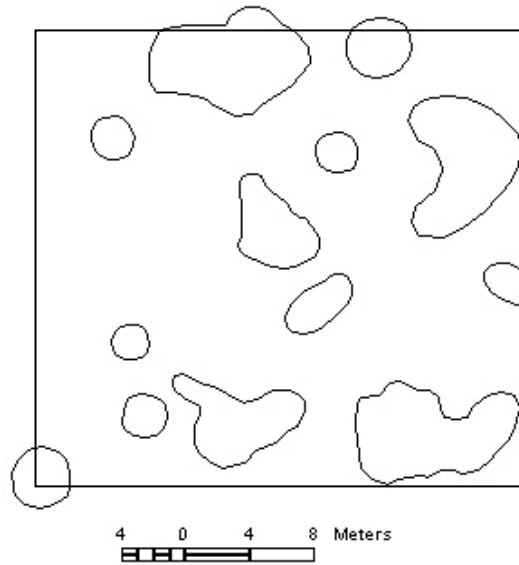


Figure 3.5 One plot of the sample crown map

Systematic Sampling was implemented to reduce the costs of field work as well as investigating larger geographical area. In the case of border trees whose crowns were not fully contained in a plot the following rule was applied, if less than 50% of the crown area was inside the plot, these border trees were excluded from the assessment process. A number of 34 trees were found to be border trees, the remaining 223 trees were the ones fully located in the plot and used for accuracy assessment.

3.4 Regression analysis

Tree height and crown area are important tree characteristics in coppice stands. Field measurement of height is more difficult and time consuming. Depending on the size of the crown and spatial resolution of the images it is feasible to derive crown area by manual or automated methods. Using the crown area-height relationship, height can be modeled from crown area. For investigating the functional relationships among variables regression analysis is a conceptually simple method (Chatterjee and Hadi 2006). In this study regression analysis was applied to determine whether there was a statistical relationship between crown area and tree height. The data of 223 trees measured in all sample plots were included in that analysis. The selection of the regression model was

based on the coefficient of determination of the model (R^2); the analyses were carried out in Microsoft Excel[®] 2002.

3.5 Image processing

3.5.1 Pre-processing

Pre-processing can be considered one of the fundamental steps in most automated tree crown delineation approaches since it prepares images for further processing. In general, pre-processing operations include: co-registration, radiometric and geometric corrections and noise reduction (Chen, 2008). The success of delineation algorithms is heavily dependent on the nature of image pre-processing. In this research pre-processing was carried out including conversion to the top of atmosphere spectral radiance and image co-registration, using ERDAS Imagine[®] software.

3.5.1.1 Conversion to top-of-atmosphere spectral radiance

In order to minimize the influence of atmospheric conditions, the digital numbers (DNs) for each band were converted to Top Of Atmosphere (TOA) radiance. To obtain band-integrated radiance [$W - m^{-2} - Sr^{-1}$] radiometrically corrected pixels of each band were multiplied by an appropriate absolute radiometric calibration factor (K factor) which was derived from the image metadata. To get spectral radiance [$W - m^{-2} - sr^{-1} - \mu m^{-1}$] the results were divided by the proper effective band width (Krause, 2003). In this research, absolute atmospheric correction did not apply since the crown delineation methods rely only on internally consistent differences within a scene (Hill, 1991; Guyot, 1994).

3.5.1.2 Precise image co-registration

Accurate and precise co-registration of multispectral data with panchromatic image is required for the image fusion process. However Pan and MS bands are collected simultaneously, there is a time delay between the collects (~0.2 seconds) depending on the scanning mode of the instrument. Since orbital velocity is equal to 7.5 km/sec, this delay can make 1.5 Km difference between the collects on orbit. Moreover, random spacecraft

motion between collects can also cause miss-registration between Pan and MS bands (Magsud and Samarakoon, 2006). Blurring edges in the fused images may arise from misalignment of features at the same location (Liu, 2000). The co-registration process implemented in this study was based on AutoSync extension of the ERDAS Imagine[®] software Package version 9.2 which allows automatic image rectification. AutoSync utilize Automatic Point Matching (APM) to deliver the coordinates of evenly distributed corresponding points between an input image and a reference image. This process requires that the user identifies initial points in both images. Then Autosync generates more tie points based on these primary points (ERDAS, 2006).

By using the panchromatic band as a reference image, the multispectral data were co-registered using 513 tie points and a second-degree polynomial geometric correction model with the nearest neighbor algorithm. The RMS error was 0.2 pixel.

3.5.2 Image fusion

3.5.2.1 Concept of image fusion

Image fusion is the combination of two or more different images to form a new image by using certain algorithm (Pohl & Van Genderen, 1998). Image fusion can be performed at 1) pixel, 2) feature, and 3) decision level. Pixel level image fusion means fusion at the lowest processing level referring to the merging of measured physical parameters. Pixel based image fusion can be used to increase the spatial resolution of the multispectral image. Various factors should be considered before performing image fusion on a set of images. Co-registration of the multispectral and panchromatic images plays an essential role because mis-registration causes artificial colors or features. Co-registration was performed in the pre-processing step. To avoid from blockiness effects the results were smoothed using a 3 by 3 low pass filter (Chavez *et al.*, 1991). The image fusion methods that are applied for comparison in this research study are Brovey, IHS, Gram-Schmidt, PCA, Ehlers, PC+Wavelet methods, they are described in the following sub chapters.

3.5.2.2 Brovey fusion method

The Brovey transform is based on the mathematical combination of the multispectral images and high resolution Pan image. This method uses addition, division and multiplication for fusion of multispectral bands (Zhang, 2002). Each multispectral image is normalized based on the other spectral bands and multiplied by the Pan image to add the spatial information to the output image. The following equation shows the mathematical algorithm for the Brovey method (Zhang, 2002).

$$F_i = \frac{M_i}{\sum_{j=1}^N M_j + c} \times P \quad (1)$$

where

F_i is a fused band,

M_i is the multispectral band to be fused,

P is the panchromatic band

$\sum M_j$ is the sum of all multispectral bands.

j is the band under consideration

and

N is the number of bands

In some cases there can be an area with zero DN values for the all bands; therefore a constant c has to be added in the denominator to produce meaningful output digital numbers.

The Brovey method provides images with excellent contrast and changes the original scene's radiometry (Švab & Oštir, 2006). This fusion method increases contrast for the 'tails' of the histogram and does not preserve the spectral characteristics of the original images (Fox *et al.*, 2002). These fused images however are not suitable to be used for

pixel-based classifications but are appropriate for visual interpretation with consideration for color distortion.

3.5.2.3 IHS fusion method

The IHS transformation is one of the common techniques used to Pan-sharpen lower resolution multispectral data (Shettigara, 1992; Vrabel, 1996; Laben, 2000). This method is based on color descriptions that are natural and intuitive to humans (Gonzalez *et al.*, 2003). *Intensity* relates to the total brightness of a color, *hue* attribute refers to the dominant wavelength and *saturation* specifies the purity of color relative to gray of light contributing to a color (Lillesand & Kieffer, 1994). In fusion, by using I transformation three bands of MS images from the RGB color space were converted to the I color space. In order to compensate for the spectral differences between the two images the Pan imagery is histogram matched to the “I” component. Then the “I” component of MS imagery is substituted by the histogram matched Pan image. Finally, the RGB of fused images are obtained by reverse transformation of replaced components from the IHS space back to the original RGB space. There are different algorithms for the computation of the IHS components. A common problem of these algorithms is that they are restricted to process only three bands at the same time (Nikolakopoulos, 2004). The basic concept of the IHS fusion is shown in Figure 3.6

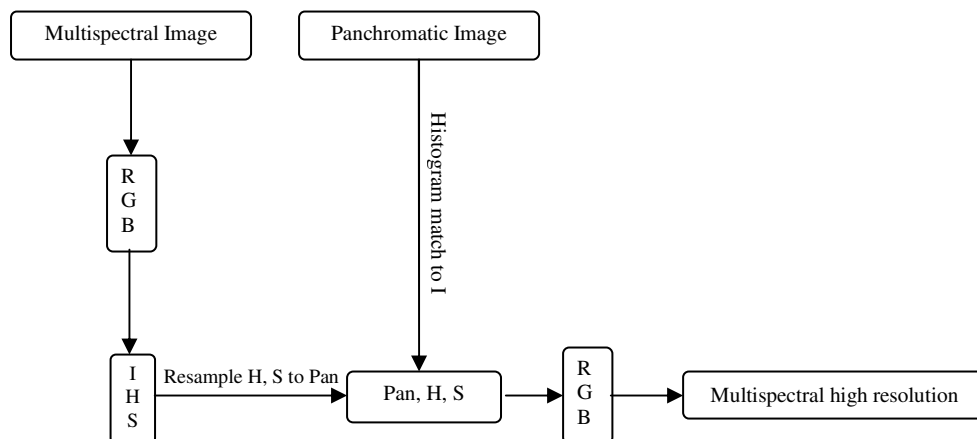


Figure 3.6 Flow chart of the IHS fusion method.

3.5.2.4 PCA fusion method

The PCA transformation is useful for image data compression, image enhancement, multitemporal dimensionality and image fusion (Pohl & Van Genderen, 1998; Zhou, 1998). This multivariate statistical technique converts inter-correlated multispectral bands into a new set of uncorrelated components (PCs) (Zhang, 2004). The first principal component PC1 accounts for maximum variance. The higher resolution image replaces PC1, since it contains the information which is common to all bands while spectral information is unique for each band (Pohl, 1999). The process flow for the PCA image fusion method is shown in Figure 3.7. First the principal components of the multispectral imagery are computed. In order to correct the albedo differences between two images, the histogram of the Pan image is matched with the PC1 image. In the next step the first PC of multispectral imagery is replaced by the histogram matched Pan. Finally, the inverse PCA transform was performed to obtain multispectral high resolution imagery.

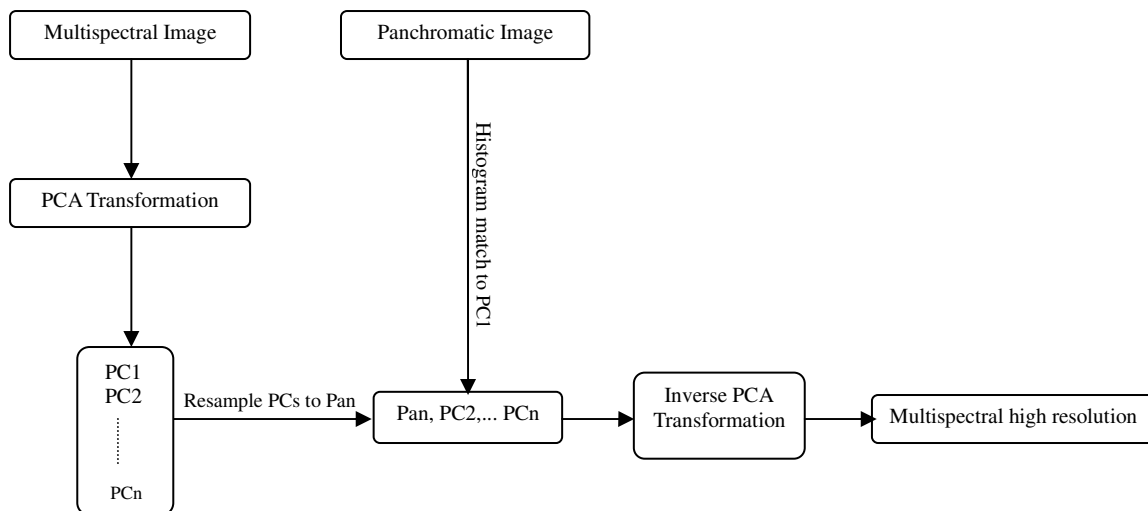


Figure 3.7 Flow chart of the PCA fusion method.

3.5.2.5 Gram-Schmidt fusion method

The Gram-Schmidt transformation is a common method in linear algebra and multivariate analysis (Nussbaum & Menz, 2008). The Gram-Schmidt (GS) fusion technique functions in a similar manner to the PCA method discussed above. However, in this case the first

Gram-Schmidt component is replaced by the Pan image. This fusion method was developed by Laben and Brower in 1998 and patented by Eastman Kodak (Aiazzi *et al.*, 2006). The GS method has been reported as a data fusion method with high fidelity of spectral information (Dou, 2007). The basic concept of GS fusion is shown in Figure 3.8. In this method, first a Lower Spatial Resolution Panchromatic image (LSRP) is simulated and combined with multispectral images (MS). Then, the Gram-Schmidt transform converts (LSRP) and the plurality of lower spatial resolution spectral band images into uncorrelated components. To obtain a Modified High Spatial resolution Pan image (MHSP) the statistics of the Pan image are adjusted to match with the statistics of the first component resulting from the Gram-Schmidt transformation. Then, the first transform component is substituted by (MHSP). Finally an inverse Gram-Schmidt transform is implemented to produce the enhanced spatial resolution multispectral images (Laben, 2000).

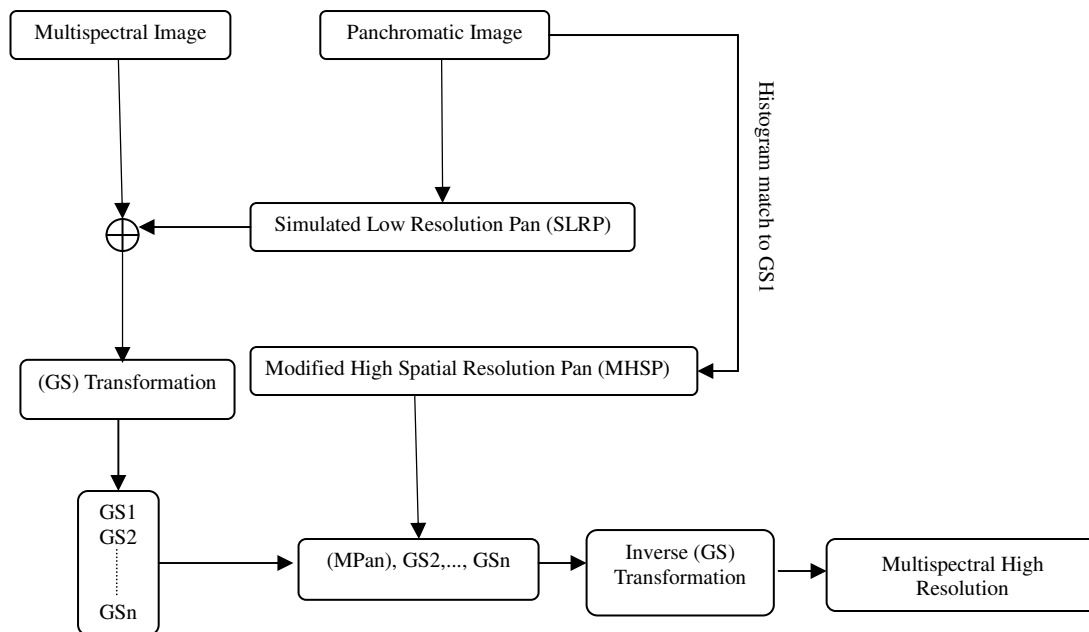


Figure 3.8 Flow chart of the Gram-Schmidt fusion method.

3.5.2.6 Ehlers fusion method

The Ehler Fusion algorithm was developed by Prof. Manfred Ehlers, University of Osnabrück (Erdas, 2008). This method is based on Fast Fourier Transformation (FFT). The idea is to modify the panchromatic image in the way that it becomes more similar to the intensity component. In the first step in order to manipulating IHS components, three low resolution multispectral RGB bands are selected and transformed into the IHS domain. Then, the intensity component I and the panchromatic image Pan are transformed into the spectral domain via a two-dimensional Fast Fourier Transform (FFT). To design the appropriate low pass filter (LP) for the intensity component and high pass filter (HP) for the high resolution panchromatic image the power spectrum of both images is used. Both low-pass and high-pass filters should be complementary. For example the high frequency part removed from the intensity component should be the only part left in the panchromatic image. The idea is to substitute the high frequency part of the intensity component with that from the panchromatic image (Ling *et al.*, 2007). The cut-off frequencies for these filters can be established from the ratio¹⁰ of pixel sizes between the high and low resolution images. Because it involves only multiplications, filtering will be directly performed in the frequency domain. To return both components back into the spatial domain an inverse FFT transform was used. Then the high pass filtered panchromatic band (Pan^{HP-1}) and low pass filtered intensity (I^{LP-1}) are added and matched to the original intensity histogram (Ehlers, 2005; Ehlers *et al.*, 2006). Finally, as can be seen in Figure 3.9 an inverse I transform converts the fused image back into the (RGB) domain to obtain high resolution multispectral image.

¹⁰ The ratios between panchromatic and multispectral imaging modes of one sensor vary between 1:2 and 1:5. For multisensor fusion, ratios can exceed 1:20 (e.g. Ikonos and SPOT merge) (Ehlers *et al.*, 2006).

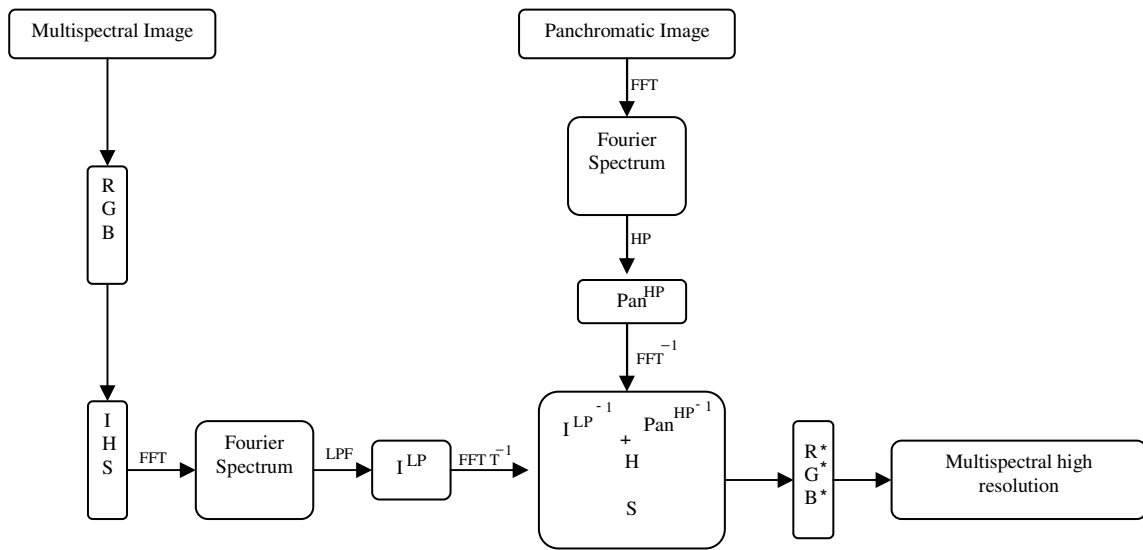


Figure 3.9 Flow chart of the Ehlers fusion method

3.5.2.7 PC + Wavelet fusion method

The wavelet transform is a mathematical tool developed in the field of signal processing (Zhang, 2002). There are two possibilities to combine Pan and MS images in the wavelet domain: substitution and addition. In the substitution method, both the Pan and MS images are decomposed and some wavelet coefficients of the MS image are substituted by the corresponding coefficients of Pan. In the addition method only the Pan image is decomposed and its coefficients are directly added to the MS image (Acerbi-Junior *et al.*, 2006). Since the Pan image is a single band the substitution image, from the multispectral image, must also be a single band. In this regards, I or PCA transform are appropriate tools to compress the multispectral image into a single band. The PCA transform plus the wavelet addition method was applied in this research. As the process flow diagram shows (Figure 3.10), in the addition method, first the principal components of the multispectral image are computed and the panchromatic image is histogram matched with PC1.

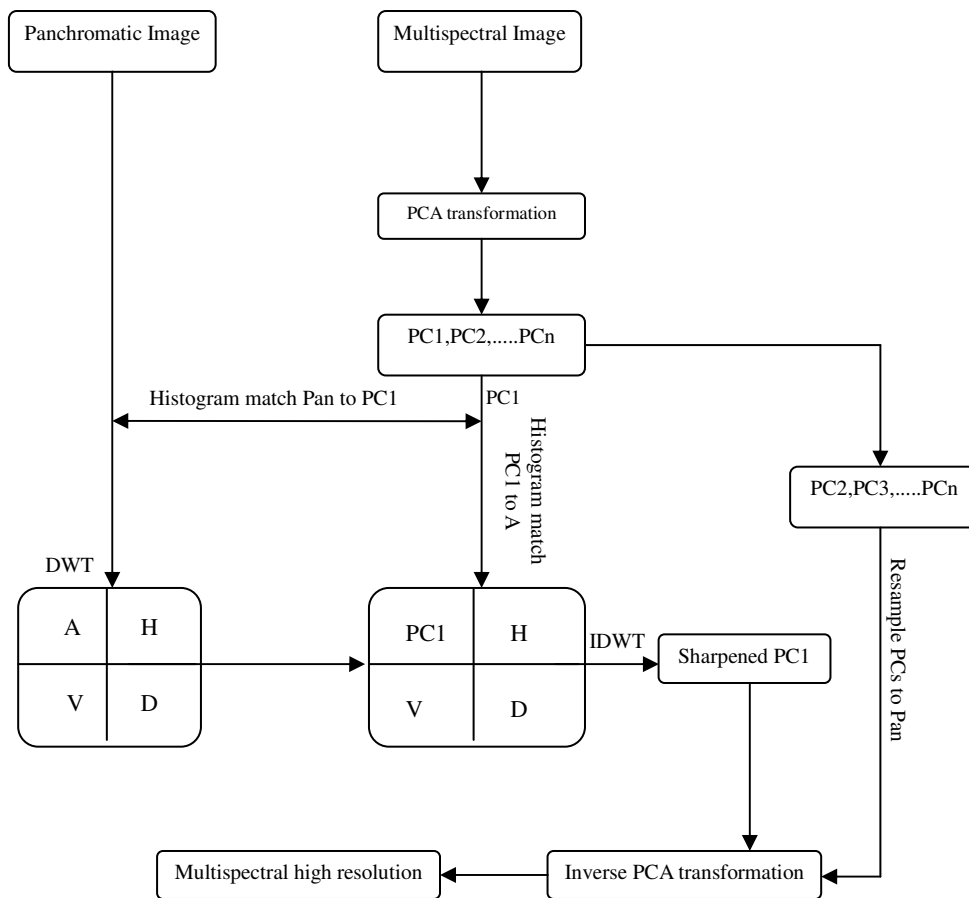


Figure 3.10 Flow chart of the PC +Wavelet fusion method.

Then the histogram matched Pan image is decomposed by the Discrete Wavelet Transform (DWT) decomposition process. By a combination of low and high pass filters vertical, horizontal and diagonal details are extracted which are denoted by V, H and D respectively. The approximation A is result of low pass filtering in vertical and horizontal direction. The PC1 replace the approximation of the Pan image in the wavelet domain and the high frequency components of Pan are introduced to the PC1 component. To obtain new sharpened PC1 the Inverse Discrete Wavelet Transform (IDWT) is done. Other PCs are resampled to the same spatial resolution of Pan. The inverse PCA transform is performed to obtain a multispectral high resolution image (ERDAS, 2005).

3.5.3 Image fusion quality assessment

3.5.3.1 Protocol for quality assessment

A number of pixel-based image fusion techniques have been developed to combine the spatial and spectral characteristics of Pan and MS images. The merit of these techniques for certain application depends on the quality of the results. A suitable fusion method has to be chosen with respect to the used spectral characteristic of the multispectral bands and high frequency information of the Pan image. Hence, it is desirable to quantitatively measure the spectral and spatial quality of the merged images. Quantitative quality assessment is a complicated task as the images to be compared are at different spatial and spectral resolutions. Great deals of efforts have been made to build a standard protocol for quality assessment. The main challenge of such protocols is how to establish and define a reference image.

Wald *et al.* (1997) proposed a standard protocol which provides a normative framework for assessing the quality of synthetic images. It is simple to implement and permits to alleviate the need for a reference image if that is not available.

According to the protocol described by Wald *et al.* (1997), a fused image must have the following three characteristics to assess the quality:

1. Any synthetic image once degraded to its original resolution, should be as identical as possible to the original image.
2. Any synthetic image should be as identical as possible to the image that the corresponding sensor would observe with the same highest resolution.
3. The multispectral set of synthetic images should be as identical as possible to the multispectral set of images that the corresponding sensor would observe with highest resolution.

These three properties were summed up to form consistency and synthesis properties. Consistency is corresponding to the first property and the synthesis aggregate the second and third properties. Wald (1997) proposed an image degradation procedure to build up reference images. The fundamental premise of his theory is that fusion performances are

not affected by variant image scales. This assumption may be reasonable in general, but may not hold for very high resolution data. The quality at higher resolution can be better or worse depending on the image high frequencies and the introduced spatial degradation procedure (Alparone *et al.*, 2006).

The consistency property was assessed by down sampling the fused images at the higher spatial resolution to their original spatial resolution, so that the reference image is the original MS bands. To evaluate synthesis properties of fused images, original data sets were down sampled to their lower resolution. In order to get fused images at low spatial resolution, fusion is performed on these two new sets and the results were evaluated by comparing with original MS and Pan images. It is expected that this consistency property provides reliable results as compared to the synthesis approach.

3.5.3.2 Quality metrics

The ultimate goal of image fusion is to obtain images of enhanced quality. It is very difficult to provide a precise definition of the term “quality” because it depends upon the application of fused datasets. For example, a better quality may be an increase in accuracy of a geophysical parameter or of a classification (Wald, 1999). In this study what actually referred to was both spatial and spectral *image fidelity*. It was assumed that a reference image was available and the quality of fused images was assessed by how close they were to the reference image. Image quality can be assessed by subjective and objective quality metrics. In subjective quality assessment the intended users evaluate fused images by performing specific visually oriented tasks. Subjective assessments are usually time consuming and expensive. Objective quality metrics on the other hand try to quantify the differences and similarities between images by exploiting the pixel values. Objective metrics are easy to calculate and independent of viewing conditions as well as individual observers (Wang, 2002). The following subsections describe objective and subjective quality metrics that are applied to evaluate the quality of fused images.

There are basically two classes of objective quality or distortion assessment approaches. The mathematically defined measures and the measures based on Human Visual System (HVS) characteristics (Wang, 2002). Various criteria and mathematical metrics regarding

the spectral fidelity aspect of image quality are proposed (Dixon *et al.*, 2006). Bias, Correlation Coefficient, Difference in Variance, Standard Deviation of the Difference, RASE and ERGAS are the criteria that applied in this study to check synthesis properties of fused images. Let M_k be the mean value for the original spectral image B_k . Subscript k denotes the band under consideration. B_{kl}^* Is the fused band created at lower resolution “ l ”. Superscript $*$ denotes the fused band. $(B_{kh}^*)_l$ is the fused band at higher resolution “ h ” which degraded to the lower resolution “ l ”.

For evaluating the synthesis property the symbol B_{kl}^* is used in the following equations.

Bias

Bias is the difference between the means of the original multispectral and the fused image. Ideally, the bias should be zero. The value is calculated relative to the mean value of the original image (Wald, 2002) by

$$Bias = \frac{M_{kl} - M_{kl}^*}{M_{kl}} \quad (2)$$

Difference In Variances (DIV)

The DIV can be defined as the difference between the variances of the original image and of the fused one. This difference expresses the quantity of information added or lost during fusion. A positive value indicates a loss of information and a negative value shows some added information. Its value is given relative to the variance of the original image. The ideal value is zero (Wald, 2002):

$$DIV = \frac{\delta_{kl}^2 - \delta_{kl}^{*2}}{\delta_{kl}^2} \quad (3)$$

where:

δ_{kl}^2 is the variance of the original band and

δ_{kl}^{*2} is the variance of the fused band.

Correlation Coefficient (CC)

The correlation coefficient measures similarity in small size structures between the original and the fused images. The higher the correlation between the original and fused images, the better the estimation of the spectral values. The range of possible values is from -1 to +1. Values close to +1 indicate that they are highly similar while a value close to -1 indicate that they are highly dissimilar (Wald, 2002). The correlation between two images A and B is computed from

$$corr(A|B) = \frac{\sum_{i=1}^N \sum_{j=1}^N (A_{i,j} - \bar{A})(B_{i,j} - \bar{B})}{\sqrt{\sum_{i=1}^N \sum_{j=1}^N (A_{i,j} - \bar{A})^2 \sum_{i=1}^N \sum_{j=1}^N (B_{i,j} - \bar{B})^2}} \quad (4)$$

where

A and B are two images,

$A_{i,j}$ is the element of original multispectral image,

$B_{i,j}$ is the element of fused image,

\bar{A} is the mean value of A and

\bar{B} is the mean value of B .

Standard Deviation of the Difference image (SDD)

The standard deviation of the difference image (SDD), as well as its value relative to the mean of the original image globally indicates the level of error at any pixel. Ideally, it should be zero (Wald, 2002), it obtains from:

$$SDD = \frac{\text{standard deviation } (M_{kl} - M_{kl}^*)}{M_{kl}} \quad (5)$$

RASE

Is the Relative Average Spectral Error (RASE) and characterizes the average performance of a method in the considered spectral bands. RASE is independent of units, the number of spectral bands, and accordingly of calibration coefficient and instrument gains. The value is expressed in percent (Wald, 2002) by

$$RASE = \frac{100}{M} \sqrt{\frac{1}{N} \sum_{k=1}^N RMSE(B_k)^2} \quad (6)$$

where

M is the mean radiance of the N spectral bands (B_k) of the original MS bands.

RMSE can be derived from:

$$RMSE(B_k) = \sqrt{(Bias)^2 + (Standard\ Deviation)^2} \quad (7)$$

ERGAS

ERGAS is from the French acronym “erreur relative globale adimensionnelle de synthèse” (dimensionless global relative error of synthesis) proposed by Wald (2002). ERGAS equals to the spectral RMSE divided by the mean radiance of each band. This quantity is independent of the number of spectral bands and offers a global view of the quality of fused images.

It is given by:

$$ERGAS = 100 \frac{h}{l} \sqrt{\frac{1}{N} \sum_{k=1}^N \left[\frac{RMSE(B_k)^2}{(M_k)^2} \right]} \quad (8)$$

where:

N is the number of bands,

h/l is the ratio of the spatial resolution of original higher resolution Pan and lower resolution MS images.

Visual metrics

The visual quality metrics are related closely to the characteristics of human perception. Visual quality assessment is the most direct and reliable method to evaluate spectral preservation and spatial details of fused images separately. However the human visual system is not equally sensitive to various types of distortion in an image so the individual opinions vary considerably (Wald, 1997). This type of evaluation requires a display supply, sophisticated panel of investigators and post processing steps that make the whole process expensive in terms of efforts, time and required equipments (Petrović *et al.*, 2004).

3.5.3.3 Visual quality assessment

Visual inspection has been done through different color composites by a panel of evaluators. The evaluators on the panel were specialists with a very good background in remote sensing. A set of criteria and specifications were established regarding the spatial and spectral fidelity of objects with different shape and size. A mosaic of the all synthesized images was produced to guarantee that the same Look-up tables (LUTs) are applied to all images. This permits a comparison between any synthesized image and the original one. Then, to check the first property, images $(B_{kh}^*)_l$ compared to the corresponding original images B_{kl} . For testing the second property the relevant images were B_{kl}^* and B_{kl} . Finally, a comparison is made between the original set B and all the sets B^* synthesized by each method. The evaluators assessed fused images with respect to the original images and assigned a score to each one. The results were grouped into five categories ranging from no spectral changes visible (1) to the complete spectral changes (5). To obtain the overall quality mean scores are derived for individual methods. The PCA spectral transform, the Ehlers fusion method, the Brovey transform and the Wavelet transform all implemented in ERDAS Imagine[®] software Package, version 9.2, the Gram-Schmidt spectral sharpening method and the IHS spectral transform implemented in ENVI[®] software package, version 4.2.

3.5.4 Image segmentation

3.5.4.1 Definition of image segmentation

Very High Spatial Resolution (VHR) imagery introduces a higher spectral variability within the homogeneous units which increases with reducing the spatial resolution. These spectral variations make traditional per-pixel supervised and unsupervised classifiers ineffective and useless. Image segmentation as an alternative approach has been proposed to automatically and efficiently extract the required information from the enormous quantity of data provided by these high-resolution remote sensing systems. Image segmentation is the process of partitioning a digital image in discrete, non-overlapping regions on the basis of internal homogeneity criteria (Devereux *et al.*, 2004). This can be homogeneity of any type, such as intensity, color, texture or higher level objects (De Bock & Philips, 2007). Image segmentation can also be viewed as the process of identifying edges that correspond to boundaries between the objects, as well as regions that correspond to surfaces of desired objects in the image (Shell & Hall, 2000).

Soille (2003) argued that image segmentation is a key step towards the quantitative interpretation of image data. Once an image has been segmented, further measurements on each region and adjacency relations between regions can be obtained. Although it is still very difficult to achieve an accurate segmentation process, all subsequent image interpretation tasks including feature extraction and object recognition, rely heavily on the quality of segmentation results (Peng & Bhanu, 1999).

3.5.4.2 Image segmentation techniques

Automatic image segmentation is one of the most challenging issues in the field of image processing. Until now considerable works have been done on the segmentation of intensity images, and a wide variety of techniques for image segmentation has been developed. These segmentation techniques can be roughly categorized into three classes:

- 1) Characteristic feature thresholding or clustering,
- 2) Edge detection,
- 3) Region extraction.

These techniques are either based on the concepts of similarity (i.e. region growing) or discontinuity (i.e. edge detectors) of pixel values (Fu and Mui, 1981; Gonzalez and Woods, 2002; Pal and Pal, 1993).

Each of these techniques has its own advantages and disadvantages in terms of accuracy, speed and complexity. None of single segmentation techniques alone work best even over one image. Consequently, different segmentation techniques are manually combined.

In this research in order to determine the best segmentation strategy for identifying and delineating individual tree crowns, knowledge based morphological Watershed segmentation and Laplacian of Gaussian (LoG) edge detector were adapted and compared.

3.5.4.2.1 Thresholding segmentation

Thresholding is one of the most commonly used techniques for image segmentation. This technique transforms grayscale images to binary images in such a way that the foreground of an image discriminates from its background. Many thresholding methods have been developed so far, which can be roughly categorized as either global or local. In global thresholding, a single threshold value applies for the entire image using the gray scale histogram. Global thresholding is simple, easy to implement and sufficient in many cases. However, when the image has an uneven background with different intensity values, global thresholding can not be adapted to these local variations. To overcome this limitation local thresholding must be applied. Local thresholding methods utilize local information such as maximum and minimum intensities, mean and standard deviation and intensity histogram of pixels in rectangular windows to select a threshold value for each pixel (Solihin & Leedham 2002).

For both of them it is desirable to determine the optimal threshold values automatically. Otsu *et al.* (1997) developed a global thresholding algorithm based on histogram information derived from source image. Otsu's method calculates an optimal threshold value that maximizes the between-class variances of the histogram or minimizes the within-class variance (Ritter *et al.*, 2001). Detailed information regarding Otsu's method can be found in Otsu *et al.* (1997).

3.5.4.2.2 Edge based segmentation methods

Edge detection is an image segmentation technique based on the detection of discontinuity of spatially adjacent pixel feature values. An edge can be defined as a place where abrupt (local) changes in intensity values occur (Bhanu and Lee, 1994). Frequently, edges are associated with the boundaries of desired objects. But in some cases, edges do not correspond to any object outlines (e.g., shadows and noise), or in other cases objects outlines can not be identified as edges, for example because of low intensity differences between neighboring objects (Bräunl *et al.*, 2001). Based on the intensity profile, edges can be classified into three types 1) step edge, 2) rump edge and 3) roof edge. More information about the edge types and their characteristics can be found in Gonzalez & Woods (2007). In this research, the term edge encompasses all mentioned types of edges. In order to determine edge locations accurately and to provide reliable edge maps, a variety of edge detectors have been reported in the literature which can be roughly categorized as 1) gradient, 2) Laplacian, 3) probabilistic and 4) wavelet methods (Horney *et al.*, 2003). The most common edge detectors are gradient-based and Laplacian-based which were applied in this research and are described in more details in the following sections.

The gradient-based edge detectors such as Sobel, Roberts Cross and Prewitt apply the first-order differentiation and highlight the edge location by looking for the maximum and minimum in the gradient of the image.

For a 2-D function, $f(x, y)$ the gradient magnitude and direction can be defined as follows (after Gonzalez *et al.*, 2003):

$$\nabla f = \begin{bmatrix} G_x \\ G_y \end{bmatrix} = \begin{bmatrix} \frac{\partial f}{\partial x} \\ \frac{\partial f}{\partial y} \end{bmatrix} \quad (9)$$

The magnitude of this vector is

$$\nabla f = \left[(\partial f / \partial x)^2 + (\partial f / \partial y)^2 \right]^{1/2} \quad (10)$$

To simplify computation, this quantity can be approximated by omitting the square-root,

$$\nabla f \approx G^2 x + G^2 y \quad (11)$$

A commonly used approximation to the above expression uses the absolute value of the gradients G_x and G_y .

$$\nabla f \approx |G_x| + |G_y| \quad (12)$$

Its direction is calculated as follows:

$$\alpha(x, y) = \tan^{-1} \left(\frac{G_x}{G_y} \right) \quad (13)$$

Each first derivative edge detectors convolve the image with two convolution kernels to extract horizontal and vertical edges. For example, Sobel masks are shown in Figure 3.11.

Convolving the input image by both Sobel kernels will produce two images, each containing only vertical or horizontal edge responses. Diagonal responses appear in both images, but weaker than vertical or horizontal responses. The gradient image ∇f will be formed by combining these two images using one of the aforementioned formulas.

-1	-2	-1
0	0	0
1	2	1

-1	0	1
-2	0	2
-1	0	1

Figure 3.11 Sobel edge detector masks.

Finally, edge detection is accomplished by extending the one-dimension thresholding scheme to two dimensions based on the following formula (after Qureshi, 2005):

$$\left(|G_x| + |G_y| \right) > T \quad \text{or} \quad \sqrt{G^2 x + G^2 y} > T \quad (14)$$

Although, the first derivatives can be used for detecting abrupt changes in intensity, they are directional operators while the Laplacian operator is isotropic and responds equally to changes in intensity in any direction (Gonzalez & Woods, 2007). The Laplacian-based edge detector has the nice property that it produces edges of zero thickness, making edge-thinning steps unnecessary (Bovik, 2005). The major disadvantage of the Laplacian operator for edge detection is the extreme sensitivity to noise (Jähne, 2005).

The Laplacian of a 2-D function $f(x, y)$ is formed from second-order derivatives, as follows (after Gonzalez *et al.*, 2003):

$$\nabla^2 f(x, y) = \frac{\partial^2 f(x, y)}{\partial x^2} + \frac{\partial^2 f(x, y)}{\partial y^2} \quad (15)$$

Typical Laplacian masks are shown in Figure 3.12

.0	-1	0
-1	4	-1
0	-1	0

-1	-1	-1
-1	8	-1
-1	-1	-1

Figure 3.12 Laplacian edge detector masks.

To improve the Laplacian operator Marr and Hilderth (1980) introduced an approach based on first smoothing the image with Gaussian operator and applying the Laplacian subsequently (Banerjee & Zetu, 2001).

The Gaussian of a 2-D function $f(x, y)$ is as follow:

$$h(r) = -e^{-\frac{r^2}{2\sigma^2}} \quad (16)$$

where $r^2 = x^2 + y^2$ and σ is standard deviation.

The Gaussian kernel acts as a low pass filter eliminating the high frequency noises and blur the image. The value of σ will determine the degree of blurring. The Gaussian filter will preserve edges much better than the basic mean filter. Nevertheless, there are undesirable effects i.e., loss of information and displacement of prominent structures in the image plane (Wei-qi & Desheng, 2006).

The Laplacian of this function (the second derivative with respect to r) is

$$\nabla^2 h(r) = -\left[\frac{r^2 - \sigma^2}{\sigma^4} \right] e^{-\frac{r^2}{2\sigma^2}} \quad (17)$$

This function is also called the Laplacian of Gaussian (LoG). The three-dimensional plot of the LoG function has a shape like *Mexican hat* as shown in Figure 3.13 (a) and the two-dimensional cross section of the zero-crossing of the Mexican hat is shown in Figure 3.14(b).

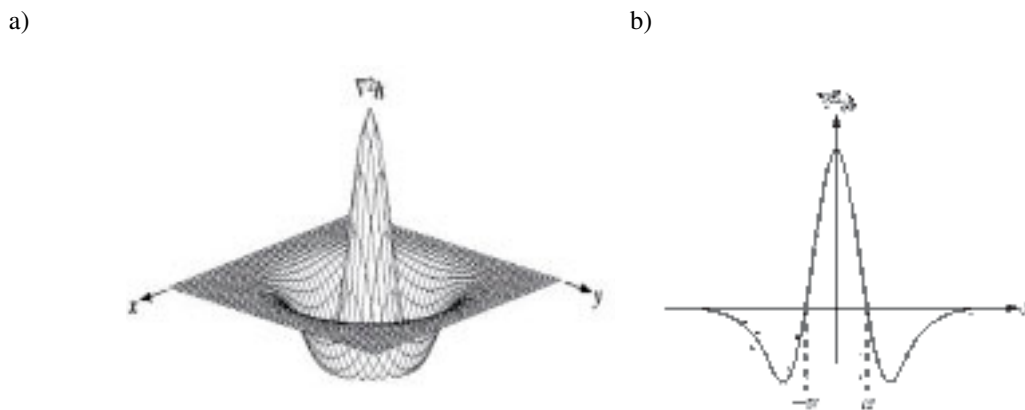


Figure 3.13 (a) 3D plot of LoG function, (b) cross section showing zero crossing (from Acharya and Ray, 2005)

By convolving an image with the LoG operator, a double-edge image will be produced. Edges can be located as the place of the points where the second derivative crosses zero between the double edges.

The main steps of the LoG operator can be summarized as follows:

- (i) Convolve the input image with a $n \times n$ Gaussian low pass kernel;

- (ii) Compute the Laplacian of the resulting image from step 1;
- (iii) Find the zero crossings of the image from step 2

3.5.4.2.3 Watershed segmentation method

The Watershed transformation is a very powerful morphological segmentation tool that incorporates the advantages of region growing and edge detection methods (Soille, 2003). Watershed extraction generally means the thinning of the gradient image with a homotopic transformation (Pesaresi, 2001).

The intuitive concept of watersheds comes from geography, where the grey scale image is considered as a topographic surface and the grey-tone of each pixel stand for its altitude. Based on this analogy, a catchment basin is corresponding to an area of the image with an associated regional minimum intensity. The watersheds are the zones dividing adjacent catchment basins and are represented by pixels having the highest gradient magnitude intensities. The concept of watersheds and catchment basins are illustrated in Figure 3.14.

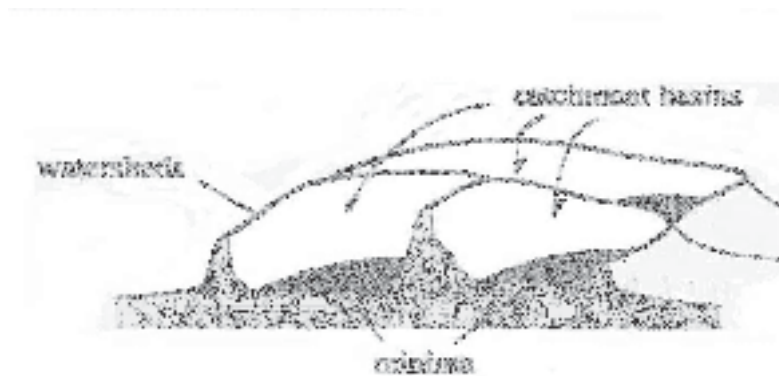


Figure 3.14 Topographic representation of a gray scale image (from Soille, 2003).

Numerous algorithms have been developed to compute a Watershed transformation. Most of them fall into two basic classes. The first class contains the immersion based Watershed algorithms. The immersion algorithm (named VS algorithm) was proposed by Vincent and Soille (1990) and basically involves simulating the immersion process of the surface (Sun *et al.*, 2005). Firstly, the metaphorical landscape is punctured at its local minima and

plunge into in a lake with constant vertical velocity. Then, the water will begin to flow through the holes, starting from the minima at the lowest altitude and gradually reach those with a greater altitude. Dams are built at the places where the water coming from the flooding of two or more different minima would meet to avoid merging of catchment basins. This concept is depicted in Figure 3.15. Finally, each minimum is surrounded by dams delineating its associated catchment basin (Soille, 2003; Osma-Ruiz *et al.*, 2007). Of all Watershed algorithms, this immersion technique was shown to be the most efficient one in terms of edge detection accuracy and processing time. Furthermore, it turns out to be very flexible, since it can be easily adapted to any kind of digital grid and extended to n-dimensional images and graphs (Vincet & Soille, 1991).

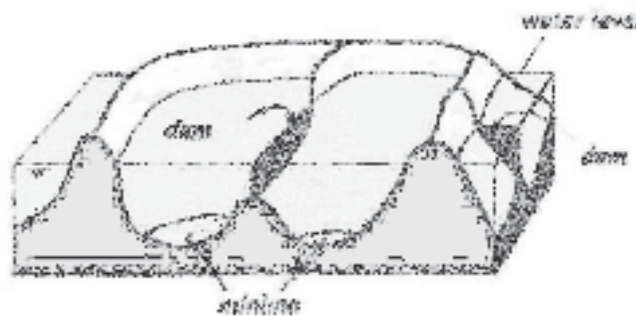


Figure 3.15 Illustration of the flooding of the relief and dam building (from Soille, 2003).

The immersion algorithm imposes a discrete set of seed points on the image and then extends each catchment basin from the seeds by iteratively adding the closest connected component regions of the next highest gray level. Any pixels that are equidistant from two catchment basins are labeled as watershed lines (Cates *et al.*, 2005).

The second class of Watershed algorithms (BM algorithm) was proposed by Bieniek and Moga (2000). This algorithm simulates the rain over the surface. The drops that fall on a point of the image surface will flow a downward path of the steepest slope until it reaches the minimum of the surface. This point is tagged as belonging to the receiving basin associated with this minimum. Figure 3.16 presents the rain-falling concept. By repeating this process for all points in the surface, every point will be assigned to a minimum and

the surface will be divided into catchment basins (Osma-Ruiz *et al.*, 2007, Sun *et al.*, 2005).

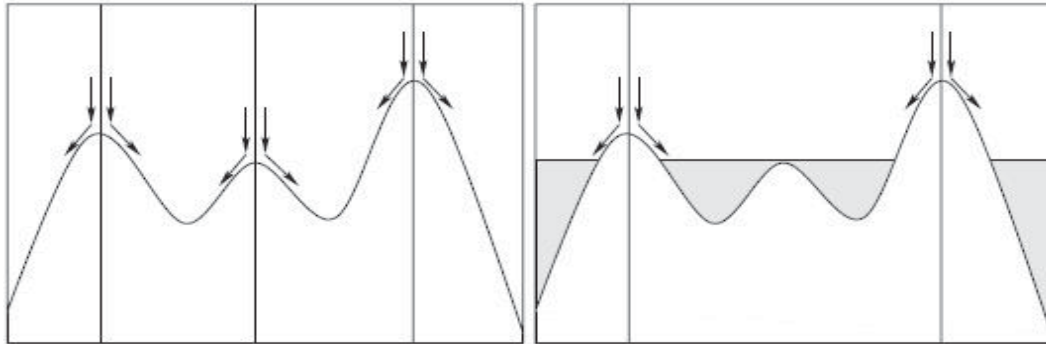


Figure 3.16 Illustration of (rain-falling) process of Watershed transform (after De Bock & Philips, 2007).

The Watershed transformation has proved to be an effective technique for image segmentation, but the sensitivity to noise and over segmentation are the two main drawbacks which may be difficult to overcome (Pesaresi, 2001; Lefèvre, 2007). To alleviate these problems, it is possible to involve prior knowledge in the Watershed transform. This knowledge comprises the number and positions of desired regions by determining some markers. Detailed explanation on the Marker-controlled segmentation, which was proposed by Beucher and Lantuejoul (1979), is introduced in the following sub section. This approach is also adapted and applied in this study.

Marker-controlled Watershed

The main idea behind the Marker-Controlled Segmentation (MCS) is to combine the concept of Watershed segmentation with morphological transformation in order to integrate a high level knowledge about the image contents into the segmentation process. This knowledge often consists in the number and the positions of the desired objects. The advantage is that the segmentation occurs only around the user defined markers (Soille, 1999, 2003; Lefèvre, 2007). Markers are used to reduce the number of the local minima of the image. It is desirable to have a unique marker per region. The size of the markers

can be varied depending on the image quality and can range from one pixel for high quality images to a large connected component of pixels for noisy images. Markers are either manually obtained from the input image or by means of the appropriate feature detectors, which rely on a priori knowledge about the characteristics of the image objects. As the process flow diagram shows (Figure 3.17) the image, which indicates the locations of the markers, is called the “*marker function*”. A model for the definition of the object boundary can be applied to determine the object boundaries. The transformed image, which highlights the object boundaries, is called “*segmentation function*”. Direct computation of the watersheds of *segmentation function* provides a large number of small catchment basins that are not actually associated with meaningful regions.

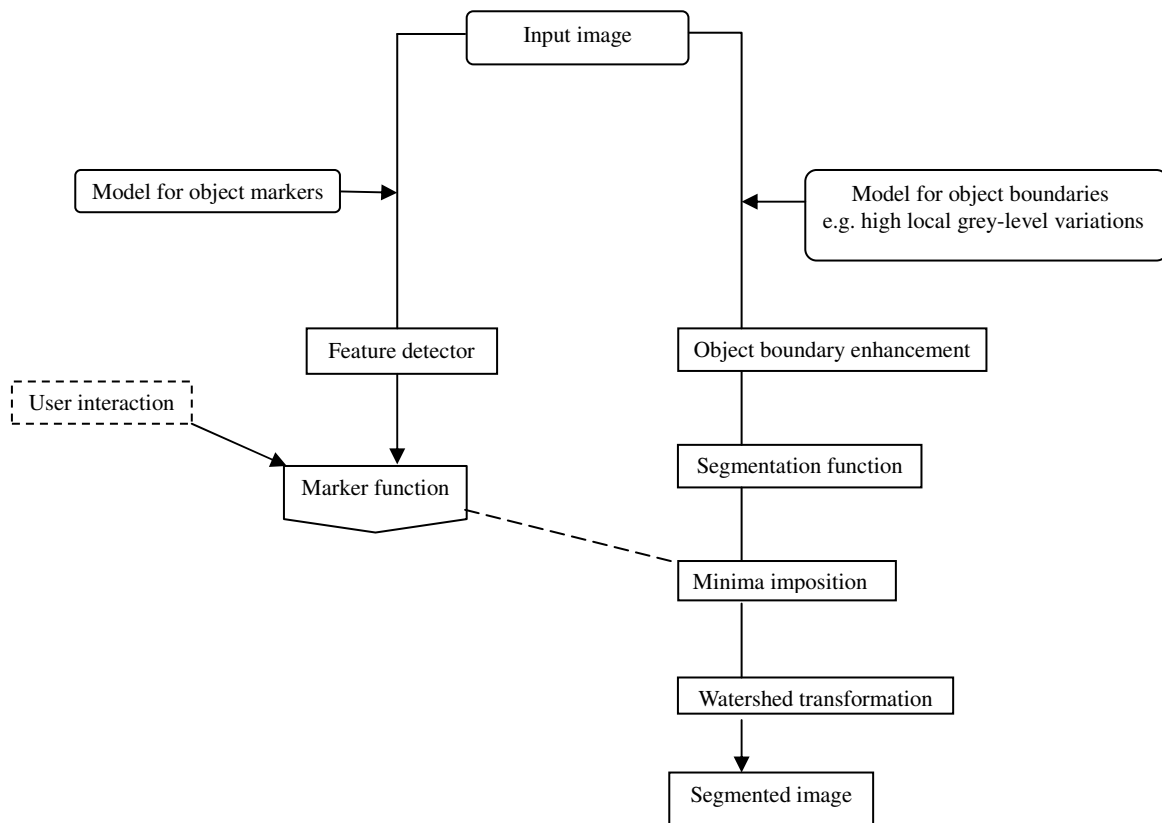


Figure 3.17 Morphological paradigm for image segmentation (after Soille, 2003).

Hence, to remove all irrelevant minima, the segmentation function must be filtered using an appropriate filtering technique (i.e. minima imposition) and *marker function*. Finally,

by computing the watershed of the filtered *segmentation function*, the object boundaries can be obtained (Soille, 2003). The main steps of the MCS procedure can be summarized as:

- (i) Enhance the intensity variations in the input image using an edge detector.
- (ii) Obtain a relevant marker set.
- (iii) Delineate the Watersheds from the combination of markers and edges.

3.5.5 Automated tree crown delineation

3.5.5.1 Initial image preparation

The best spectral band and enhancement operations should be selected to maximize crown discrimination from background and optimize algorithms fulfillment. Since most of the segmentation techniques were defined for gray level images, in the present study the Principal Component Analysis (PCA) was applied on the multispectral fused images to obtain an appropriate single band image. The Principal Component Analysis partitions the total variance of the image data set in the way that the first component accounts for the maximum variance of the linear combination of spectral bands (Mather, 2004). Therefore the first principal component, which contains the most spatial and spectral information was selected as initial image for the further processing steps. Following the selection of the initial image, a crown mask must be produced to remove undesirable backgrounds. Background is the main challenge of tree crown segmentation in the disperse forests. In this type of forests bare soils, rain-fed fields, ploughed soils, riverbeds, manmade structures (such as roads, buildings with a diverse intensity levels) comprise the heterogeneous canopy background. Finding a proper threshold value is a difficult task, because some features (e.g. ploughed soils and rain-fed fields) have either a same rough texture or a similar intensity value to the tree crowns. On the other hand, features like roads and riverbeds show a large difference in gray tones compared to the tree crowns. Moreover, because of the large distances between trees, the presence of discrete and narrow crown shadows make obstacle for successful crown delineation. Therefore these shadows must be eliminated from the image in such a way that spectral and spatial fidelity

of the crowns were preserved. In this complex situation, simple thresholding or contrast enhancements cannot properly remove the undesirable backgrounds and might lead to losing some useful information.

3.5.5.2 Mask generation

The tree delineation algorithms can easily misinterpret minor inhomogeneity within a background texture as tree crowns. To avoid such artifacts which usually need to be remedied by human intervention, it is necessary to make a mask image. Multispectral images provide an opportunity to develop various vegetation indices. The Normalized Difference Vegetation Index (NDVI) is one of the most widely used vegetation indexes and its correlation with certain biophysical properties of the vegetation canopy, such as leaf area index (LAI), fractional vegetation cover, vegetation condition, and biomass has been well demonstrated in many approaches (Jiang *et al.*, 2006) in many applications. In order to cope with the mentioned problems in this research, an NDVI mask image was applied. Fortunately there was no visible green vegetation in the background and the NDVI helped to remove non-tree areas (buildings, roads, shadows) while preserving spectral and spatial fidelity of vegetation information for further segmentation process.

3.5.5.3 Tree crown delineation using the LoG edge detector

As discussed in the previous section, eliminating the background provided a high contrast image with a bimodal histogram which facilitates determination of the threshold value. The threshold value T was automatically determined using Otsu's method. This algorithm was implemented in the MATLAB image processing toolbox. All the pixels with a gray value greater than T were identified as tree crowns and those below formed the background. The result was obtained as a binary image. Prior to gradient extraction, the threshold image was filtered with a 3×3 median kernel. The median filter was applied because it preserves the edges reasonably well while it tends to remove the noise from the image (Florencio, 1994). The smoothed image was convolved with the Laplacian of Gaussian filter (3×3 pixel size) to extract significant edges using the MATLAB image processing toolbox.

3.5.5.4 Tree crown delineation using marker-controlled Watershed segmentation

The Sobel operator was selected as an edge detector to obtain a 2-D spatial gradient magnitude. The Sobel operator was applied to the masked image as input to produce the *segmentation function* image. Edge pixels defined by the Sobel edge detector formed closed contours around each tree crown. Figure 3.18 shows the results of the Sobel edge detector using an image subset.

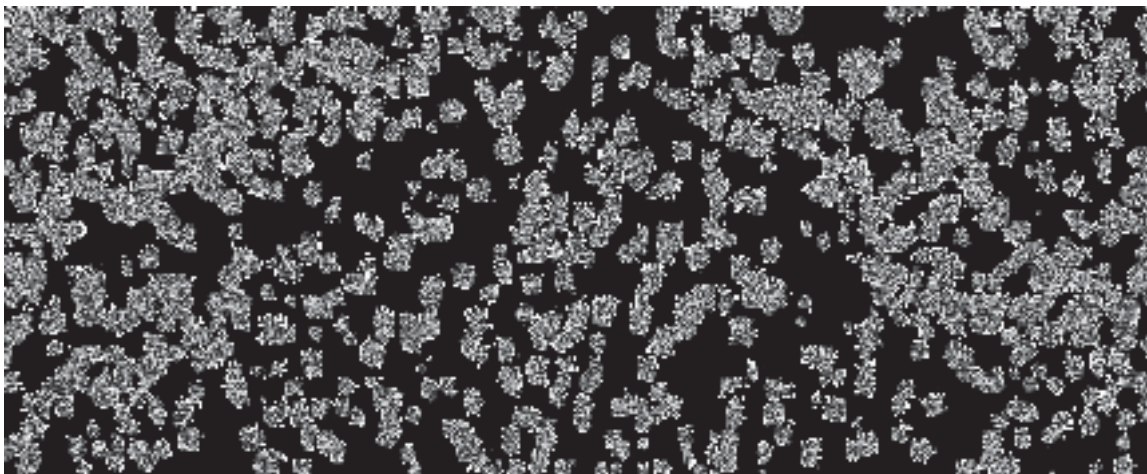


Figure 3.18 Illustration of the resultant image after Sobel edge detection.

But, further segmentation of these contours is necessary to reach the ultimate objective of the tree crown extraction. According to Brandtberg (1999c) and Wang *et al.* (2004), there are three possible cases of closed contours (Figure 3.19). Although, the isolated case might contain a simple one, or in slightly touching and compact group case, it is not easy to define the individual tree crown boundaries without visible edges existing on the image. Determination of the number of trees in each closed contours may alleviate this problem.

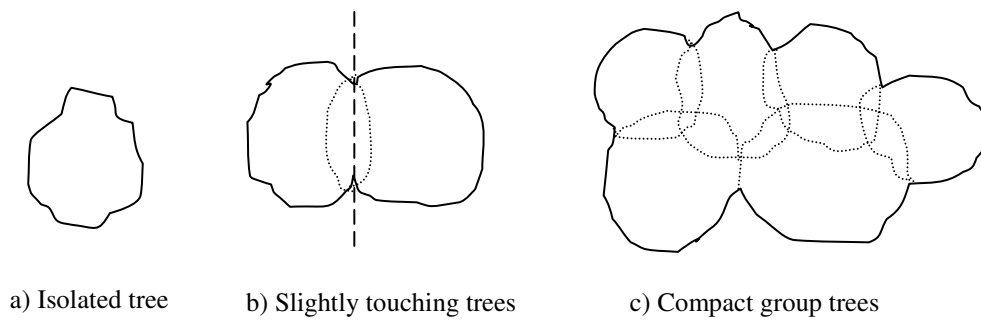


Figure 3.19 Three typical cases of closed contours after smoothing and edge detection (modified from Brandtberg, 1999)

The marker controlled method requires the identification of the markers or seeds inside each region of interest. The success of this method highly depends on the correct marker selection. Tree top location is an appropriate choice to automatically determine an internal marker inside each closed contours. Since oak trees have a relatively flat canopy surface, each crown may represent multiple local maxima which make it difficult to detect accurate tree tops from the gray scale imagery. Alternatively, the crown centre can be used to find tree tops. It was assumed that each tree top is located in the vicinity of the centre of tree crown. The concept of distance transform is widely used in image analysis and especially in mathematical morphology (Soille, 2003).

Euclidean distance transform assigns to each pixel in the binary image the Euclidean distance from that pixel and the nearest nonzero pixel of the image. The morphological distance transformation was applied on the binary NDVI imagery. The result was an image that represents the higher values at each crown centre, gradually decreases towards the boundary of the crown. By combining the spatial and radiometric structure of distance imagery, a mountainous landscape can be assumed. In such three-dimensional analogy, the spatial information can be assigned to the x and y dimension, while the intensity value of each pixel to the z dimension. In this image, local radiometric maxima (peaks) correspond to the top of a tree while local radiometric minima (valleys) correspond to the area between trees. Figure 3.20 shows a distance transform of a subset of QuickBird data and its corresponding radiometric topography.

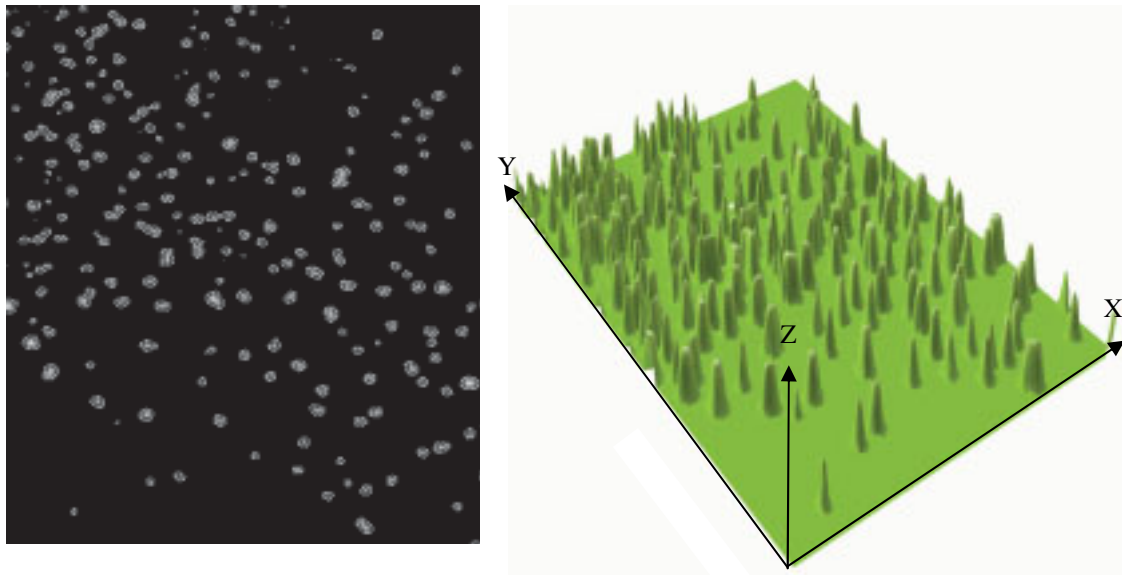


Figure 3.20 An example of distance image and its corresponding 3D view.

Subsequently, to determine the location of potential tree tops, the regional maximum of the distance image was calculated using the eight-connected neighborhoods. The result is a marker function image, which identifies tree tops by connected components of pixels that are set to 1 and all other external pixels to 0. This image stands for desired minima locations to be imposed on the segmentation function image. Morphological reconstruction of the gradient image with the marker function image imposes all markers as minima of the gradient while it removes those that do not correspond to any markers by increasing their value until the value of the closest regional maximum is attained. The imposition of minima is illustrated in Figure 3.21.

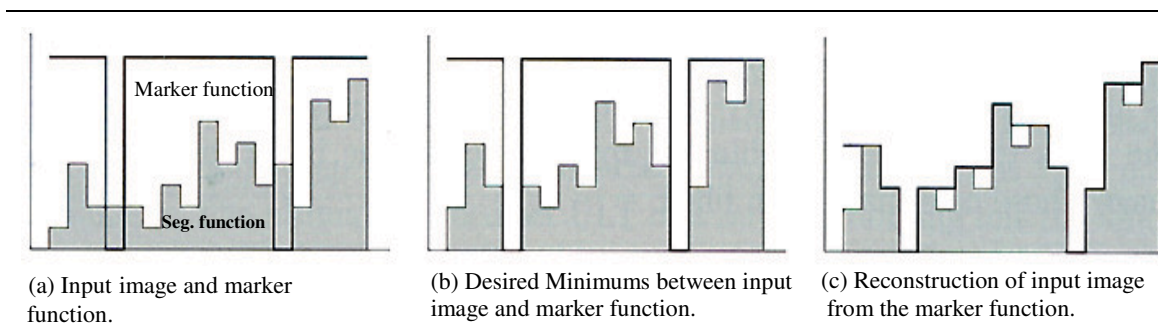


Figure 3.21 Minima imposition technique.

The input image, segmentation function contains 7 minima. The two desired minima of the marker image were imposed to the segmentation function image by a morphological reconstruction. Next, the MATLAB Watershed segmentation was applied on the modified image to precisely outline the boundaries of each crown. The result is a binary image in which, values “0” corresponded to the background and “1” is assigned to the trees or tree clusters.

3.6 Crown delineation quality assessment

A variety of different approaches for assessing the accuracy of the delineation results can be found in the literature but none of them has been accepted as a standard procedure. So far accuracy can be defined as the degree of correspondence between Computer-Generated Segments (CGS) and the actual Ground Reference Segments (GRS). The purpose of an accuracy assessment is the identification and measure of map errors. For many reasons the accuracy of the crown map should be evaluated. The accuracy of crown delineation is often crucial to perform further image analysis. High level of precision and accuracy of a crown map is required to meet the needs of recognition and classification of individual tree species as well as biomass and tree volume estimation. In addition, identifying and understanding the nature of map errors can help to improve the delineation techniques. If the information derived from crown map is being used in some level of decision-making processes, several measures of its quality should be known. The results of applying different techniques on the same image are usually dissimilar and it is necessary to indicate clearly which of these techniques performs a better tree crown delineation of the image. A standard procedure to express the delineation accuracy is essential to compare the results of each new study with that of one made already. While development of new tree crown delineation techniques has attracted significant attention (Pinz, 1989; Culvenor, 2002), relatively fewer efforts have been done on their evaluation (Pouliot *et al.*, 2002; Leckie *et al.*, 2005) hence comparison and adaptation of these techniques to other studies is difficult (Pouliot & King, 2005). In this study extensive use is made of the Leckie *et al.*, (2005) model, a specific representation for delineation evaluation based on the quantity of mutual overlaps between CGS and GRS.

Individual tree crown delineation has been implemented in the MATLAB software using QuickBird sub-images and the segmentation methods given in section 3.5.5.3 & 3.5.5.4. In order to evaluate results quantitatively and qualitatively, a ground reference map which represents individual tree crown outline was acquired during the field work. The accuracy assessment of crown maps was achieved with delineation evaluation.

Delineation evaluation

Delineation evaluation involves the comparison of the crown maps in terms of the spatial similarity with ground reference data on a crown-by-crown basis. The performance of the algorithm can be evaluated by judging the quality of the segmented image. The quality of automatically generated segments depends on the quantity of the overlap one has with the ground reference segments as well as the number of spatial overlaps. For any given CGS, it is critical to know the probability of being delineated correctly and the amount of confusion with one another. To carry out this work certain quality measures and conditions should be defined. Comparing the area of overlap to the area of GRS and CGS will permit a decision about the spatial similarity, and quantitative assessment of this decision. Since numerous topological relations can be distinguished between CGSs with the GRSs, subsequently, one combination of conditions that leads to the set of existing relation between CGS and GRS should be presented. Each condition should be represented by clear and distinct criteria. Alternative criteria and approaches for determining spatial correspondence of the CGS and GRS were developed by Leckie *et al.*, 2005. In this study extensive use is made of Leckie intersection model. Based on the mutual relation between segments, this model was revised in this study and recategorized in three main groups see also Figure 3.24.

- i) 1:1 means GRS only has one CGS overlapping it and that CGS only has that GRS associated it.
- ii) 1: n means a GRS has several CGS associated with it.
- iii)n:1 means a CGS has several GRS associated with it.

For the 1:1 category, based on the size of the CGS comparing to GRS and the area of their overlap different degrees and types of correspondence were considered. Perfect matches are considered those where the size of CGS and GRS are almost the same and the overlap is more than 50%. If the CGS is too big or too small it can represent an overlap, cover the GRS or be covered by the GRS configurations. Good matches are defined when more than 85% of the CGS is covered by GRS or vice versa.

For the 1:n category, good matches are defined as cases where CGS and GRS have more than 50% overlap (one perfect match) but the GRS has a slight association with secondary CGS's. Different types of poor matches (split) occur when more than one CGS occupies a GRS, and at least GRS covers more than 50% of each CGS's area.

For the n:1 category, good matches are characterized as each cases where CGS and GRS have more than 50% overlap (one perfect match) but the CGS shows a small overlap with secondary GRSs. Poor matches (grouped) occur when more than one GRS is associated with one CGS, more than 50% of each GRS area must be covered by the same CGS. Omission and commission are two particular cases of no match or overlap. Omission occurs when a reference crown was not matched and excluded from the delineation. If a computer generated crown did not match a reference segment then it is considered as commission.

Figure 3.22 illustrates a set of 12 configurations between GRS and CGS applied in this study. The perfect match, good and poor matches plus omission and commission errors comprise all possible relationships between GRS and CGS. Appendix 1 shows a detail description of altogether 20 overlap types.

Finally, an overall evaluation method proposed is applied to evaluate the delineation results of different techniques.

The final outcomes of the automatic delineation techniques were converted to vector polygons, and each polygon was labeled with a unique ID that corresponded to an actual ground tree. In order to ease the pain of manual evaluation of the results and to assist in the accuracy assessment, a software (DELIN) was developed at the Chair of Forest Inventory and Remote Sensing University of Göttingen, written in Visual Basic 6.0.

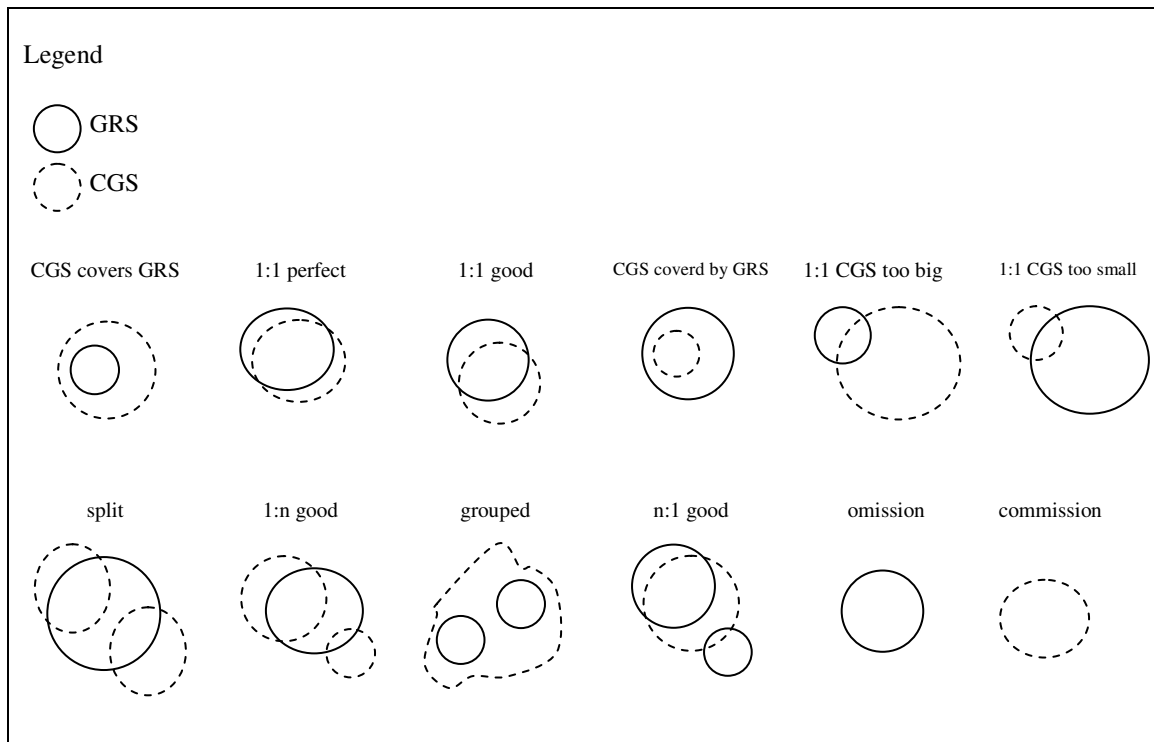


Figure 3.22 The 12 categories of GRS and CGS configurations for crown by crown comparison (after Leckie *et al.*, 1999).

The user interface of that software consists of three parts termed Plots-Shape, Reference-Shape and Methods-Shape to input plots, GRS, and CGS shapefiles respectively. Figure 3.23 shows the interface of the program. First every polygon of two layers (CGS & GRS) was sorted by plot ID and in each plot by GRS-ID. To determine the amount of intersection area between CGS: GRS, every CGS polygon was compared with the GRS inside the plot. The minimum spatial overlap threshold was defined as 5% to ensure small overlapping segments are not considered. If more than one CGS was overlapped with the same GRS, the CGS which has the largest overlap is assigned as the correct match to the reference the others were treated as secondary overlaps. The DELIN software computes the overlap percentage and the number of overlaps for each GRS. This information was stored as an ASCII file and imported in the MS Excel software. The comparison between the resulting percentages for each polygon and the 20 overlap types has been done by the VBA-macro in Excel. Based on the definitions in Appendix 1, the type of each configuration was determined.

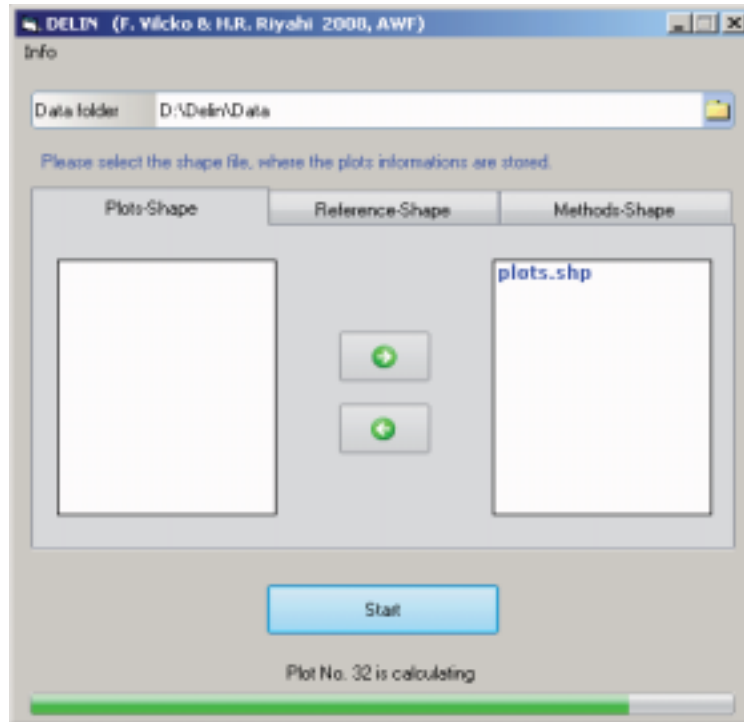


Figure 3.23 User interface of DELIN program.

The DELIN software generates a table for each method that contains seven fields whose item names are plot NO, GRS-ID, GRS-Area, Method-ID, Method Area, Intersected Area (the common area of the CGS and GRS that is associated with each match), Accuracy (the name of an appropriate configuration for each match), CGS/GRS (the percent of each GRS which is occupied by correspondence CGS), GRS/CGS (the percent of each CGS which is occupied by the correspondence GRS) (Figure 3.24). The unique GRS ID makes it possible to retrieve each polygon and its associated CGS easily in the GIS environment. Moreover it is feasible to determine the number and size of individual crowns in each overlap type.

Plot NO.	GRS- ID	GRS-Area	LOG -ID	LOG -Area	Intersect Area	Accuracy	CGS/GRS	GRS/CGS
2	80	7.58	0	0	0	Omission	0	0
2	245	14.87	177	12.52	12.5	1:1 Perfect match	84.06	99.84
2	54	26.21	178	24.06	22.43	1:1 Perfect match	85.58	93.23
2	69	41.66	179	44.21	39.57	1:1 Perfect match	94.98	89.50
3	175	64.26	23	68.27	63.59	1:1 Perfect match	98.96	93.14
4	32	44.86	183	51.92	44.85	1:1 Perfect match	99.98	86.38
4	239	5.87	182	4.88	4.28	1:1 Perfect match	72.91	87.70

Figure 3.24 A sample output of the DELIN software.

3.7 Crown detection assessment

The detection accuracy can be evaluated using the accuracy index (AI) which was defined by Pouliot *et al.* (2002). The AI index counts all errors against the correct number of crowns to be detected. GRS not matched to CGS were taken as omission errors, CGS not matched to GRS were taken as commission errors, and perfect matched trees were considered as correctly identified trees. The accuracy index can be defined as:

$$AI = \left[\frac{(n - o - c)}{n} \right] \times 100 \quad (18)$$

where *AI* is an accuracy index in percent, *o* and *c* represent the number of omission and commission errors, and *n* is the total number of trees in the image to be detected.

Chapter 4

Results

4.1 Regression analysis

Based on the field inventory data, the relationship of tree height versus crown area was plotted. In this relationship crown area and tree height were taken as the independent and dependent variables, respectively. The scatterplot was used to examine the relationship between variables and to check for linear and non-linear relations. To improve the regression, outliers (n = 4) either because of unrealistic values or because they were actually measured in wrong way, were identified by visual inspection and removed. For this study, a logarithmic relationship was selected as follows, owing to its higher coefficient of determination. $Y = 1.6136\text{Ln}(x) + 1.8985$

Figure 4.1 shows the regression line.

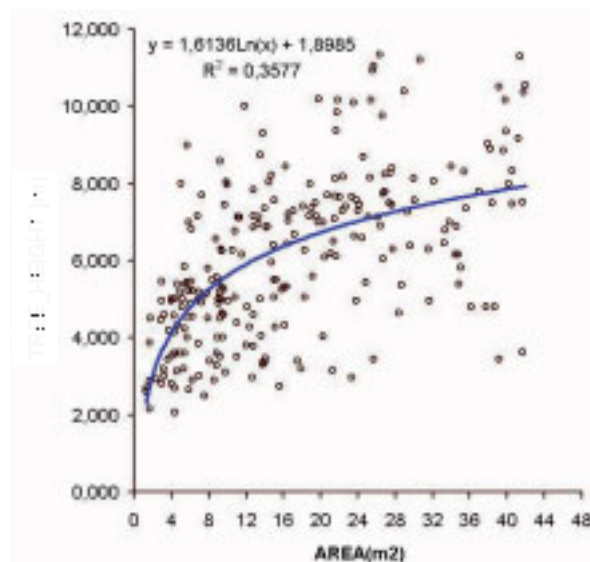


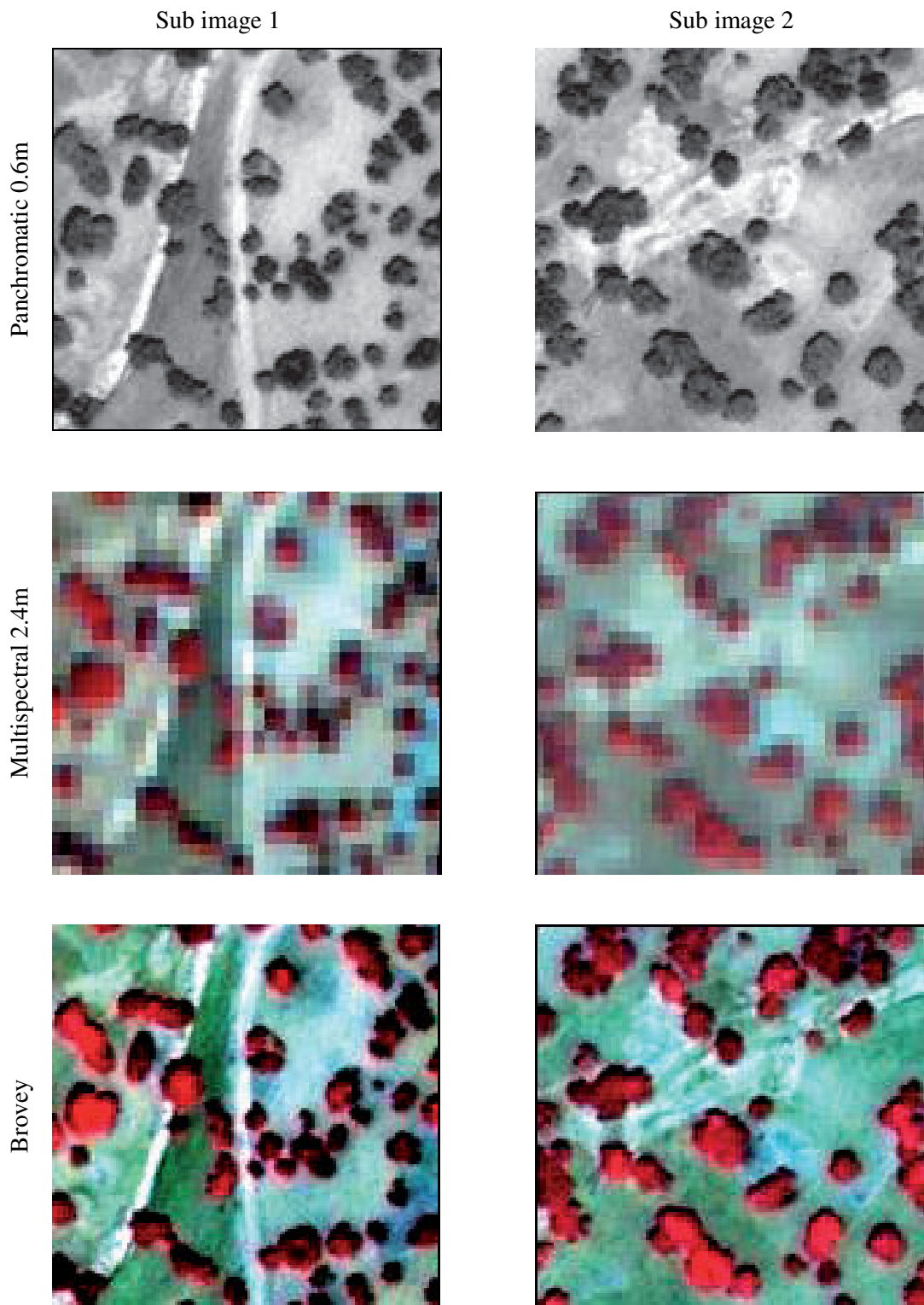
Figure 4.1 Scatter plot and fitted regression line of tree height vs. crown area.

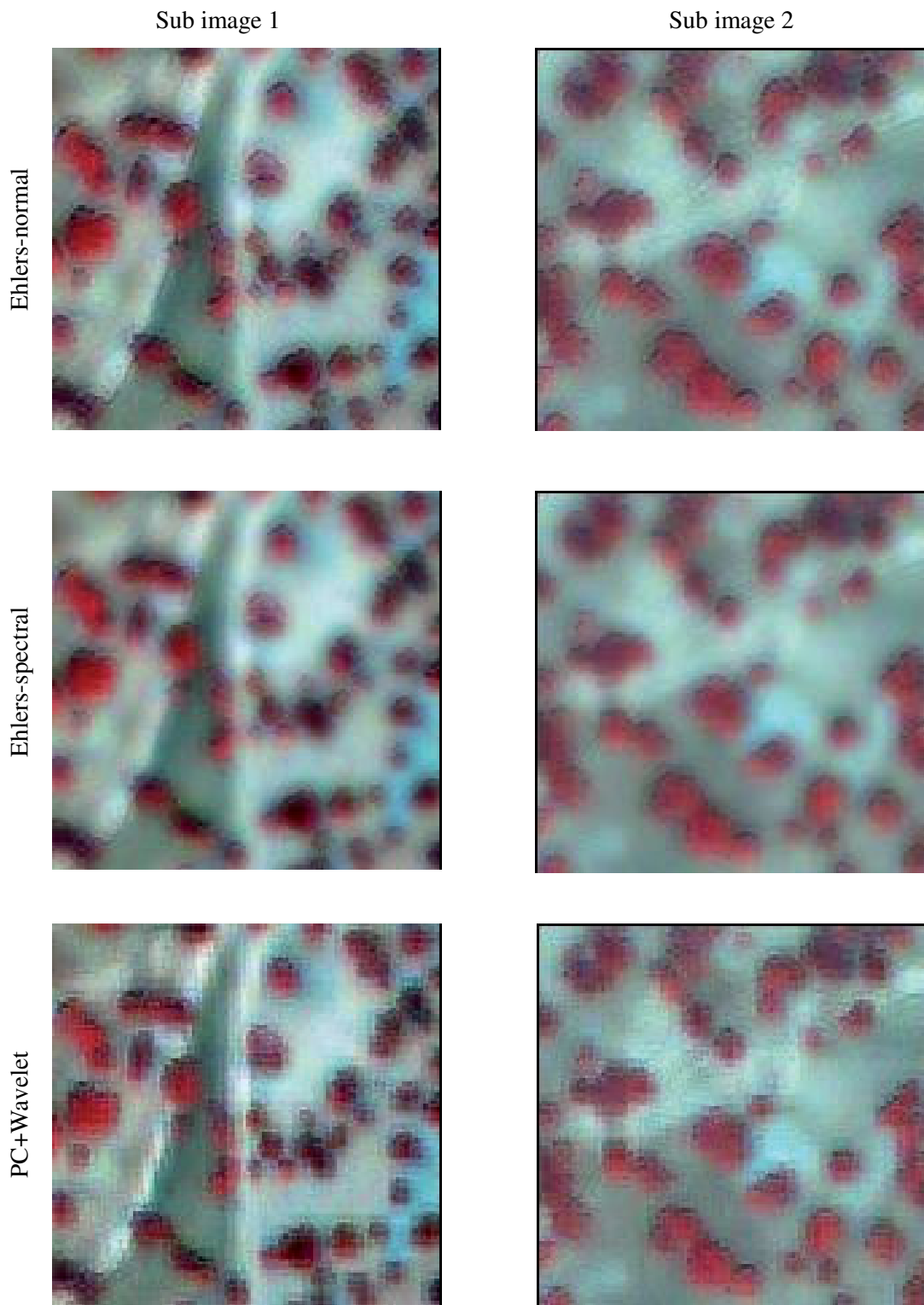
The coefficient of determination was $R^2 = 0.36$ and the regression coefficient was statistically significant ($P < 0.0001$). Thus, it is seen that there is a positive, nonlinear relationship between tree height and crown area.

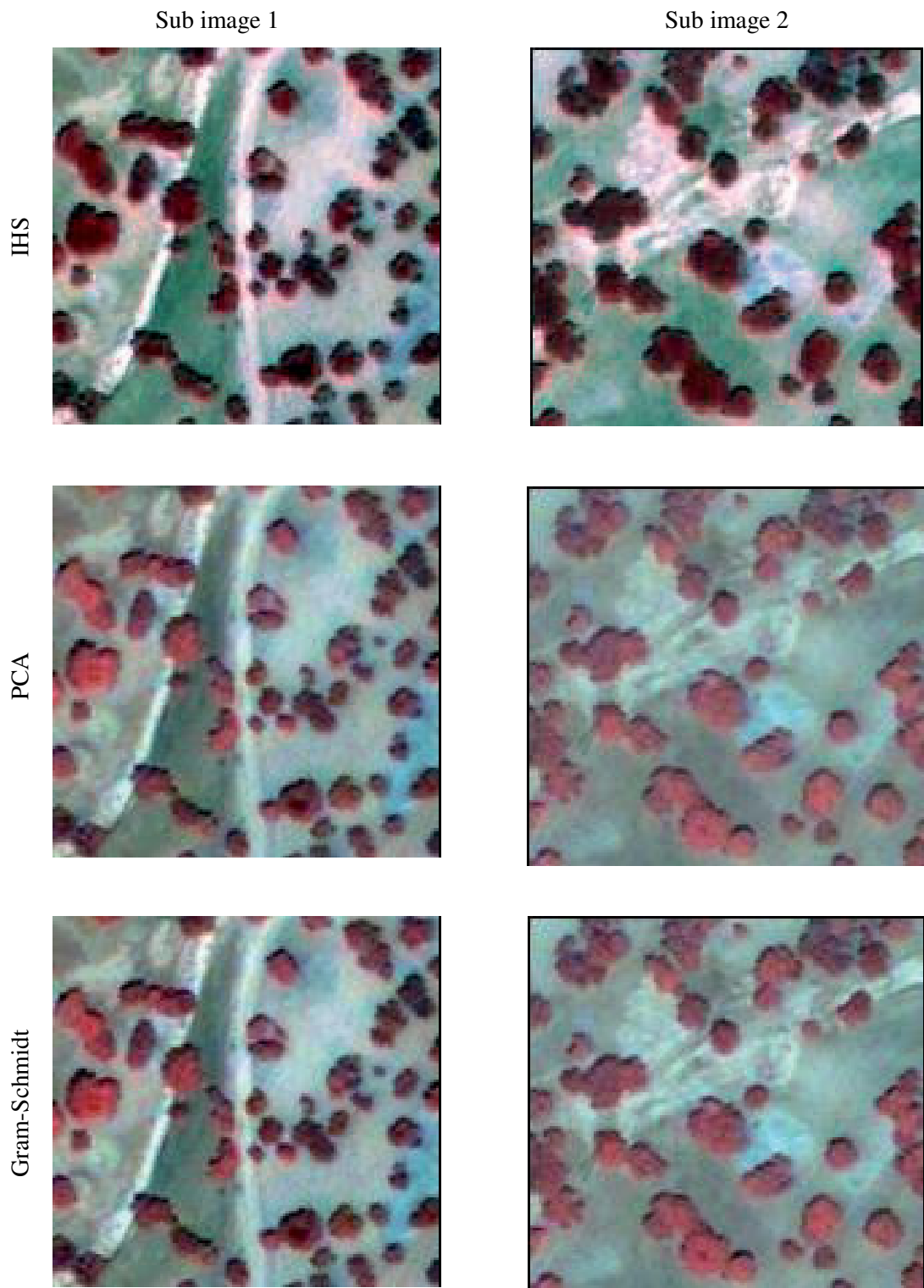
4.2 Image fusion evaluation

4.2.1 Results of visual quality assessment

The results showed that the Ehlers-spectral and Ehlers-spatial fused images represented fewer details and sharp contours, compared to the original Pan. The colors were not similar to the actual one and the blur in the whole image was obvious. The images synthesized by the PC + Wavelet method exhibit less high frequencies. The Brovey method provided nice images which present sharp details but close examination indicated that the dark areas became darker, and the white one whiter than the original images. The images synthesized by IHS method are visually acceptable. However they present sharp details, it is clearly observed from the color of tree crowns that the variation in color tones is low. This would make a lower intensity in a color composite. This clearly appears in Figure 4.2. Comparison of color composites made from the Ehlers-spatial with the actual one reveals that the relative spectral values of different structures have been preserved. However, too many spatial details are introduced to the image. The images from the Gram-Schmidt and PCA methods are visually satisfactory. High frequencies are present and the contours are sharp. Spatial as well as spectral characteristics are similar to the actual one but small differences may appear when a group of pixels is observed closely. Outcome results showed that that both PCA and Gram-Schmidt methods can preserve spectral and spatial information contents of original data better than the others.







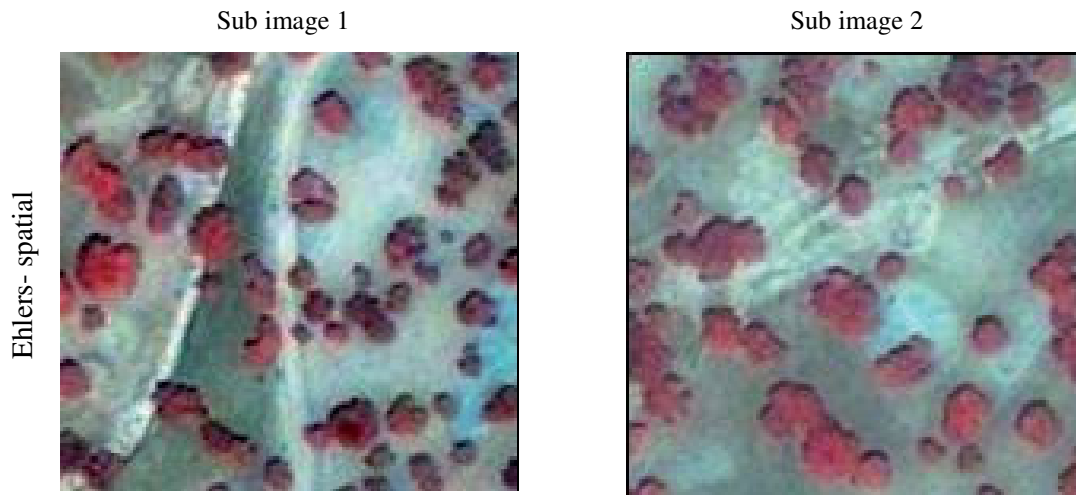


Figure 4.2 Results of QuickBird fused sub images of Dasht-e Barm, Iran. The first row: Pan sub images, the second row: Multispectral sub images. The rest are color composites (RGB = 4, 3, 2) of fused sub images named based on the fusion methods.

4.2.2 Results of statistical quality assessment

As the IHS method can merge only three bands at one time, different band combinations are possible. Based on the further processing steps in this research, green, red and NIR bands were selected. Wald (2002) suggested using the second property because it enhances the quality and drawbacks of the methods better than the other properties.

In this study, to evaluate the synthesis property, some statistics on differences between the original B_k and synthesized images B_{kl}^* were calculated. The bias value is calculated relative to the mean value of the original image. The difference in variances is calculated relative to the variance of the original image and expressed in percent. The correlation coefficient between the original images and the synthetic images was calculated using a pixel-based comparison. These statistical measures are presented in Table 4.1- 4.4.

Table 4.1 Statistics on the difference between the original and synthesized images (in radiance or relative value) for band 1 (Blue).

	<i>Brovey</i>	<i>Ehlers Normal</i>	<i>Ehlers Spatial</i>	<i>Ehlers Spectral</i>	<i>Gram-Schmidt</i>	<i>PCA</i>	<i>PCA+Wavelet</i>
Bias relative to the actual mean value	-3%	2%	1%	2%	-2%	-2%	-76%
Correlation coefficient between original and synthesized images	0.61	0.66	0.73	0.66	0.75	0.96	0.53
Standard deviation of differences relative to the actual mean value	36%	31%	28%	32%	12%	12%	35%
Difference in variance relative to the actual variance	-12%	23%	26%	23%	-7%	-6%	58%

Table 4.2 Statistics on the difference between the original and synthesized images (in radiance or relative value) for band 2 (Green).

	<i>Brovey</i>	<i>Ehlers Normal</i>	<i>Ehlers Spatial</i>	<i>Ehlers Spectral</i>	<i>Gram-Schmidt</i>	<i>IHS</i>	<i>PCA</i>	<i>PCA+Wavelet</i>
Bias relative to the actual mean value	5%	9%	9%	10%	1%	-22%	2%	-65%
Correlation coefficient between original and synthesized images	0.64	0.65	0.74	0.65	0.76	0.93	0.97	0.54
Standard deviation of differences relative to the actual mean value	34%	32%	28%	32%	28%	91%	9%	35%
Difference in variance relative to the actual variance	8%	34%	34%	33%	5%	-210%	6%	64%

Table 4.3 Statistics on the difference between the original and synthesized images (in radiance or relative value) for band 3 (Red).

	<i>Brovey</i>	<i>Ehlers Normal</i>	<i>Ehlers Spatial</i>	<i>Ehlers Spectral</i>	<i>Gram-Schmidt</i>	<i>IHS</i>	<i>PCA</i>	<i>PCA+Wavelet</i>
Bias relative to the actual mean value	10%	15%	15%	15%	1%	-18%	2%	-48%
Correlation coefficient between original and synthesized images	0.64	0.65	0.73	0.64	0.74	0.92	0.97	0.50
Standard deviation of differences relative to the actual mean value	33%	31%	28%	32%	29%	89%	10%	31%
Difference in variance relative to the actual variance	20%	44%	42%	44%	14%	-169%	16%	68%

Table 4.4 Statistics on the difference between the original and synthesized images (in radiance or relative value) for band 4 (Near-IR).

	<i>Brovey</i>	<i>Ehlers Normal</i>	<i>Ehlers Spatial</i>	<i>Ehlers Spectral</i>	<i>Gram-Schmidt</i>	<i>IHS</i>	<i>PCA</i>	<i>PCA+Wavelet</i>
Bias relative to the actual mean value	6%	10%	6%	16%	9%	-16%	5%	-51%
Correlation coefficient between original and synthesized images	0.62	0.70	0.76	0.70	0.82	0.78	0.84	0.54
Standard deviation of differences relative to the actual mean value	26%	20%	17%	20%	16%	81%	16%	24%
Difference in variance relative to the actual variance	-70%	-6%	4%	-12%	-27%	-619%	-40%	25%

The PCA+Wavelet method gave very poor results in all aspects of table 4.1 through 4.4, due to bias and spectral distortion it generated. The visual appearance of the Brovey method appears fine but the results remain of poor quality (Figure 4.2), it induced a low bias, but standard deviation of the difference is large and the correlation coefficients indicate that more Pan information has been introduced to the synthesized images.

The IHS method introduces too much high frequencies from the Pan image into the synthesized images especially in the NIR band. The difference in variance is negative and too large, especially for NIR band that means fusion provides too much information that can be noise or artifacts. The bias is high and the results still remain of low quality. The three methods using Ehlers concept offer approximately the same level of quality: high bias especially in green, red and NIR bands and low correlation coefficients. These clearly indicate the weak similarities between the actual images and the synthesized ones. The high and positive difference in variance in the blue, green and red bands, expresses the information lost in these bands during the enhancement of spatial resolution. However, the Ehlers-spatial approach exhibits superior in green, blue and NIR compared to the other Ehlers methods but the results still are not satisfactory.

The Gram-Schmidt and PCA method provide acceptable results. The Gram-Schmidt method gives the lowest bias in the green and red bands. The correlation coefficient and standard deviation of differences are acceptable in all bands. The difference in variance is the lowest in blue, green and red but it is high and negative in NIR. This indicates that more information has been introduced into the NIR band.

The PCA method performs slightly better than the Gram-Schmidt method as a whole. The bias is less than that of the Gram-Schmidt method in the NIR band. The standard deviation is the smallest in all bands for the PCA approach. Thus, the PCA method produces less error in the blue, green, red and NIR bands. The highest correlation coefficient between the synthesized images and the original one in all bands denotes good similarities in small structures.

Global errors

The global errors are based on the spectral error presented in each pixel. Global image measures summarize the discussed quality metrics and allow a comparison of all methods of a glance. ERGAS is the normalized average error of each band. Wald (2002) argued that ERGAS values larger than 3 stand for synthesized images of low quality, while values less than 3 represent a satisfactory quality. The RASE delineate the average performance of a method in the considered spectral bands and has a tendency to decrease

as the quality increases. Global evaluation index ERGAS and RASE are used to evaluate quality of fused images. Table 4.5 compares the obtained results.

Table 4.5 The global errors of the compared methods.

	<i>RASE (%)</i>	<i>ERGAS</i>
Brovey	14.39	3.58
Ehlers Normal	14.66	3.74
Ehlers Spatial	14.84	3.78
Ehlers Spectral	14.91	3.81
Gram-Schmidt	12.39	3.36
IHS	45.00	13.10
PCA	9.34	2.37
PC+ Wavelet	13.53	3.37

The PCA method presented the lowest value of the RASE and the ERGAS index. Hence, the spectral quality of images fused by the PCA method is much better than the others. In contrast, the IHS method has highest values for the both RASE and ERGAS indices.

4.3 Tree crown delineation results

In order to compress the information content of multispectral bands into one single band the principle component analysis (PCA) was performed in a preparation step. The first principle component was selected as initial image for the delineation process. To eliminate the effects of background the NDVI mask was multiplied by the initial image to create the crown mask. Figure 4.3 shows an example of an initial image, the crown mask image and their correspondent histograms.

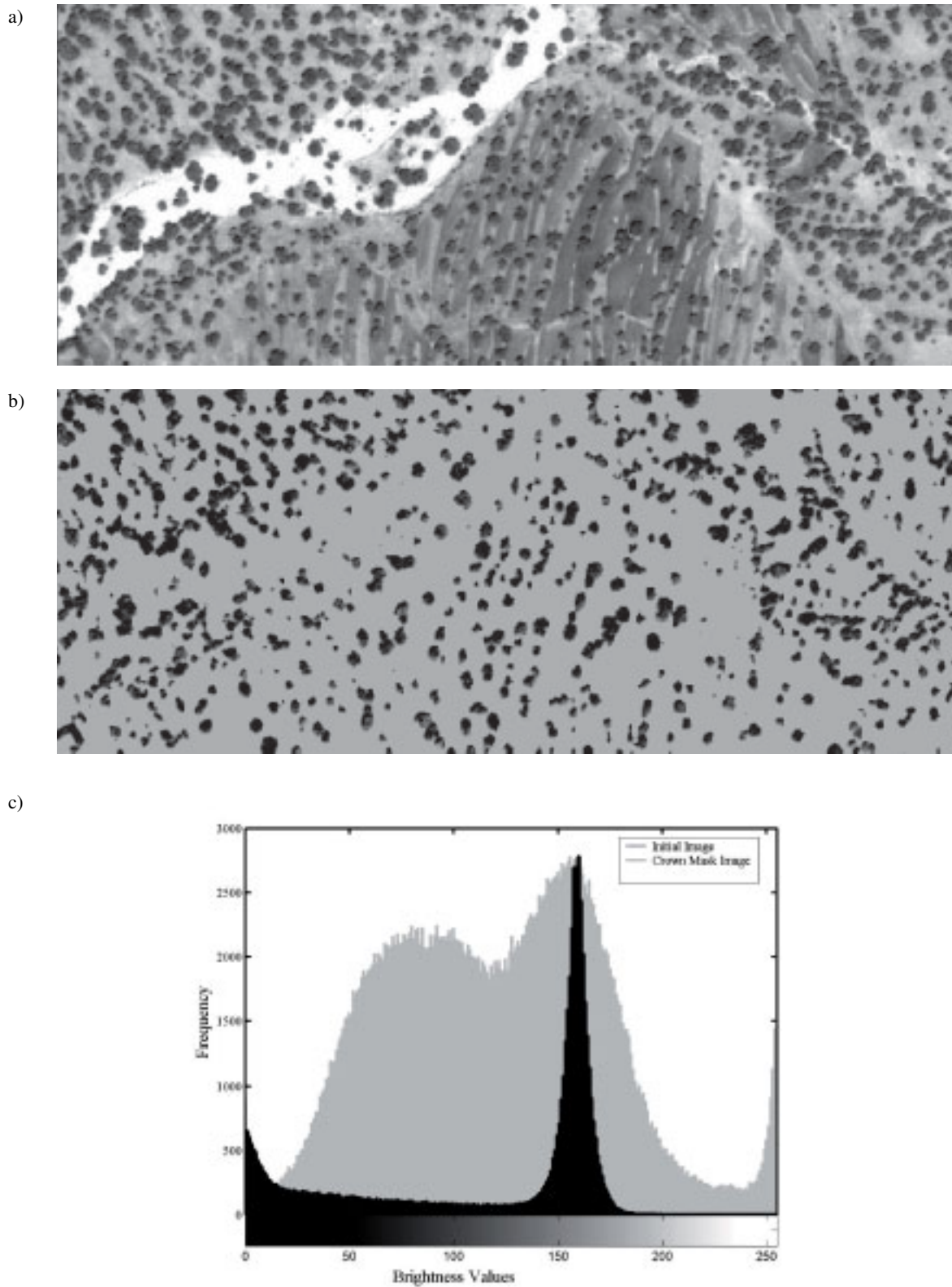


Figure 4.3 (a) Initial image. (b) Crown mask image. (c) Histogram of the initial (gray) and histogram of the crown mask image (black).

To delineate individual tree crowns the Log edge detector was performed on the crown mask image. Figure 4.4 shows the delineation results of the LoG method using the image subset displayed in Figure 4.3. For further processing steps, this binary image was converted to vector format using standard GIS software. An example overview of the delineation results overlaid on the color composite image is in Figure 4.6.

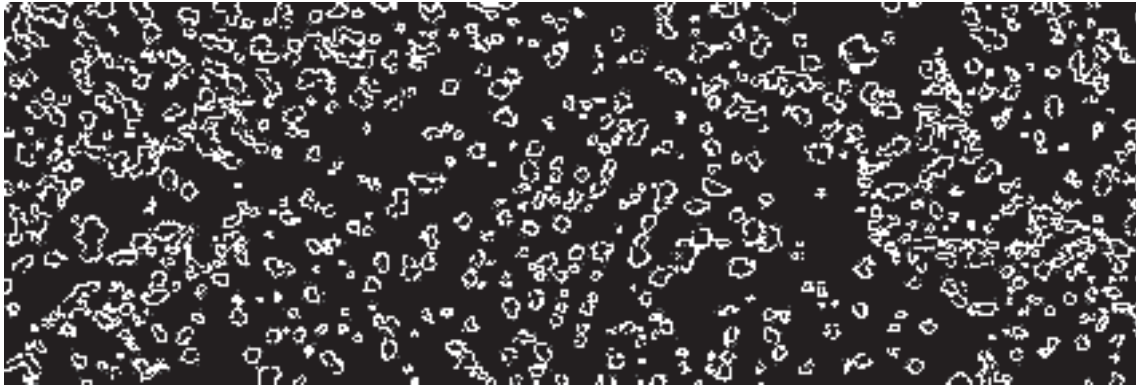


Figure 4.4 An example of automatically delineated tree crowns by the LoG method.

Marker-controlled watershed segmentation was applied on the initial image for the tree crown delineation. Figure 4.5 shows the delineation results using marker controlled Watershed segmentation. The final step involves converting contiguous selected pixels from the binary image to a polygon vector using standard GIS software. Figure 4.7 gives an example overview of the delineation results overlaid on the color composite image for the Watershed method.

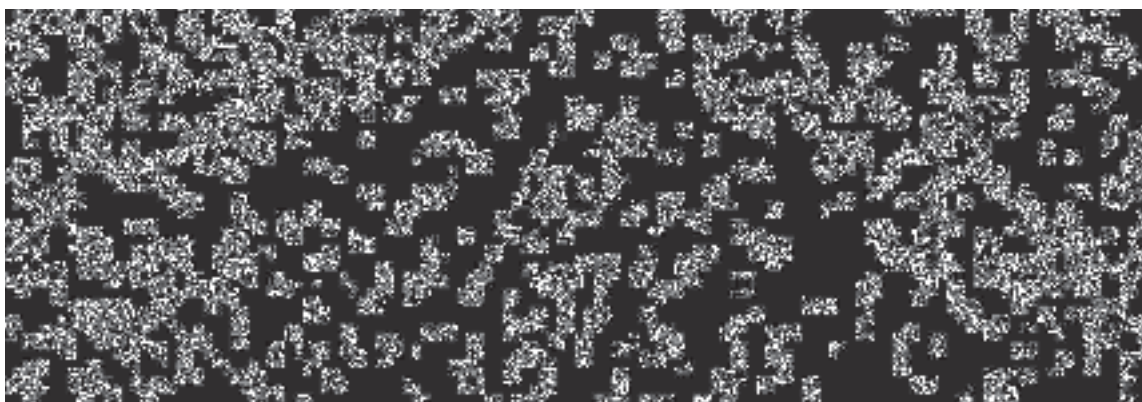


Figure 4.5 An example of automatically delineated tree crowns by marker controlled Watershed segmentation.

The results are binary images such that all pixels that correspond to individual tree crowns have the value 1, and all the other pixels are set to 0. Very high variability in crown shape and size can be seen in both resultant images. In general it can be said that the number of delineated crowns are not the same and most of small segments which identified by the LoG method could not be recognized by the Watershed method. It is not feasible to quantify the quality of the segmentation results visually. Indeed the human eye is not able to distinguish the differences between two regions with very close shape.

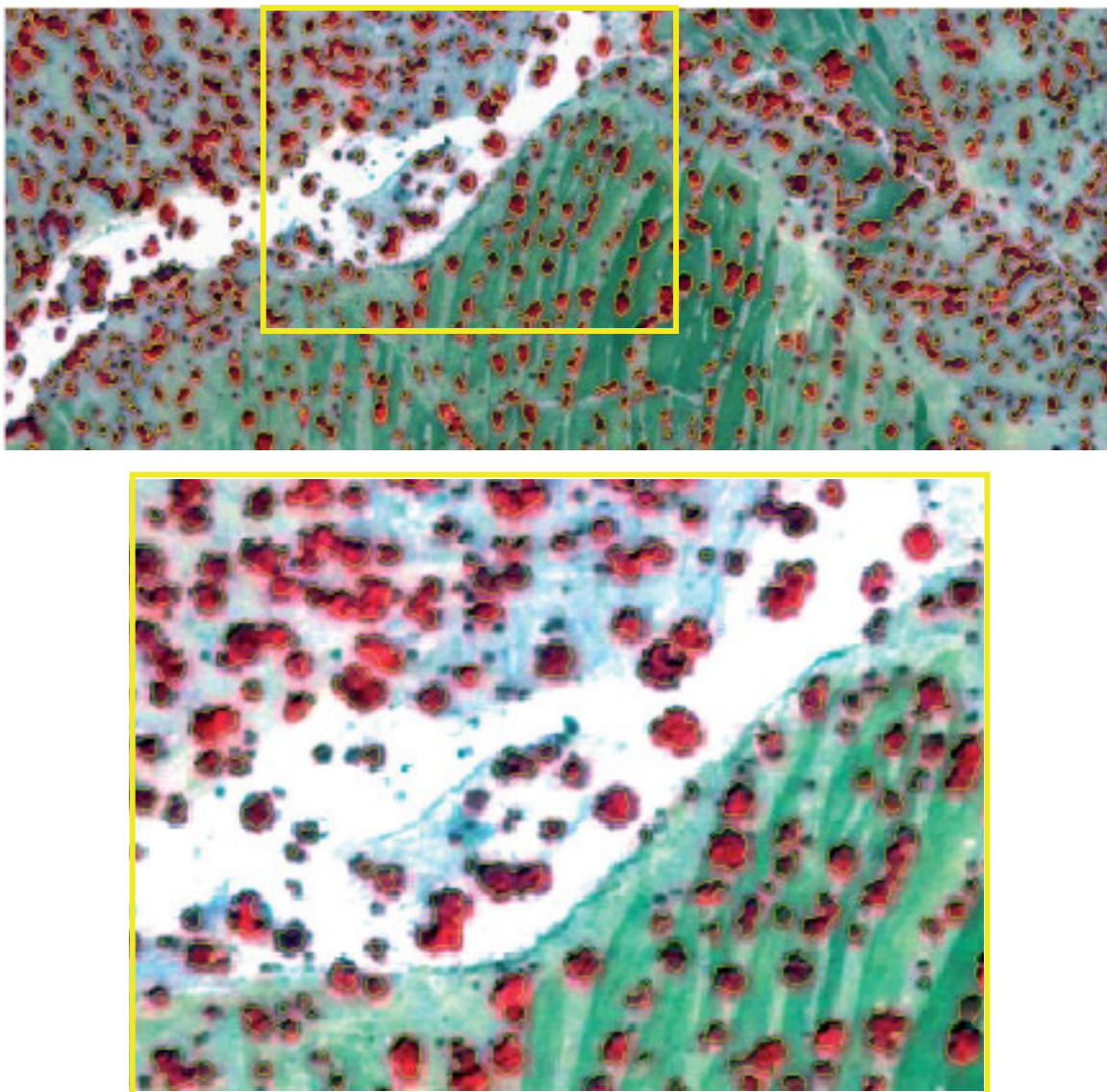


Figure 4.6 An example of crown delineation results of the LoG method overlaid on color composite (R G B = 4, 3, 2). To allow better discrimination of the output results, a zoom subset is included. Successful delineation of small crowns is obvious.

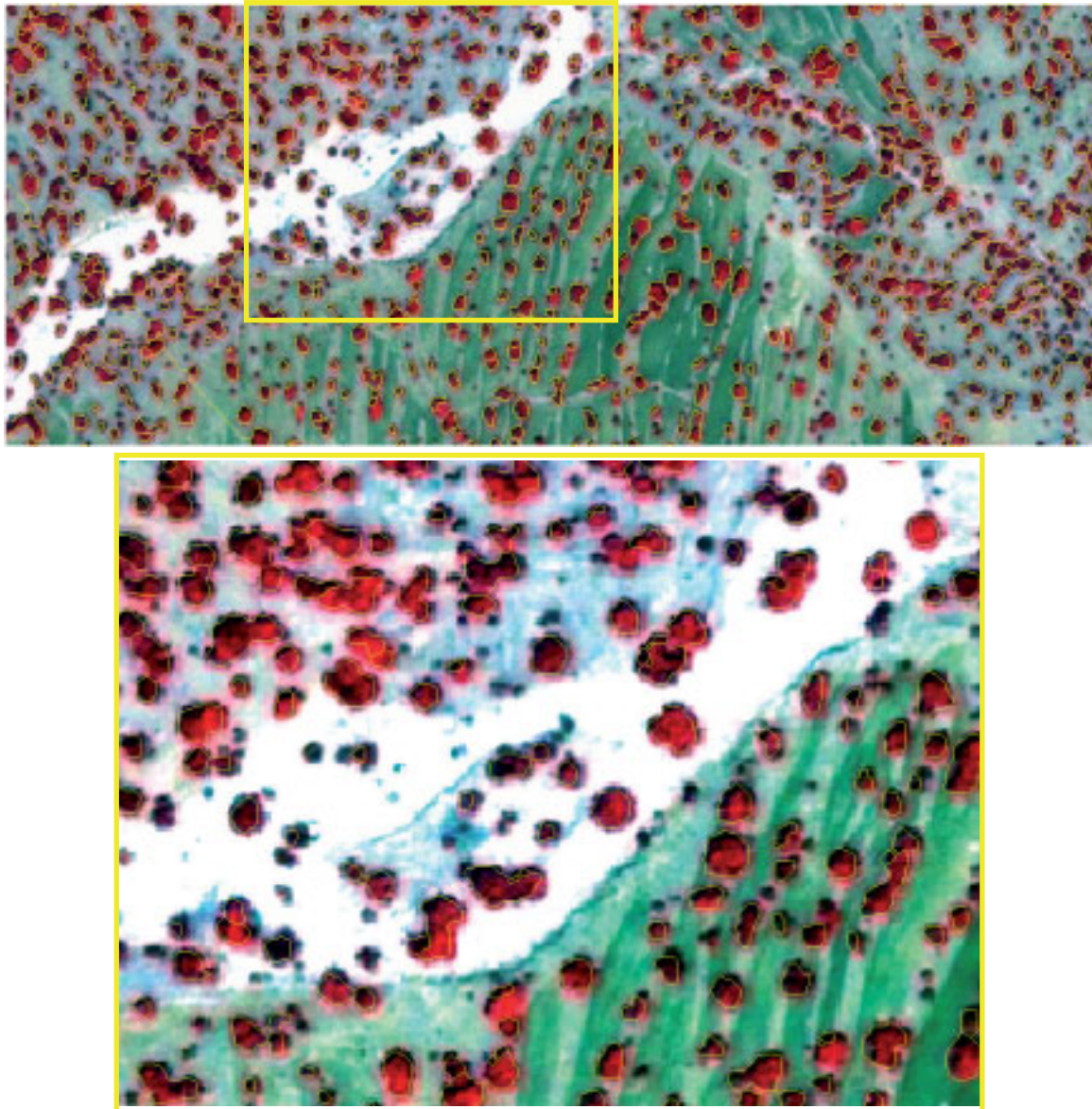


Figure 4.7 An example of crown delineation results of the Watershed method overlaid on color composite (RGB = 4, 3, 2). To allow better discrimination of the output results a zoom subset is included. Omission of small crowns can be observed.

4.3.1 Delineation evaluation of LoG method

In order to investigate the potential of the LoG approach, the results were compared with the ground reference using the “DELIN” software. Table 4.6 examines the automatic delineation results of the LoG method on a crown by crown basis.

Table 4.6 Results of the delineation evaluation of LoG method.

	Cover type	Number of crowns	Percentage	Total percentage	Average Area (m ²)	Total Average Area (m ²)
Perfect	1:1 Perfect match	129	58.1%	58.1%	29.9	29.9
	1:1 Good	3	1.3%		13.7	
	1:n Multiple major	4	1.8%		38	
Good	1:n Multiple minor	2	0.9%	9.8%	76.9	31.5
	n:1 Multiple major	4	1.8%		29.1	
	n:1 Multiple minor	10	4.5%		26.9	
Poor	1:1 Poor	7	3.1%		11	
	1:n Split	1	0.4%		14.1	
	1:n Split one dominant	1	0.4%	31.8%	13.9	19.6
	n:1 Grouped	53	23.8%		22.6	
	Omission	8	3.6%		9.1	

Values show the number, percent and average area of ground reference crowns in each correspondence category as given in Appendix 1. The results were categorized in three main groups (e.g. perfect match, good matches and poor matches). 58.1% of crowns showed a perfect match with the average crown area of 29.9 m². Approximately 72% of

the intermediate crowns ($11 - 40 \text{ m}^2$) had perfect match. The larger trees were delineated better, 75% of the large trees ($>40\text{m}^2$) showed a perfect match. About 1.3% of the trees had a good match 1:1, 2.2% good match 1:n, and 6.3% good match n:1 defined as types 2, 4, 6 in Appendix 1 respectively. The total rate of good matches for this method was 9.8%. For this method there were no commission errors. Eight trees with greater proportion of small crowns ($<10\text{m}^2$) were omitted. Only 2 trees were split into one or two trees. About 53 trees with the average area of 22m^2 were grouped.

4.3.2 Delineation evaluation of the Watershed method

To evaluate the performance of the Watershed method, the results were compared with the ground reference on a crown by crown basis. The number, percentage and average area of ground reference crowns in each correspondence category are listed in Table 4.8. For better observation the results are categorized into three main groups (e.g. perfect match, good matches and poor matches). About 48.6 % (108 trees) of the total crowns had a perfect match. The average reference area of perfect matched trees was 31 m^2 . The smaller crowns ($<10\text{m}^2$) with a proportion of 19% showed the smallest contribution. About 55% of the intermediate crowns ($11-40 \text{ m}^2$) had a perfect match while the large crowns ($>40\text{m}^2$) with the greatest proportion, (61%) showed better delineation. A number of 36 trees had good matches defined as types 2, 4, 6 in Appendix 1. The total rate of good matches for this method was 16%. Just 3 trees were split into two or more crowns. About 37 trees were considered to be grouped, (i.e., having several GRS strongly associated with CGS; types 7.1, 7.2 in Appendix 1) with the greater proportion 19.8% of the intermediate trees. 31 trees with the greater proportion 53% of small trees were omitted.

4.4 Tree crown detection results

For each delineation method, the number of omission and commission errors was determined. The overall detection accuracy of each method was calculated using equation (18). The detection error and accuracy for the LoG and Watershed methods are shown in Table 4.7.

Table 4.7 Tree crown detection error and accuracy.

Method	Correct	Omission	Commission	Total	Correct (%)	AI (%)
LoG	152	8	62	222	68.4	68
Watershed	144	31	47	222	64.8	64

Table 4.8 Results of the delineation evaluation of the Watershed method.

	Cover type	Number of crowns	Percentage	Total percentage	Average Area (m ²)	Total Average Area (m ²)
Perfect	1:1 Perfect match	108	48.6%	48.6%	31	31
	1:1 Good	2	0.9%		17.7	
	1:n Multiple major	5	2.2%		34.5	
Good	1:n Multiple minor	6	2.7%	16.1%	59.1	32.6
	n:1 Multiple major	9	4%		25.4	
	n:1 Multiple minor	14	6.3%		27.3	
Poor	1:1 Poor	5	2.2%		24.2	
	1:n Split	2	0.9%		41.6	
	1:n Split many small	1	0.4%		89.2	
	n:1 Commission impure	2	0.9%	34.9%	11.2	18.1
	n:1 Grouped	37	16.6%		21.6	
	Omission	31	13.9%		10.3	

Chapter 5

Discussion

5.1 The delineation algorithms

As comprehensively discussed in section 2.4, there are various algorithms used to delineate individual tree crowns. Briefly mentioning, they are listed as template matching, valley following, and vision expert methods. Since these algorithms need prerequisite conditions to work properly, application of them in the case of current study may face some difficulties. To have a better overview on these difficulties, let us briefly recall from section 2.4 the mentioned algorithms and their required conditions.

To perform the template matching technique, predefined templates are required (section 2.4.1.3). These templates incorporate variables such as tree geometry as well as sun and view angles. Therefore the variation in representation of trees on the image is controlled by these parameters. As a clear prerequisite, this algorithm requires the templates to match each tree separately. To apply this technique in Zagros forests, with different tree crown shapes and sizes, it is necessary to have a unique template for each tree separately. This, however, requires predefining many individual templates. So, quite clear that in this case, man work expenses, computational time, and omission errors will be increased. Needless to mention that, creating any individual template for each tree requires a significant time. Comparing numerous templates with the base image requires higher computational power and time. To this the higher probability of missing many matching cases between templates and the base image can also be added.

Briefly, the valley following approach utilizes the intensity pattern of shaded areas between trees and a rule-based system to outline the boundaries of each crown (see section 2.4.1.2). This algorithm assumes that image structure is analogous to image intensity topography. Valleys of shade between trees have the lowest spectral reflectance

which gradually increases towards the crown boundary (Gougeon 1995). This technique at first tries to find local minimum and then follows the network of minima between trees. Next a rule based system refines the network and delineates the crown boundaries. Therefore, this approach by its nature can not do properly with optical imagery for Zagros forests, because trees are positioned far from each other and there is not continuous shadow between them. In this case the high reflectances of the bare soil between trees do not permit a complete network of minima to be constructed. Hence the prerequisite condition for application of this method is lost.

Another common algorithm used to find tree location is Local Maxima (LM) filtering (Wulder *et al.*, 2000; Deralle & Rudemo, 1997). Local maximum can be used as a starting point for some delineation methods such as TIDA and region growing (see section 2.4.2). It is assumed that the top of a tree or crown apex has the highest spectral reflectance. After finding a maximum point, by clustering the neighboring pixels in all directions, pixels of a crown that are directly adjacent to those points are identified. To halt the process a threshold value is needed to be defined. This threshold can be the minimum value of spectral reflectance in a tree crown. However, this principle works well with coniferous trees which have the conic shapes with a single peak. But in Zagros forests with the deciduous trees, which have the broad crown with multiple local maxima, this algorithm can not work properly. Clearly in this case, the algorithm recognizes several maxima for a single tree and leads to over-segmentation.

These were some few algorithms (among the others) commonly used to delineate individual trees and we saw how they are unable to handle the problem of crown delineation in Zagros forests. Now let us look at the adapted algorithms suitable for deciduous sparse forest.

In the color composite QuickBird imagery of the study area (see Figure 3.3) individual tree crowns are visually distinguishable from the background (due to a highly coverage of the bare soils). In order to utilize this opportunity to delineate individual trees it is necessary to increase the spatial resolution of multispectral bands. To do so, different image fusion techniques were used to fuse multispectral bands with Pan imagery. The Normalized Difference Vegetation Index (NDVI) is one of the most widely used

vegetation indexes (Jiang *et al.*, 2006). In this NDVI image, intensity discontinuity occurs at the boundary of the tree crown and the background. The concept presented in this work was based on the application of NDVI image and different edge detection methods to improve the application of QuickBird imagery for automatic delineation of individual tree crowns in sparse forests. In this condition Marker-controlled Watershed segmentation and the LoG edge detection methods were used.

Watershed method assumes the grey tone of an intensity image as altitude of a topographic surface. To construct the watershed line this surface is flooding from regional minima. Since each tiny and insignificant regional minimum can form its own catchments basin, application of the Watershed method directly on the QuickBird imagery may result in over-segmentation. To avoid this problem, one solution is to use markers to remove undesirable minima that may arise due to noise and reflectance of other objects than tree crowns. In the current study the marker-controlled Watershed segmentation was optimized by proposing the following major steps:

- 1) Separate tree crowns from the background using an NDVI mask.
- 2) Produce segmentation function by Sobel operator.
- 3) Morphological techniques, so-called “Euclidean distance transform”, and “regional maximum” are used to provide marker image.
- 4) Minima imposition technique is applied to modify the gradient magnitude image such that the only remaining minima are those given by the marker image.
- 5) Calculate the Watershed transform using modified gradient magnitude image to outline the boundaries of individual crowns.

The main suitability of this method is the capability to control the segmentation process by priori knowledge about the location of individual crowns. The algorithm consisted of a combination of edge detection and region growing approaches. Sobel operator produces closed contours that may be advantageously used for the detection of individual crowns. However, it is very difficult to find the individual tree tops for deciduous trees using intensity imagery. But it can be assumed that the tree top is located in the vicinity of

crown centre. In this case, we can therefore consider the crown center as the tree top. Now the question is how to find the crown center.

To find the crown center, the Euclidean distance transform was applied on the NDVI binary image. This morphological transform assigns each crown pixel a value that corresponds to the shortest distance between the crown pixel and the background. In this way the central pixel of each individual crown shows the highest intensity value (see Figure 3.22). Using morphological processing, these maxima are used to identify crowns center in the image, and therefore, based on the mentioned assumption can be considered as tree tops. These tree tops should be extracted from the image in a way to be used as a marker image for the next step.

To extract the individual tree top, regional maximum function was applied on the intensity image as input. This function sets the regional maxima to 1 and all other pixels to 0 in the output binary image. After providing the marker image, it is necessary to modify the gradient image such that the resulting image has regional minima at the marker locations. To reach this goal the minima imposition technique (section 3.5.4.2.3 Watershed segmentation method) was used. Then the morphological Watershed segmentation is carried out on this image. The quality of the Watershed segmentation is directly linked to the marker image. The over-segmentation mainly occurs when the markers are not perfectly appropriate to the individual crowns to be delineated. However, choosing too few markers lead to the under-segmentation.

For further investigation the Laplacian of Gaussian (LoG) edge detector was adapted and applied to delineate individual tree crowns in this study. The major advantage of Laplacian edge detector for Zagros forest condition is the capability to cope with the irregularities in the tree crown, forms and sizes. However, successful performance of this method requires the abrupt changes in the crown boundary. On the QuickBird data of the study area individual crowns made a discrete and narrow shadow that is not appropriate for successful edge detection. An NDVI mask was used to eliminate these shadows from the image, while preserving the spectral and spatial fidelity of individual crowns. The result is a mask image that contains homogenous background and individual crowns with variable intensity. Since the second derivative operators like Laplacian method are

extremely sensitive to noise, application of Laplacian operator on the mask image may yield edge detection errors like false edges, and broken or missing edge segments. To suppress the noise and to get better results, image thresholding was applied on the mask image before the gradient operator is used. Selection of an appropriate threshold is essential for reliable segmentation. In this study from several techniques, Otsu's method was selected to determine the optimal threshold values automatically. This method assumes two classes of pixels for the image and then calculates the optimum threshold to separate these two classes (Otsu *et al.*, 1997). By performing this method on crown mask image all pixels with grey value less than the threshold level were assigned to 0 and a value of 255 to all pixels with a grey level greater than the threshold level. In this way the image was segmented into two regions, one corresponding to the background and the other to tree crown. This image was convolved with the LoG filter to extract significant edges. It should be noted that the LoG method is able to detect edges at different scales. When choosing a too small scale often results in severe over-segmentation with too small regions within the individual crowns. When choosing a too large scale results in under-segmentation with too big regions of grouped trees. In this work, we concentrate on the detection of possible edge points at one scale.

5.2 Comparing the applied methods

The accuracy of the results of two different crown delineation methods was assessed using crown by crown comparison. Grouping of adjacent trees to one was the common problem in two different algorithms we used. The analysis revealed that the grouping error was mainly caused by intermediate trees and trees in close proximity. One possible reason for a higher number of grouped crowns from the LoG method could be the image thresholding. By thresholding the intensity image, small valleys between the adjacent crowns will be destroyed. Similarly, in the marker controlled Watershed method which the number of crowns in each polygon is determined by the markers, choosing too few markers in each polygon resulted from distance transformation lead to grouping of adjacent trees. That is; independent of the applied algorithm, the most important criteria was separation between two touching trees. When the space is less than one pixel, there is

no distinct brightness gradient on the image to be used to separate crowns. In other word, automatic delineation techniques require at least a distance of one pixel to separate neighboring trees. This would be important for accuracy assessment based on ground reference, because the composition and vertical structure of tree crowns that is observed from the ground can be different from those visible from above. It means, in a field measurement we may consider a small gap between trees as a clear separation. However, in a space observation, this gap cannot be shown due to a size of less than a pixel. Therefore, some of the errors in our work may come from this fact.

The results demonstrate that the proposed Watershed algorithm performs well in delineating tree crowns for larger trees while for small crowns the result was not satisfactory. In the Watershed method, 13.9% of trees were omitted while it was just 3.6% in the LoG method. Decreasing the number of omitted trees by the LoG method indicates that the spatial resolution of the QuickBird imagery was not a limiting factor for small tree detection.

The high omission error introduced by the Watershed method was due to two factors. First, in the pre-processing step, the NDVI image was selected to extract markers, since small trees with a low foliage density have a low NDVI value. Consequently their location were not identified properly in the marker function image and considered as background. Second, low contrast edges of small trees may generate small magnitude gradients which can not be detected properly by the Sobel edge detector. But, a significant improvement in the results can be achieved by thresholding the crown sizes. Increasing the minimum crown area to $>10 \text{ m}^2$, decreases the omission error dramatically to 3.1% of the trees. However, if delineation of the small trees is not interested, the Watershed algorithm gives a more acceptable result.

Splitting of large crowns to the small fragmentations due to large branches and inter crown shadows was rare. It seems that the spatial resolution of data used in this research (60 cm) and applied smoothing filters, were suitable to diminish the inter crown variation effects.

5.3 The image fusion methods

Six of the most common pixel-based image fusion techniques were applied and evaluated qualitatively and quantitatively in this research. Some methods showed clear advantages over other methods. These results were obtained from the examining QuickBird imagery over a forested area. It should be noted that the results from different fusion methods are strongly dependent on the types of regions contained in the imagery and sensor characteristics. Good results of a particular method in a forested area may not valid for example, for an urban area and vice versa. Furthermore the evaluation of the fusion results depends on the application of fused data for instance when enhancing the visual properties of data is considered for visual interpretation purposes the definition of quality may be different from the case that the data are fused for digital image classification. In this research enhancing all aspects of fused data was desirable. Therefore, general and global evaluation techniques were applied to assess all properties of fused data. From the visual inspection, the color distortion in the fused IHS and Brovey QuickBird sub images is more noticeable than the original color composites (Figure 4.2). As the Brovey method uses a ratio technique and changes the DN values considerably, the statistical characteristics of the fused multispectral images show high differences to the original one. The Brovey method can achieve higher spatial results but preserve less spectral fidelity. The IHS method, as also stated by Yocky (1996) distorts the colors (with red darkening). The reason could be because the intensity image that was replaced by the Pan was not equivalent to the Pan image. Moreover, various intensity images can be obtained from the applied QuickBird band combination. For instance the intensity image of QuickBird bands 1, 2, 4 is different from the intensity image of QuickBird bands 2, 3, 4 and both have large differences to the Pan image. The quantitative analyses also confirmed the findings of the visual inspection. A comparison to the other fusion methods reveals that color information is better preserved in the Ehlers method than in the standard IHS method. One possible reason may be because of improved capability of the Ehlers method by using multiple IHS transforms which make it possible to include more than 3 bands until the number of bands is exhausted (Klonus *et al.*, 2008). In this way the intensity component becomes much more equivalent to the panchromatic image. Moreover, as declared by Ling *et al.* (2006) in the standard IHS method some low

frequency information of the intensity component is lost in fused images due to replacement of the intensity component by whole panchromatic image. Consequently the color information of the original image is modified by the panchromatic image. While in the Ehlers method because the high frequency part of the panchromatic image is fused to the multispectral image the color information is better preserved in fused images.

Visual and statistical comparisons demonstrated that poor results were obtained by the PC + Wavelet method. Possible reasons could be related to the shift variant and the number of applied decomposition levels. Based on the Mallat description (1989) the Discrete Wavelet Transform (DWT) acts as a set of high and low pass filters and downsampling of the convolved images. DWT of an image produces four output images, which increases the data volume fourfold. The DWT downsamples each coefficient image by the factor of two to balance the increment of data volume. Thus each decomposition level results in losing information and the transform is termed as shift variant. As Bradley (2003) stated the shift invariant means any small shift in input can cause large changes in reconstructed waveforms especially when coefficients are not included in the IDWT. This sometimes leads to spatial artifacts (blurring, shadowing) in the fused image.

Visual comparison of the resulting images shows a close similarity between the Gram-Schmidt and PCA methods but the statistical metrics indicate a somewhat better preservation of the spectral properties by the PCA method. The PCA method distorted the spectral characteristics of the data the least. However the IHS, PCA and Gram-Schmidt methods work with a component substitution strategy but the PCA method can combine Pan with all QuickBird multispectral bands at the same time. The Gram-Schmidt method functions in a similar manner and constructs the simulated panchromatic band exploiting the mean of all the multispectral bands. Consequently, the first principal component and the first Gram-Schmidt component are more equivalent to Pan than the intensity component.

5.4 Regression analysis

The regression results between tree height and crown area were rather poor. Visual inspection of the regression line revealed that these data don't have such a strong

relationship and single regression can not estimate tree height well. One reason for the poor results is that crown sizes are highly variable while tree heights are relatively uniform without marked variation. Several small trees may be combined and make one big crown while one single large tree can produce the same crown size. Thus increasing the crown area may lead to increase the tree height especially for small crowns but it stops in one point and after that with increasing the crown area tree height does not increase. These results proved that predicting individual tree height from measuring crown area or crown diameters is not a powerful approach for the tree species in the Zagros forests.

5.5 Comparison with other research

Comparing obtained results of the current study with other studies, despite the similarity of the applied delineation methods, is not a fair comparison, because conditions under which those analyses were performed are not the same as conditions used in our study. These conditions include spatial and spectral resolution, the sun-sensor geometry, forest structure and accuracy assessment methods which have a significant influence on the outcome of the tree delineation process. The literature of crown delineation covers a high variety of sensors with different spatial resolution ranging from 0.1 m to 1 m (Table 1.1). The spatial resolution in relation with the forest type and crown size dictates the success of delineation algorithms. Omission errors caused by small trees as well as commission errors due to over-segmentation of large crowns are errors mainly related to spatial resolution. However, the probability of correctly detecting small trees and trees in close proximity at finer spatial resolution is higher. But, for large crowns, fine scales tend to increase the within-crown brightness variability, leading to false crown delineation. At coarser spatial resolution large crowns are delineated properly while smaller trees may be missed or trees in close proximity of neighbors may be detected as a single crown. Pouliot *et al.* (2002) examined various spatial resolutions from 5 to 30 cm pixel sizes to determine the most appropriate spatial resolution to use for crown delineation of 6-year-old trees. As expected, they conclude that delineation accuracy is more sensitive to image resolution, decreasing consistently and nonlinearly with increasing spatial resolution.

From the literature, there are several sensors (i.e. MEIS II, CASI, and IKONOS) with various spectral resolution that have been used for delineating individual tree crowns. Spectral information provided by hyperspectral sets of bands, can increase the accuracy of the delineation and discrimination of the neighboring tree species comparing to the gray scale images. Moreover, higher spectral resolution makes it possible to use different ratio and synthetic bands which may increase the separability of different trees from each other and from background. Color segmentation methods can exploit the variation of color within the tree crown and among trees to improve individual tree crown delineation comparing to the segmentation methods that work based gray scale images (Erikson, 2004).

Sun-sensor geometry has strong effects on both radiometric and geometric properties of tree crowns. Sun elevation varies not only in different latitude but time of day and time of year. This variation can not be fixed among different crown delineation studies which have been done in different time and locations. Changes in sun angle or direction will result in different shadow size and orientation, which may result smaller trees become hidden in the shadow of larger crowns. Wulder *et al.* (2008) showed that a change in view angle causes not only apparent change in the position of tree crowns, but also on the shape and size of the crowns. In general, the best delineation accuracy can be achieved with small off-nadir view angles. The assumption that tree tops are located around the vicinity of the center of a crown can be met only when the view angle is $\pm 15^\circ$ off-nadir (Wang *et al.*, 2004).

The vertical and horizontal structure of the forest in conjunction with the forest type control the visibility and separability of tree crowns in the images. In general, delineation of coniferous forests with mono-layered structure is much easier than uneven-aged deciduous forests with multi-layered structure (Warner *et al.*, 1998). According to recent publications (Leckie *et al.*, 2005; Bunting and Lucas, 2006) delineations are less successful as the structural complexity of the forest increases. Lower accuracies are expected for the forests with greater density and proximity of crowns.

The evaluation procedures applied either for tree detection or crown delineation can be mainly divided into two groups: individual tree assessment and aggregated assessment.

The first group utilizes more detailed information such as the number of individual trees or the area of the individual crowns to compare tree by tree with a reference. The second group of evaluation utilizes the aggregated estimates that are obtained by averaging the results of automated crown delineation or tree detection in the plot or the given area. In some studies aggregated estimates were used and in the other individual assessments. Aggregated estimates generally provide higher accuracies than individual estimates (Pouliot *et al.*, 2002).

The wide range of applied accuracy evaluation methods makes it difficult to directly compare different studies. Accuracy assessment methods which developed for evaluating tree detection results are simple, easy to be implemented and require few input parameters. For instance Accuracy Index (AI) that was proposed by Pouliot *et al.* (2002) only counts the number of perfect match, omission and commission errors. While the crown delineation accuracy assessment methods are very complicated and require precise measurements of tree crown characteristics such as area, diameter and boundary. For example Correctness and Completeness are two accuracy measures which proposed and applied by Straub & Heipke (2007) for evaluating the delineation results. These two accuracy measures were developed based on three overlapping configurations between GRS and CGS, see section (2.5.3) for more details. Pouliot *et al.* (2002) used crown diameters of two different directions and individual tree positions to evaluate crown delineation and tree detection accuracy respectively at plot and stand level. The crown area provides an ideal means to evaluate the delineation accuracy. However few studies to date have conducted such validation. Culvenor *et al.* (1998) evaluate TIDA performance on simulated forest imagery using average crown area. The delineation results were compared with the crowns of known area that served as reference data. The average area of the delineated crowns was 61 m^2 , compare with 67 m^2 for average area of simulated crowns. Tree-for-tree isolation accuracy assessment which is the most complicated and precise area based method was proposed and applied by Leckie *et al.* (2004). This accuracy considers not only the number of matches but how well each automated delineated crown represents the reference. They defined a categorization of 20 different configuration types based on the quantity and the number of the overlaps

between automatically delineated and the reference crown. Approximately 56 –73% of the trees had a good match between manual and automated delineations. Since there is not a unique way for representing the accuracy of different studies, comparing the outcomes of this work with the other studies is not easy even if the same delineation methods were applied.

Another important factor is the precision and reliability of reference data. There are two ways to provide the reference data for accuracy assessment of automated crown delineation. One is based on visual interpretation of high resolution imagery and the other is by field measurements. In the literature there are few authors that applied field measurements due to the difficulty, and associated costs and errors of identifying and locating individual trees (Bunting & Lucas, 2006; Wulder *et al.*, 2000). Whiles, manually interpreted reference data are more common since it is easier and cheaper to be implemented (Gougeon, 1995; Gougeon & Leckie, 1998). It is obvious that the studies which applied manually interpreted reference for accuracy assessment tend to have higher accuracy than studies which applied field based reference. Because when the reference was provided by visual interpretation, errors relating to the tree positioning, crown projection, separating tightly overlap or clumped crowns are minimized.

Although the above mentioned conditions (i.e. spatial and spectral resolution, the sun-sensor geometry, forest structure and accuracy assessment methods) precluded the capability of making rigorous comparisons among different studies, it was still of interest to compare our work with other research results. In the following, where possible, two studies with at least one equivalent property with the current study were selected to be compared.

Leckie *et al.*, 2005 used two datasets of CASI imagery with a pixel size of 70 cm. CASI imagery was obtained on two occasions, one in 1996 and the second in 1998 over a multi species old coniferous forest in British Columbia, Canada. Trees were delineated with the valley following approach of the Individual Tree Crown (ITC) software suite. Tree-for-tree accuracy assessment was applied. For the 1996 and 1998 data, 59% and 47% of the ground reference trees within the plots were considered as a good match respectively. Only six trees in the 1996 data were missed, seven trees were split into two or three

crowns. Only two trees were omitted for the 1998 data, 20 trees split into two crowns. Both dates of imagery had high rates of commission errors (25%).

The marker controlled Watershed segmentation and LOG methods were presented in this study. Based on the definition of Leckie *et al.*, 2005 good matches consist of correspondence types 1, 2, 4.1, 4.2 as of appendix 1; 62.1% and 54.4% were good matches for the LoG and the Watershed methods respectively. The LoG method only 2 trees were split and 8 trees missed. For Watershed method 31 trees omitted and 3 trees were split into two or more crowns.

Wang *et al.* (2004) used a two-stage approach with edge detection followed by marker-controlled watershed segmentation to delineate individual tree crowns in an 80-years old coniferous forest. The method used the prior information of the actual number of trees in the image. The CASI imagery with the nominal spatial resolution of 0.6 m was collected in October 1996 over British Columbia, Canada. The accuracy of the automatic method was assessed from using manual delineation and average agreement accuracy assessment method. Comparison showed that about 75.6% of the total pixels are classified identically (crown or non-crown). They found that misclassification was primarily associated with large, circular shaped clumps in the image. The algorithm detected most of the visually interpreted tree crowns.

The average agreement accuracy assessment method was applied to calculate the accuracy of detected crowns using field measured ground truth for the current study. This accuracy assessment showed about 97% average agreement for both the marker controlled Watershed and LoG methods. This accuracy measure utilizes the area of both individual tree crowns and the background. In the Zagros forest trees are in a large distance therefore a large proportion of the total area is covered by background. Most of the background is consisted of bare soil which has a great chance to be classified correctly. It is obvious that when a large class is classified correctly the overall accuracy will increase. Therefore, comparing to the Wang *et al.*, research the average agreement increased in the current study. The average agreement accuracy assessment method can not provide a reliable base for reporting or comparing the accuracy of the tree crown delineation methods since the accuracy of other objects such as background can alter the

average accuracy of the crown delineation. Moreover this method does not use overlapping configurations between GRS and CGS.

In the following accuracy index (AI) was used as a base for comparing previous research results with this study (see section 3.7). The results of other studies were converted to AI where it was possible. Brandtberg and Walter (1998) applied edge detection at multiple scales for estimating each tree crown area in mature and naturally regenerated mixed European forests. Aerial color infrared images with pixel size corresponding to 10 cm on the ground were used. Reported accuracy was AI = 52% with ground truth which was measured on sample plots. The method had trouble to detect non circular crowns. A considerable number of hidden trees, or trees standing very close to each other was indicated in ground truth that were not possible to be detected. Pouliot *et al.* (2002) developed the Local Maximum Refinement and Delineation Algorithm (LMRDA) package, which consists of two separate programs for automated detection and delineation of individual crowns in coniferous forest regeneration. It achieved a best result AI of 90% for 15 cm spatial resolution airborne imagery as compared to the field delineation. Wulder *et al.* (2000) observed an AI of 51% using variable window-size LM filter on airborne multispectral MEIS-II imagery with 1-m spatial resolution. Study areas were a 40-year-old plantation and a 150-year-old naturally regenerating mature coniferous stands. Tree crown locations from the different filtering combinations were compared to a detailed digital ground survey stem map. Erikson (2003) used a region growing approach to find trees in color infrared aerial images with pixel size of 10 cm on the ground. The study area consisted of both pure and mixed naturally regenerated and mainly mature stands. Comparing with the manual delineated reference data an AI \approx 85% was reported. However the results do not include the regions found in the background. Individual tree detection accuracy for the Watershed method was AI = 48% and for the LoG method was AI \approx 60%. These results show that applied algorithms produced individual tree detection accuracies within the range of the cited studies. As mentioned before the obtained accuracy is highly dependent on the specific conditions.

5.6 Wider application of the delineation algorithms

Most of the tree crown delineation algorithms are developed for a certain forest type and condition. For instance Pouliot *et al.* (2005) developed an algorithm for automated detection-delineation of coniferous tree regeneration, Culvenor (2002) developed tree identification and delineation algorithms for application to imagery of native Eucalypt forests in Australia, Warner *et al.* (2006) proposed a shadow-based delineation program for identifying trees in imagery of a closed canopy, deciduous forest, in West Virginia, USA. In the current study two different crown delineation procedures were applied to delineate individual trees in deciduous forests in Zagros area. These forests are relatively open and structurally complex in terms of crown shape and size. The approaches adapted in this study are also recommendable to be applied in arid and semi arid forests for forest mapping and monitoring purposes. Arid and semi-arid regions of Iran are affected by the process of desertification. The UN Convention to Combat Desertification (UNCCD) defines desertification as: “land degradation in arid, semiarid and sub-humid tropics caused by a combination of climatic factors and human activities.” A critical consequence of desertification is vegetation loss and reduction of productive capability of land. For long-term desertification monitoring and assessment arguments built upon reliable benchmarks and indicators are required. Vegetation indicator is among the most important indicators to assess desertification which can potentially be obtained using individual tree based information. Moreover, application of the delineation methods to the remote sensing data archives allows both spatial and temporal trends in degradation to be determined.

In Iran, the main forestry activity aimed at combating desertification is afforestation. Since 1965, two million hectares have been successfully planted mainly by *Haloxylon* spp. (Ferydoony –Nasry, & Rahbar, 2004) in the wide range of areas with the high risk of desertification. A prerequisite for a successful plantation program is to put the plantation under a proper monitoring program. The algorithms applied in this study have the potential to provide valuable information regarding crown size, tree species, and tree distribution patterns of forest plantations in arid areas. The procedures outlined in this study in conjunction with multispectral capability of QuickBird imagery may provide a

good opportunity for individual tree based health monitoring of forest plantations in arid areas.

Another promising application may be achieved in assessing and mapping Tree Resources Outside Forests (TROF). The Food & Agricultural Organization (FAO) of the United Nations defines (TROF) as “trees on land not defined as forest and not as other wooded land”. A detailed discussion concerning definition and classification of (TROF) can be found in Kleinn (2000). The tree resources outside forests not only serve many ecological functions, such as biodiversity conservation, protection of soil and water resources, contributions to the scenic beauty of the landscape and carbon sequestration, but also many economic functions, such as wood and non-wood products (Kleinn *et al.*, 2001). The TROF exhibit a variety of different shape and spatial patterns ranging from single scattered isolated trees, linear patches to the groups of trees which actually form clusters of different shapes. It includes woody vegetation like date palm, citrus trees, orchards, poplar plantations, linear plantation along roads, rivers and canals. These distributions are similar as that of Zagros forests. The delineation approaches in this study have been optimized for variable tree crown shape and sizes, in open forests but satisfactory results could potentially be achieved in forest plantations and orchards (e.g., date palm plantations in South, South East, and South West of Iran) which support more regularly shaped crowns with a certain space between individual trees. However, the approaches developed for the Zagros forests based on single species and mono-layered open structure are likely to be less applicable to the uneven-aged and multi-layered dense forests in the North of Iran.

Some factors contributed to the successful performance of the delineation approaches over the forests occurring in Dasht-e Barm. In particular, the Zagros forests are open and many individual trees, tree clusters or groups of trees are separated by large gaps which may be covered by any type of herbs, cultivation or bare soil. Fortunately, QuickBird images were acquired over a period of time when rainfed crops were harvested and the grass and herbs were dried so that there were no green ground covers of grasses and herbaceous plants. Under this condition, an NDVI mask was applied successfully to eliminate the background. It is obvious that the performance of the NDVI mask is less

successful in the forest environments where surface vegetations or under canopy cultivations are existed. Alternative methods of discrimination are necessary to be developed for these conditions.

Chapter 6

Summary

Forest information procurement and inventory are integral components of target oriented planning and decision making in forest management and forest policy. Depending on the specific circumstances of the resource, different combinations of data sources are employed. This thesis research analysed the options provided by high resolution satellite imagery (e.g. QuickBird) for the inventory and mapping of the forest resource, on an individual tree basis, in the open and dry forests of the Zagros Mountains in southwest Iran.

The continued advancements in satellite sensor technologies have increased the potential use of satellite data in the context of the individual tree crown delineation. The new generation of earth observation satellites like OrbView-3, QuickBird-2, and IKONOS are simultaneously capturing high resolution panchromatic and lower resolution multispectral images. In the first phase of this study, a number of pixel-based image fusion techniques were used to increase the spatial resolution of multispectral bands. Spectral and spatial quality of the fused images was indeed the most important feature of the crown delineation process. A quality assessment was performed with statistical and visual metrics. This assessment revealed that the techniques based on the component substitution strategy (i.e. PCA, GS) performed better than the others, with the PC + Wavelet method showing the weakest results. Some information loss and distortions are unavoidable in the fusion process. Nevertheless, the fused data has enough spatial information required for individual tree level analysis. Due to the presence of the near-infrared spectral band, with fused data, it was possible to provide ratio bands as well as synthetic bands. The effects of background were mitigated by using the NDVI mask. The first principal component (PC1) provided the optimal exploitation of spatial and spectral information for the delineation process.

Very high spatial resolution QuickBird imagery with good spectral quality and efficient geometric correction provides excellent possibilities for tree-scale analysis. The second phase of this study involved our attempts to adapt the delineation techniques to derive tree based information in Zagros forests. These techniques should be able to delineate individual crowns with variable shapes and sizes in sparse stands. To this end, we applied the marker controlled watershed method and the LoG method. The marker controlled watershed method effectively combines the edge detector method, the local maximum, and the watershed segmentation techniques to produce individual crown segments. The success of the watershed segmentation method relies on the existence of reliable markers for each crown. Since we explicitly used the NDVI image to extract markers, the delineation of small trees with low NDVI values was not promising. The LoG method combines global thresholding, to identify the brightness delimiter between background and adjacent crowns, and the Laplacian of Gaussian filter, to extract significant edges. In this method, crowns with light signals and low contrast with background could not be detected properly. For the data sets studied, the LoG method was found to be better suited than the marker controlled watershed method. Therefore, if we had to choose a delineation method for such conditions, we would recommend the LoG method. The obtained results also suggest that, if small crowns are neglected we can reasonably assume that the difference between these two methods is small. Overall, the accuracy of both methods is promising, especially considering the strict criteria used in accuracy assessment. The results of this study showed that individual trees or clusters of trees can be automatically delineated with high accuracy in sparse forests.

This study described the wide capabilities of QuickBird imagery for individual tree crown delineation in the open forests of the Zagros region. There are still several open questions, for example how to document the potential of QuickBird in different acquisition and forest types, such as more heterogeneous stands, complex topography and on sloping and rough terrain. In this research, we selected flat terrain for crown delineation. However, to a large extent, the Zagros forests are located on a mountainous landscape. Sun-target-sensor geometry, in conjunction with topography affects the orientation, shape and size of individual crowns. Since a single date image was applied in this research, it was not feasible to systematically investigate and analyse the effects of

sun-target-sensor geometry. However, promising results were obtained here with single date imagery. Further research, based on images acquired with multi-view angle is needed to determine the best time and view angle for tree crown extraction in this area. Moreover, various methods for topographic effects correction have been proposed. How to deal with spectral and spatial distortions due to topographic effects is a challenge for future research.

There are numerous avenues of future research for high resolution satellite imagery. Perhaps the most interesting is to combine QuickBird imagery with laser data, to improve individual crown segmentation results, to precisely measure the height of the individual trees, and to estimate the above ground biomass in this area with an integrated remote sensing and field sampling approach.

Improving the delineation methods applied in this study is also a possible path for future research. As previously mentioned, the markers are found using an NDVI image. The design of more robust marker detection is required for successfully delineating both small and large crowns by the watershed method.

Certainly, incorporating the spectral information in the segmentation process is one of the future research plans. By including the color component of the image, the edge detector would be able to detect edges in regions with high color variations. Also, color information of the tree crown, in conjunction with shape information of the corresponding segment, provides a good basis for species classification of individual trees. QuickBird, with its spectral resolution in near-infrared, red, green, and blue, has a good potential also for forest health monitoring.

A standard and universally accepted method to assess the accuracy of individual crown delineation has not yet been introduced. The crown by crown method applied in this research is probably the most complete and powerful technique. This method not only determines the number of matches but also describes how well two segments cover each other. The development of a unique accuracy assessment method is an urgently required research area for the improvement of individual crown delineation processes.

From the forest manager's point of view, very high spatial resolution data offers detailed information such as tree species, tree crown area, tree crown location, and the capability for monitoring of individual trees over time. Individual tree based information can also be used to scale up to the stand and forest level. Consequently, stand attributes can be estimated precisely and can support monitoring and management of forests with higher levels of accuracy than with traditional medium resolution sensors. Very high-spatial resolution remote sensing will be a core component of precision forestry.

Appendix 1 Categories of CGS – GRS overlap

(after Leckie *et al.*, 2004, modified)

Notes:

- 1:1 means a GRS only has one CGS associated with(overlapping) it and that CGS only has that GRS associated it.
- 1: n means a GRS has several CGSs associated with it.
- n :1 means an CGS has several GRSs associated with it.
- K is the area of CGS which occupied by the GRS.
- L is the area of GRS which occupied by the CGS.
- a minimum percent area of overlap is required before an CGS and GRS are considered associated (this was set at 5%, but can be changed).

A. (1:1)

(1) Perfect match (1:1)

- Only one CGS overlapping the GRS; that GRS is the only GRS associated with the CGS;

$$K = 50 - 100\%$$

$$L = 50 - 100\%$$

(2) Good matches (1:1)

(2.1) CGS too small

- Only one CGS overlapping the GRS; that GRS is the only GRS associated with the CGS; but the GRS covers most of the CGS (i.e., more than 85% of the CGSs area is occupied by the GRS).

$$K = 85 - 100\%$$

$$L = 20 - 50\%$$

(2.2) CGS too big

- Only one CGS overlapping the GRS; that GRS is the only GRS associated with the CGS; a very good 1:1 overlap of a CGS with the GRS, but the CGS is too big. Therefore, it is considered a good match.

$K = 20 - 50\%$

$L = 85 - 100$

(3) Poor matches (1:1)

(3.1) CGS too small

- Only one CGS overlapping the GRS; that GRS is the only GRS associated with the CGS; but the match is poor. Represents a case in which the GRS mostly covers the CGS, but the CGS is too small to cover most of the GRS.

$K = 50 - 85\%$

$L = 20 - 50\%$

(3.2) CGS too big

- Only one CGS overlapping the GRS; that GRS is the only GRS associated with the CGS; it is considered a poor match as the coverage of the GRS by the CGS is not good enough to compensate for the poor coverage of the CGS by the GRS.

$K = 20 - 50\%$

$L = 50 - 80\%$

(3.3) GRS inside CGS

- Only one CGS overlapping the GRS; that GRS is the only GRS associated with the CGS; but the match is poor. Represents a case in which the GRS is covered by CGS, but the GRS is too small to cover most of the CGS.

$K = 20 - 85\%$

$L = 85 - 100\%$

(3.4) CGS inside GRS

- Only one CGS overlapping the GRS; that GRS is the only GRS associated with the CGS; but the match is poor. Represents a case in which the GRS covers the CGS, but the CGS is too small to cover most of the GRS.

K = 85 – 100%

L = 20 – 85%

B. (1: n)

(4) Good matches (1: n)

(4.1) multiple minor

- One CGS overlapping the GRS; that GRS is the only GRS associated with the CGS. But GRS has a minor association with secondary CGS (i.e., less than 20% of the GRS is occupied by the secondary CGS).

K = 50 – 100%

L = 50 – 100 %

(4.2) multiple major

- Only one CGS overlapping the GRS; that GRS is the only GRS associated with the CGS. But other CGS have some significant (major) overlap with the GRS (i.e., between 20% and 50% of GRS is occupied by the secondary CGS).

K = 50 – 100%

L = 50 – 100 %

(5) Poor matches (1: n)

(5.1) Split

- A GRS that contains several CGS within it; more than 20% of the GRS must be occupied by each CGS and more than 50% of each CGS area is occupied by the GRS.

(5.2) Split (many small)

- A GRS that contains many small CGS within it; less than 20% of the GRS must be occupied by each CGS and more than 50% of each CGS area is occupied by the GRS.

(5.3) Split (one dominant)

- A GRS that contains many small CGS within it but one of the CGS is not small (i.e., more than 20% of the GRS is occupied by the dominant CGS).

(5.4) Omission (complete, pure; 1:0)

GRS with no overlap with any CGS

(5.5) Omission (impure) (1:1 or 1: n omission)

– GRS with some CGS that have only a small overlap with the GRS; an almost 1:0 pure omission, but with one to three CGS occupying only a small area (less than 20%) of the GRS; the second and third most dominant CGSs must not have more than 50% of their area occupied by the GRS.

C. (n: 1)

(6) Good matches (n: 1)

(6.1) (multiple minor)

- Only one CGS overlapping the GRS; that GRS is the only GRS associated with the CGS. But CGS has a minor association with secondary GRS (i.e., less than 20% of the CGS is occupied by the secondary GRS).

$K1 = 50 - 100\%$

$L1 = 50 - 100\%$

$K2 < 20\%$

(6.2) (multiple major)

- Only one CGS overlapping the GRS; that GRS is the only GRS associated with the CGS. But other GRS have some significant (major) overlap with the CGS (i.e., between 20% and 50% of CGS is occupied by the secondary GRS).

K1 = 50 – 100%

L1 = 50 – 100 %

K2 = 20 – 50%

(7) Poor matches (n: 1)

(7.1) grouped

– A CGS that contains several GRS grouped within it; more than 20% of the CGS must be occupied by each GRS and 50 -100% of each GRS area can be occupied by the CGS.

(7.2) grouped (many GRS in a CGS; severely grouped/under separated CGS)

–A CGS that contains many small GRS within it; less than 20% of the CGS must be occupied by each GRS and more than 50% of each GRS area is occupied by the CGS.

(7.3) commission (complete, pure; 0:1)

– CGS with no overlap with any GRS

(7.4) commission (impure) (1:1 or n:1 commission)

– CGS with some GRS that have only a small overlap with the CGS; an almost 0:1 pure commission, but with one to three GRS occupying only a small area (less than 20%) of the CGS; the second and third most dominant GRS must not have more than 50% of their area occupied by the CGS.

References

Acerbi-Junior, F.W., Clevers, J.G.P.W., & Schaepman, M.E. (2006). The assessment of multi-sensor image fusion using wavelet transforms for mapping the Brazilian Savanna. *International Journal of applied Earth Observation and Geoinformation*, 8(4), 278 – 288.

Ahmadi Sani, N., Darvishsefat, A.A., Zobeiri, M., & Farzaneh, A. (2006). Potentiality of ASTER images for forest density mapping in Zagros. *The 13th Australasian Remote Sensing and Photogrammetry Conference*.

Aiazzi, B., Alparone, L., Baronti, S., & Selva, M. (2006). MS + Pan Image Fusion by an Enhanced Gram-Schmidt Spectral Sharpening, 26th EARSeL Symposium, Warsaw, Poland, 29May-2 June.

Alparone, L., Aiazzi B., Baronti S., Garzelli A., & Nencini F. (2006). Information-Theoretic Image Fusion Assessment Without Reference. 4th. *ESA- EUSC conference on Image Mining*, Madrid Spain.

Bai, Y., Walsworth, N., Roddan, B.D., Hill, A., Broersma, K., & Thompson, D. (2005). Quantifying tree cover in the forest grassland ecotone of British Columbia using crown delineation and pattern detection. *Forest Ecology Management*, 212, 82-100.

Banerjee P., Zetu D. (2001). *Virtual Manufacturing: Virtual Reality and Computer Vision Techniques* John Wiley and Sons, ISBN 0471354430, 9780471354437, 320 pages.

Becker, G. (2001). Precision forestry in central Europe – new perspectives for a classical management concept. In: *Proc. Of the First International Precision Forestry Symposium*, Seattle, Washington. 6-9.

Beucher, S., & Lantuéjoul, C. (1979). Use of watersheds in contour detection. In: *Proceeding of International Workshop on Image Processing, Real-Time Edge and Motion Detection/Estimation*. Rennes, France, 17-21.

Bhanu, B., & Lee, S. (1994). *Genetic Learning for Adaptive Image Segmentation*. Springer, ISBN 0792394917, 9780792394914 , 271 pages.

Bieniek, A., & Moga, A.N. (2000). An efficient watershed algorithm based on connected components. *Pattern Recognition*, 33(6). 907-916.

Bovik A. C. (2005). *Handbook of Image and Video Processing*. 2 edition, Published by Academic Press, ISBN 0121197921, 9780121197926, 1372 pages.

De Bock, J.D., & Philips, W. (2007). Line Segment Based Watershed Segmentation. In *Proceedings of MIRAGE*, 579-586.

Bradley, A. (2003). Shift-invariance in the discrete wavelet transform. In *proceedings of VIIth Digital Image Computing: Techniques and Applications*, Sun C., Talbot H., Ourselin S. and Adriaansen T. (Eds.), 10-12 Dec., Sydney, 29–38.

Brandtberg, T. (1999a). Algorithms for structure- and contour-based tree species classification using digital image analysis. In *Proceedings of the International Forum on Automated Interpretation of High Spatial Resolution Digital Imagery for Forestry*, Victoria, B.C., 10–12 February 1998. Canadian Forest Service, Natural Resources Canada, Victoria, B.C., 199–205.

Brandtberg, T. (1999b). Automatic individual tree-based analysis of high spatial resolution aerial images on naturally regenerated boreal forests, *Canadian Journal of Forest Research*, 29, 1464-1478.

References

- Brandtberg, T. (1999c). Remote sensing for forestry applications – a historical retrospect. (http://www.dai.ed.ac.uk/CVonline/LOCAL_COPIES/BRANDTBERG/UK.html)
- Brandtberg, T. (2002). Individual tree-based species classification in high spatial resolution aerial images of forests using fuzzy sets. *Fuzzy Sets and Systems*, 132, 371–387.
- Brandtberg, T., & Walter, F. (1998). Automated delineation of individual tree crowns in high spatial resolution aerial images by multiple-scale analysis. *Machine Vision and Applications*. 11(2), 64-73.
- Bräunl, T., Feyrer, S., Rapf, W., & Reinhardt, M. (2001). *Parallel Image Processing*. Springer, ISBN 3540674004, 9783540674009, 203 pages.
- Bunting, P., & Lucas, R. (2006). The delineation of tree crowns in Australian mixed species forests using hyperspectral Compact Airborne Spectrographic Imager (CASI) data. *Remote Sensing of Environment*, 101(2), 230-248.
- Cates, J.E., Whitaker, R.T., & Jones, G.M. (2005). Case study: an evaluation of user-assisted hierarchical watershed segmentation. *Med. Image Anal.* 9(6), 566-578.
- Chatterjee, S., & Hadi, A. (2006). *Regression Analysis by Example*. John Wiley & Sons, Ltd. ISBN: 978-0-471-74696-6, 375 pages
- Chavez, P.S., Sides, S.C., & Anderson, J.A. (1991). Comparison of three different methods to merge multiresolution and multispectral data: Landsat TM and SPOT Panchromatic. *Photogrammetric Engineering and Remote Sensing*, 57 (3), 295-303.
- Chen, C.H., (2008). *Image Processing for Remote Sensing*. Published by CRC Press, 2008, ISBN 1420066641, 9781420066647, 400 pages.
- Choi, M.S., & Kim, W.Y. (2002). A novel two stage template matching method for rotation and illumination invariance. *Pattern Recognition*, 35(1), 119-129.
- Chubey, M.S., Franklin, S.E., & Wulder, M.A. (2006). Object-based Analysis of Ikonos-2 Imagery for Extraction of Forest Inventory Parameters. *Photogrammetric Engineering & Remote Sensing*, 72(4), 383-394.
- Coops, N.C., Johnson, M., Wulder, M.A., & White, J.C. (2006). Assessment of QuickBird high spatial resolution imagery to detect red attack damage due to mountain pine beetle infestation. *Remote Sensing of Environment*, 103(1), 67-80.
- Culvenor, D.S. (2002). TIDA: an algorithm for the delineation of tree crowns in high spatial resolution remotely sensed imagery, *Comput. Geosci.* 28, 33-44.
- Culvenor, D.S. (2003). Extracting individual tree information: a survey of techniques for high spatial resolution imagery. In *Remote sensing of forest environments: concepts and case studies*. Edited by M.A. Wulder and S.E. Franklin. Kluwer Academic Publishers, Boston, Mass, 255-277.
- Culvenor, D.S., Coops, N., Preston, R., & Tolhurst, K.G. (1998). A spatial clustering approach to automated tree crown delineation. In D. A. Hill, D. G. Leckie (Eds.), *Proceedings of the International Forum on Automated Interpretation of High Spatial Resolution Digital Imagery for Forestry* (pp. 67– 80). Victoria, BC: Canadian Forest Service, PacificForestry Centre.
- Darvishsefat, A.A., & Saroei, S. (2003). Evaluation of the potential of Landsat ETM+ for forest density

- mapping in zagros forests of Iran. *Geoscience and Remote Sensing Symposium*, 2003. IGARSS Proceedings. IEEE International, 4, 2529-2531.
- De Wulf, R.R., & Goossens, R.E. (1990). Extraction of forest. Stand parameters from panchromatic and multispectral SPOT-1. data, *International Journal of Remote Sensing*, 8, 1571-1575.
- Descombes, X., & Pechersky, E. (2006). Tree Crown Extraction using a Three States Markov Random Field, Research Report, INRIA, France, 5982, 14 pages.
- Devereux, B.J., Amable, G.S., & Costa Posada, C. (2004), An efficient image segmentation algorithm for landscape analysis. *International Journal of Applied Earth Observation and Geoinformation*, 6 (1), 47-61.
- Dixon, T.D., Canga, E.F., Noyes, J.M., Troscianko, T., Nikolov, S.G., Bull, D.R., & Canagarajah, C.N. (2006). Methods for the assessment of fused images, *ACM Transactions on Applied Perception (TAP)*, 3(3), 309-332.
- Dou, W., Chen, Y.H., Li, X. B., & Sui, D. Z. (2007). A general framework for component substitution image fusion: An implementation using the fast image fusion method. *Computers & Geosciences* 33, pp219-228.
- Dralle, K., & Rudemo, M. (1996). Stem number estimation by kernel smoothing in aerial photos. *Canadian Journal of Forest Research*, 26, 1228-1236.
- Dralle, K., & Rudemo, M. (1997). Automatic estimation of individual tree positions from aerial photos. *Canadian Journal of Forest Research*, 27, 1728-1736.
- Dyck, B. (2003). Precision forestry-The path to increased profitability in. Proc. Precision Forestry Conf., Seattle, WA, Jun. 15-17, pp. 3-8.
- Ehlers, M. (2005). Beyond Pansharpening: Advances in Data Fusion for Very High Resolution Remote Sensing Data, *Proceedings, ISPRS Workshop 'High-Resolution Earth Imaging for Geospatial Information'*, Hannover
- Ehlers, M., Greiwe, A., & Tomowski, D. (2006). On image fusion and segmentation. 1st International Conference on Object-based Image Analysis. Salzburg University, Austria
- El-Moslimany, A. (1986). Ecology and late Quaternary history of the Kurdo-Zagrosian oak forest near Lake Zeribar, Kurdistan (western Iran). *Vegetatio*, 68, 55-63.
- Erikson, M. (2003). Segmentation of individual tree crowns in colour aerial photographs using region growing supported by fuzzy rules. *Canadian Journal of Forest Research*, 33, 1557-1563.
- Erikson, M. (2004). Species classification of individually segmented tree crowns in high-resolution aerial images using radiometric and morphologic image measures. *Remote Sensing of Environment*, 91, 469-477.
- FAO, (2002). Twenty-Sixth FAO Regional Conference for the Near East. Tehran, Islamic Republic of Iran, 9 - 13 March. Available in <http://www.fao.org/DOCREP/MEETING/004/Y2687E.HTM>.
- Fattahi, M. (2003). Forest management trends in the Zagros region of Iran. XII world forestry congress, Quebec, Canada.
- Ferydoony -Nasry, M. & Rahbar, E. (2004). Effect of thinning on growth and vigourity of Haloxylon spp. plantation in Gonabad. *Iranian Journal of Range and Desert Research* Vol. 11 No. 1, 19-30. (in Persian)

- Florencio, D.A., & Schafer, R.W. (1994). Decision-based median filter based on local signal statistics, Proceedings of VCIP'94, SPIE Vol.2308, pp.268-275.
- Fox, L., Garrett, M.L., Heasty, R., & Torres, E. (2002). Classifying wildlife habitat with pan-sharpened Landsat 7 Imagery. Proceedings of the ISPRS Commission I Symposium and Pecora 15/Land Satellite Information IV Conference
- Franklin, J., & Turner, D.L. (1992). The application of a geometric optical canopy reflectance model to semiarid shrub vegetation, IEEE Transactions on Geoscience and Remote Sensing, 30(2), 293-301.
- Franklin, S.E., & Mcdermid, G.J. (1993). Empirical relations between digital SPOT-HRV and CASI spectral response and Lodgepole Pine (*Pinus contorta*) forest stand parameters, International Journal of Remote Sensing, 14(12), 2331–2348.
- Fu, K.S., & Mui, J.K. (1981). A survey on image segmentation. Pattern Recognition Letter, 13, 3-16.
- Fuchs, H.-J. (2005). Methods for the assessment of forest trees using digitized large-scale colour infrared aerial photos. In: C. Kleinn, J. Nieschulze and B. Sloboda, Editors, GGRS Proceedings: Göttingen GIS & Remote Sensing Days, Remote Sensing and Geographical Information Systems for Environmental Studies—Applications in Forestry Göttingen, Germany, p 35-42.
- Fuchs, H.-j. (2003). Methodische Ansätze zur Erfassung von Waldbäumen mittels digitaler Luftbilddauswertung. Dissertation university Göttingen. Available in <http://webdoc.sub.gwdg.de/diss/2004/fuchs/fuchs.pdf>
- Gadow, K. v. & Hui, G.Y., (1999). Modelling forest development. Kluwer Academic Publishers, Dordrecht: 212 pages.
- Gemmell, F. (1998). An Investigation of Terrain Effects on the Inversion of a Forest Reflectance Model. Remote Sensing of Environment, 65(2), 155-169.
- Ghazanfari, H., Namiranian, M., Sobhani, H., & Mohajer, M. R. M. (2004). Traditional forest management and its application to encourage public participation for sustainable forest management in the northern Zagros Mountains of Kurdistan province, Iran. Scandinavian Journal of Forest Research, 19(4), 65–71.
- Gonzalez R.C., Woods R. E. (2007). Digital Image Processing. Prentice Hall, ISBN 013168728X, 9780131687288, 954 pages.
- Gonzalez, R.C., & Woods, R.E. (2002). Digital Image Processing, (second ed.), Prentice-Hall, ISBN 0201180758, 9780201180756, 793 pages.
- Gonzalez, R.C., & Woods, R.E., Eddins, S.L. (2003). Digital Image Processing Using MATLAB, Pearson Prentice Hall, ISBN 0130085197, 9780130085191, 609 pages.
- Goodwin, N., Turner, R., & Merton, R.N. (2005). Classifying Eucalyptus forests with high spatial and spectral resolution imagery: an investigation of individual species and vegetation communities'. *Australian Journal of Botany*, 53(4), 337 – 345.
- Gougeon, F., & Leckie, D. (2001). Individual tree crown image analysis – a step towards precision forestry. In: Proc. Of the First International Precision Forestry Symposium, Seattle, Washington. 43-50.
- Gougeon, F.; Cormier, R.; Labrecque, P.; Cole, B. ; Pitt, D.; & Leckie, D. (2003). Individual Tree Crown (ITC) Delineation on Ikonos and QuickBird Imagery: the Cockburn Island Study. In *25rd Canadian Symposium on Remote Sensing / 11^e Congrès de l'Association québécoise de télédétection*, Montréal (Québec), Canada, Oct. 14-17.

References

- Gougeon, F.A. (1995a). Comparison of possible multispectral classification schemes for tree crowns individually delineated on high spatial resolution MEIS Images. *Canadian Journal of Remote Sensing*, 21(1), 1-9.
- Gougeon, F.A. (1995b). A crown-following approach to the automatic delineation of individual tree crowns in high spatial resolution aerial images. *Canadian Journal of Remote Sensing*, 21 (3), 274-284.
- Gougeon, F.A. (1997). A locally adaptive technique for forest regeneration assessments from high resolution aerial images. In *Proceeding of 19th Can. Symposium Remote Sensing*, Ottawa, Ontario, Canada, May 24-30.
- Gougeon, F.A. (1998). Automatic individual tree crown delineation using a valley-following algorithm and a rulebased system. *International Forum on Automated Interpretation of High Resolution Digital Imagery for Forestry*, Natural Resources Canada, Canadian Forest Service, Victoria, British Columbia, Canada.
- Gougeon, F.A. (2000). Towards semi-automatic forest inventories using individual tree crown (ITC) recognition. Pacific Forestry Centre Technology Transfer Note 22:1-6. Canadian Forest Service, Natural Resources Canada, Victoria, B.C. 6 p.
- Gougeon, F.A., & Leckie, D.G. (1999). Forest regeneration: individual tree crown detection techniques for density and stocking assessments. In *Proceedings of the International Forum on Automated Interpretation of High Spatial Resolution Digital Imagery for Forestry*, Victoria, B.C., 10-12 February 1998. Canadian Forest Service, Natural Resources Canada, Victoria, B.C., 169-177.
- Gougeon, F.A., & Leckie, D.G. (2006). The individual tree crown approach applied to IKONOS images of a coniferous plantation area. *Photogrammetric Engineering & Remote Sensing*, 72(11), 1287-1297.
- Gougeon, F.A., D. Leckie, Scott, I., & Paradine, D. (1999). Individual tree crown species recognition: the Nahmint study. Pages 209-223 in Hill, D.A. and Leckie, D.G., eds. *Proceeding of Int'l Forum on Automated Interpretation of High Spatial Resolution Digital Imagery for Forestry*. February 10-12, 1998. Victoria, British Columbia, Canada. Natural Resources Canada, Canadian Forest Service, Victoria, Canada.
- Gougeon, F.A.; & Leckie, D.G. (2003). Forest information extraction from high spatial resolution images using an individual tree crown approach. *PFC Information Report*. BC-X-396 (and in French BC-X-396-F) Natural Resources Canada, Canadian Forest Service, Victoria, B.C., Canada. 26 p.
- Guyot, G., & Gu, X. (1994). Effect of Radiometric Corrections on NDVI-Determined from SPOT-HRV and Landsat-TM Data. *Remote Sensing of Environment*, 49, 169-180.
- Haara, A., & Haarala, M. (2002). Tree species classification using semi-automatic delineation of trees on aerial images. *Scandinavian Journal of Forest Research*, 17, 556-565.
- Haara, A., & Nevalainen, S. (2002). Detection of dead or defoliated spruces using. Digital aerial data, *Forest Ecology and Management*, 160, 97-107.
- Hill, J., & Sturm, B. (1991). Radiometric correction of multi-temporal thematic mapper data for the use in agricultural land-cover classification and vegetation monitoring", *International Journal of Remote Sensing*, 12(7), 1471-1491.
- Horney, R.B., Svalbe, I.D., & Wells, P. (2003). Isotropic Subpixel Measurement of Circular Objects. *Proceeding of VIIth Digital Image Computing: Techniques and Applications*, Sun C., Talbot H., Ourselin S. and Adriaansen T. (Eds.), Sydney

References

- Hupp, C.R., & Osterkamp, W.R. (1985). Bottomland vegetation distribution along Passage Creek, Virginia, in relation to fluvial landforms. *Ecology*, 66, 670-681.
- Hyypä, J., Kelle, O., Lehikoinen, M., & Inkinen, M. (2001). A segmentation-based method to retrieve stem volume estimates from 3-dimensional tree height models produced by laser scanner. *IEEE Transactions on Geoscience and Remote Sensing*, 39, 969-975.
- Hyypä, J., Mielonen, T., Hyypä, H., Maltamo, M., Honkavaara, E., Yu, X., & Kaartinen, H. (2005). Using individual tree crown approach for forest volume extraction with aerial images and laser point clouds. Proceedings of ISPRS Workshop "Laser scanning 2005", September 12-14, 2005, Enschede, *The Netherlands, International Archives of Photogrammetry, Remote Sensing and Spatial Information Sciences*, XXXVI(Part 3/W19), 144-149.
- Jähne, B. (2005). *Digital Image Processing: Concepts, Algorithms, and Scientific Applications* Springer, ISBN 3540240357, 9783540240358, 607 pages.
- Jiang, Z.Y., Huete, A.R., Chen, J., Chen, Y.H., Li, J., Yan, G.J., & Zhang, X.Y. (2006). Analysis of NDVI and scaled difference vegetation index retrievals of vegetation fraction. *Remote Sensing of the Environment*, 101(3), 366-378.
- Kass, M., Witkin, A., and Terzopoulos, D. (1988). Snakes: Active contour models. *International Journal of Computer Vision*, 321-331.
- Kleinn, C. (2007). Lecture notes for the teaching module Forest Inventory. 1st revised edition. Forest inventory and Remote Sensing department, Georg August University Göttingen. 164 pages.
- Kleinn, C. (2000). On large-area inventory and assessment of trees outside the forest. *Unasylva*, 200(51): 3-10.
- Kleinn C, D Morales, C Ramírez. (2001). Large Area Inventory of Tree Resources Outside the Forest: What is the Problem? IUFRO 4.11 Conference, Greenwich: Forest Biometry, Modelling and Information Science.
- Kleinschmit, B., Förster, M., Frick, A. And Oehmichen, K. (2007). QuickBird Data – experiences with ordering, quality and pan sharpening. In: *Photogrammetrie, Fernerkundung, Geoinformation – PFG 2007*, Heft 2, S. 73-84.
- Klonus, S., Rosso P., Ehlers M. (2008). Image Fusion of High Resolution TerraSAR-X and Multispectral Electro-Optical Data for Improved Spatial Resolution. *Proceedings of the EARSeI joint workshop "Remote Sensing-New Challenges of High Resolution"* Bochum.
- Korpela, I., Anttila, P., & Pitkänen, J. (2006). The performance of a local maxima method for detecting individual tree tops in aerial photographs. *International Journal of Remote Sensing*, 27(6), 1159-1175.
- Krause K. (2003). Radiance Conversion of QuickBird Data. Technical Note. Available in <http://www.pci.on.ca/discuss-archive/pdf00001.pdf>
- Laben, C.A., & Brower, B.V. (2000). Process for enhancing the spatial resolution of multispectral imagery using pan-sharpening, Eastman Kodak Company, US Patent # 6,011,875.
- Lamar, W.R., McGraw, J.B., & Warner, T. (2005). Multitemporal Censusing of a Population of Eastern Hemlock from Remotely Sensed Imagery Using an Automated Segmentation and Reconciliation Procedure. *Remote Sensing of Environment*, 94(1), 133-143.

References

- Larsen, M. (2007). Single tree species classification with a hypothetical multi-spectral satellite. *Remote Sensing of Environment*, 110(4), 523-532.
- Larsen, M., & Rudemo, M. (1997). Estimation of Tree Positions from Aerial Photos. In Lindeberg, Tony, editor, *Proceedings of the Swedish Symposium on Image Analysis*, 130-134, Stockholm, Sweden.
- Larsen, M., & Rudemo, M. (1998). Optimizing templates for finding trees in aerial photographs. *Pattern Recognition Letters*, 19, 1153-1162.
- Larsen, M., (1998). Finding an Optimal Match Window for Spruce Top Detection Based on an Optical Tree Model. In *proceedings of the the International Forum on Automated Interpretation of High Spatial Resolution Digital Imagery for Forestry*, pages 55-66. Natural Resources Canada / Canadian Forest Service. Victoria, British Columbia, Canada.
- Leckie, D., Burnett, C., Nelson, T., Jay, C., Walsworth, N., Gougeon, F., & Cloney, E. (1999). Forest parameter extraction through computer-based analysis of high resolution imagery. Pages 205-213, In *Proceeding of Fourth Int. Airborne Rem. Sens. Conf. and Exh. / 21st Can. Symp. Rem. Sens*, Vol. II. Ottawa, Canada, June 21-24.
- Leckie, D.G., & Gougeon, F.A. (1999). An assessment of both visual and automated tree counting and species identification with high spatial resolution multispectral imagery, *Proceeding of International Forum: Automated Interpretation of High Spatial Resolution Digital Imagery for Forestry*, Canadian Forest Service, Pacific Forestry Centre Victoria, British Columbia, February 10–12, 1998 pp. 141–152.
- Leckie, D.G., Gillis, M., Gougeon, F., Lodin, M., Wakelin, J., & Yuan, X. (1999). Computer-assisted photointerpretation aids to forest inventory mapping: some possible approaches. Pages 335-343 in Hill, D. A.; Leckie, D.G. (1998). *Int'l Forum on Automated Interpretation of High Spatial Resolution Digital Imagery for Forestry*. February 10-12, Victoria, British Columbia, Canada. *Natural Resources Canada, Canadian Forest Service*, Victoria, B.C.; Canada.
- Leckie, D.G., Gougeon, F.A., Tinis, S., Nelson, T., Burnet, C.N., & Paradine, D. (2005). Automated tree recognition in old growth conifer stands with high resolution digital imagery. *Remote Sensing of the Environment*, 94, 311-326.
- Leckie, D.G., Gougeon, F.A., Walsworth, N., & Paradine, D. (2003). Stand delineation and composition estimation using semi-automated individual tree crown analysis. *Remote Sensing of Environment*, 85, 355-369.
- Leckie, D. G., Jay, C., Gougeon, F. A., Sturrock, R. N. and Paradine, D.(2004) Detection and assessment of trees with *Phellinus weirii* (laminated root rot) using high resolution multi-spectral imagery. *International Journal of Remote Sensing* 25(4), 793-818.
- Leckie, D.G., Yuan, X., Ostaff, D.P., Piene, H., & MacLean, D.A. (1992). Analysis of High Resolution Multispectral MEIS Imagery for Spruce Budworm Damage Assessment on a Single Tree Basis. *Remote sensing of Environment*, 40(2), 125-136.
- Lefèvre, S. (2007). Knowledge from markers in watershed segmentation, IAPR International Conference on Computer Analysis of Images and Patterns (CAIP), Vienna, *Springer-Verlag Lecture Notes in Computer Sciences*, 4673, 579-586.
- Leica Geosystems. (2005). *Erdas Field Guide*. Geospatial Imaging, LLC Atlanta Georgia.
- Leica Geosystems. (2006). *Imagine AutoSync White paper*.

- Li, X. and Strahler, A.H. (1986). Geometric-optical bidirectional reflectance modeling of a conifer forest canopy, *IEEE Trans. on Geoscience and Remote Sensing*, 24(6), 906-919.
- Li, X. and Strahler, A.H. (1992). Geometrical-optical bidirectional reflectance modeling of the discrete crown vegetation canopy: effect of crown shape and mutual shadowing, *IEEE Transact. Geoscience and Remote Sensing*, 30(2), 276-292.
- Lillesand, T.M., & Kiefer, R.W. (1994). *Remote Sensing and Image Interpretation*, Third Edition. John Wiley and Sons, ISBN 0471577839, 9780471577836, 750 pages.
- Ling, Y., Ehlers, M., Usery, L., & Madden, M., (2007). FFTenhanced IHS transform method for fusing high-resolution satellite images. *ISPRS Journal of Photogrammetry and Remote Sensing*, 61, 6, 381–392.
- Liu, J.G. (2000). Smoothing filter-based intensity modulation: a spectral preserve image fusion technique for improving spatial details, *International Journal of Remote Sensing* 21(18), 3461–3472.
- Mallat, S. (1989). A theory for multiresolution signal decomposition: The wavelet representation, *IEEE Transactions on Pattern Analysis and Machine Intelligence*, 11(7), 674–693.
- Maltamo, M., Tokola, T., & Lehtikoinen, M. (2003). Estimating stand characteristics by combining single tree pattern recognition of digital video imagery and a theoretical diameter distribution model. *Forest Society*, 49, 98-109.
- Marr D., & Hildreth, E. (1980). A theory of edge detection, *Proc. Roy. Soc. (London)*, B, 207, 187–217.
- Mather, P.M. (2004). *Computer Processing of Remotely-Sensed Images: An Introduction* John Wiley and Sons ISBN 0470849193, 9780470849194, 324 pages.
- Navulur, K., (2006). *Multispectral image analysis using object-oriented paradigm*. CRC press, ISBN 1420043064, 165 pages.
- Nikolakopoulos, K.G. (2004). Comparison of four different fusion techniques for IKONOS data. *IEEE Intl. Geoscience and Remote Sensing Symposium*, 4, 2534-2537.
- Nussbaum, S., Menz, G. (2008). *Object-Based Image Analysis and Treaty Verification*. Springer. ISBN: 978-1-4020-6960-4, 172 pages.
- Olofsson, K., Wallerman, J., Holmgren, J., & Olsson, H. (2006). Tree species discrimination using Z/I DMC imagery and template matching of single trees. *Scandinavian Journal of Forest Research*, 21, 106–110.
- Osma-Ruiz, V., Godino-Llorente, J.I., Sáenz-Lechón, N., & Gómez-Vilda, P. (2007). An improved watershed algorithm based on efficient computation of shortest paths, *Pattern Recognition*, 40(3), 1078-1090.
- Otsu, N. (1979). A threshold selection method from gray-level histograms. *IEEE Transactions on Systems, Man, and Cybernetics*, 9 (1), 62-66.
- Pal, N.R., & Pal, S.K. (1993). A review on image segmentation techniques. *Pattern Recognition*, 26(9), 1277-1294.
- Peng, J., & Bhanu, B. (1999). Learning to perceive objects for autonomous navigation. *Autonomous Robots*, 6(2), 187-201.
- Perrin, G. and Descombes, X. and Zerubia, J. and Boureau, J.G. (2006). *Forest Resource Assessment*

using Stochastic Geometry. In Proc. International Precision Forestry Symposium Stellenbosch University, South Africa. 105-115.

Pesaresi, M., & Benediktsson, J.A. (2001). A new approach for the morphological segmentation of high-resolution satellite imagery. *Geoscience and Remote Sensing, IEEE Transactions*, 39(2), 309–320.

Petrović, V., & Xydeas, C. (2004). Evaluation of image fusion performance with visible differences, in: Proceedings of Prague, LNCS 3023, 380–391.

Philipson, W. (1997). Manual of photographic interpretation. *American Society for Photogrammetry and Remote Sensing*, 689 pages.

Pinz, A. (1989). Final Results of the Vision Expert System VES: Finding Trees in Aerial Photographs. In Axel Pinz, editor, *Wissensbasierte Mustererkennung*, volume 49 of OCG-Schriftenreihe, 90–111.

Pinz, A. (1991). A Computer Vision System for the Recognition of Trees in Aerial Photographs. In James Tilton, editor, *Multisource Data Integration in Remote Sensing*, volume 3099 of NASA Conference Publication, 111–124.

Pinz, A. (1999). Tree isolation and species classification. In Proceedings of the International Forum on Automated Interpretation of High Spatial Resolution Digital Imagery for Forestry, Victoria, B.C., *Canadian Forest Service, Natural Resources Canada*, Victoria, B.C., 127–139.

Pinz, A., Zaremba, M.B., Bischof, H., Gougeon, F.A., & Locas, M. (1993). Neuromorphic methods for recognition of compact image objects. *Machine Graphics and Vision*, 2, 209-229.

Pitkänen, J. (2001). Individual tree detection in digital aerial images by combining locally adaptive binarization and local maxima methods. *Canadian Journal of Forest Research*, 31, 832–844.

Pitkänen, J., Maltamo, M., Hyypä, J., & Yu, X. (2004). Adaptive methods for individual tree detection on airborne laser based canopy height model. *International Archives of Photogrammetry, Remote Sensing and Spatial Information Sciences*, 36, 187-191.

Pitt, D.G., & Glover, G.R. (1993). Large-scale 35-mm aerial photographs for assessment of vegetation-management research plots in Eastern Canada. *Canadian Journal of Forest Research*, 23, 2159–2169.

Pohl, C. (1999). Tools and methods for fusion of images of different spatial resolution. *International Archives of Photogrammetry and Remote Sensing*, 32, Part 7-4-3 W6, Valladolid, Spain.

Pohl, C., & Van Genderen, J.L. (1998). Multisensor image fusion in remote sensing: concepts, methods and applications. *International Journal of Remote Sensing*, 19 (5), 823-854.

Pollock, R. (1998). Development of a highly automated system for the remote evaluation of individual tree parameters. *Integrated Tools Proceedings*, Idaho, USA, August 16–20, 638–645.

Pollock, R. (1999). Individual tree recognition based on a synthetic tree crown image model. A spatial clustering approach to automated tree crown delineation. In *Proceedings of the International Forum on Automated Interpretation of High Spatial Resolution Digital Imagery for Forestry*, Victoria, B.C., 10–12 February 1998. Canadian Forest Service, Natural Resources Canada, Victoria, B.C., 25–34.

Pollock, R.J. (1994). Model-based approach to automatically locating tree crowns in high spatial resolution images (1994). *Proceedings of SPIE - The International Society for Optical Engineering*, 2315, 526-537.

Pouliot, D.A., & King, D.J. (2005). Approaches for optimal automated individual tree crown detection in young regenerating coniferous forests. *Canadian Journal of Remote Sensing*, 31, 256-267.

- Pouliot, D.A., King, D.J., & Pitt, D.G. (2005). Development and evaluation of an automated tree detection-delineation algorithm for monitoring regenerating coniferous forests. *Canadian Journal of Forest Research*, 35, 2332-2345.
- Pouliot, D.A., King, D.J., Bell, F.W., & Pitt, D.G. (2002). Automated tree crown detection and delineation in high-resolution digital camera imagery of coniferous forest regeneration. *Remote Sensing of Environment*, 82, 322-334.
- Pourhashemi, M., Mohajer, M.R.M., Zobeiri, M., Zahedi, G., & Panahi, P. (2004). Identification of forest vegetation units in support of government management objectives in Zagros forests, Iran. *Scandinavian Journal of Forest Research*, 19(4), 72-77.
- Pukkala, T. (1990). A method for incorporating the within-stand variation into forest management planning. *Scandinavian Journal of Forest Research*, 5, 263-275.
- Qureshi, S. (2005). *Embedded Image Processing on the TMS320C6000 DSP: Examples in Code Composer Studio and MATLAB*. Springer, ISBN 0387252800, 9780387252803, 433 pages.
- Raich, J.W., & Tufekcioglu, A. (2000). Vegetation and soil respiration: Correlations and controls. *Biogeochemistry*, 48, 71-90.
- Ritter, G.X., & Wilson, J.N. (2001). *Handbook of Computer Vision Algorithms in Image Algebra*. CRC Press, ISBN 0849300754, 9780849300752, 417 pages.
- Riyahi, R. (2001). Determination of the most suitable methods for natural resources mapping (1:250000) with satellite data in Dasht-e Arzhan region. *University of Tehran. MSc Thesis*. (in Persian).
- Sagheb-Talebi, K., Sajedi, T., & Yazdian, F. (2004). Forests of Iran. *Iran: Research Institute of Forests and Rangelands, Forest Research Division*, 27, 28 pages.
- Saroe, S. (1996). Investigating the possibility of forest density mapping in Zagros area using satellite data. *University of Tehran. MSc Thesis*, (in Persian).
- Shell R.L., & Hall, E.L. (2000). *Handbook of Industrial Automation*, CRC Press ISBN 0824703731, 9780824703738, 887 pages.
- Shettigara, V.K. (1992). A generalized component substitution technique for spatial enhancement of multispectral images using a higher resolution data set. *Photogrammetric Engineering and Remote Sensing*, 58, 561-567.
- Soille, P. (1999). *Morphological Image Analysis. Principles and Applications*. Berlin; New York; Springer Verlag. ISBN 3-540-65671-5
- Soille, P. (2003). *Morphological Image Analysis: Principles and Applications*. Springer, ISBN 3540429883, 9783540429883, 391 pages.
- Solihin, Y., & Leedham, C.G. (2002). *The Multi-stage Approach to Grey-Scale Image Thresholding for Specific Applications*, School of Computer Engineering, Nanyang Technological University, Singapore.
- Stephenson, N.L. (1990). Climatic controls on vegetation distribution: the role of the water balance, *The American Naturalist*, 135, 649-670.
- Straub, B. (2003a). A Top-down operator for the automatic extraction of trees-concept and performance

- evaluation. *The international archives of the photogrammetry, remote sensing and spatial information sciences* (eds.) H.G. Maas G. Vosselmann A. Streilein, ISPRS, Dresden, Germany, Vol. WG III/4, 34-39.
- Straub, B. (2003b). Automatic extraction of trees from aerial images and surface models. ISPRS, München, Germany, September 17-19, Vol. xxxiv, part3/W8, 157-164.
- Straub, B.M.A. (2004). Multiscale Approach for the Automatic Extraction of Tree Tops from Remote Sensing Data: IntArchPhRS. Band XXXV, Teil B3. Istanbul, 418-423.
- Straub, B.M.A., & Heipke, C. (2007). Automatic extraction and delineation of single trees from remote sensing data *Machine Vision and Applications*, 18, 317–330.
- Suárez, J.C., Ontiveros, C., Rorke, D., Snape, S., & Smith, S. (2003). Tree counting and standing volume methods for even-aged mature spruce stands using aerial photography. In: *Proceedings of the 6th AGILE Conference on Geographic Information Science*—Lyon, France, 24–26 April 2003.
- Sun, H., Yang, J., & Ren, M. (2005). A fast watershed algorithm based on chain code and its application in image segmentation, *Pattern Recognition Letters*, 26(9), 1266-1274.
- Surovy, P., Ribeiro, N.A., Scheer, L., & Sloboda, B. (2006). Assessment of tree positions from aerial photos by combining three basic techniques: tree top searching, valley following and template matching. *Proceeding 2nd Göttingen GIS and Remote Sensing Days*. 115-121.
- Švab A., & Ošti, K. (2006). High-resolution Image Fusion: Methods to Preserve Spectral and Spatial Resolution. *Photogrammetric Engineering & Remote Sensing*, 72(5), 565–572.
- Tappeiner, U., Tasser, E., & Tappeiner, G. (1998). Modelling vegetation patterns using natural and anthropogenic influence factors: Preliminary experience with a GIS based model applied to an alpine area. *Ecological Modelling*, 113(2), 225-237.
- Trotter, C.M., Dymond J.R., & Goulding, C.J. (1997). Estimation of timber volume in a coniferous plantation forest using Landsat TM, *International Journal of Remote Sensing*, 18 (10), 2209–2223.
- Tu, T.-M., Su, S.C., Shyu, H.C., & Huang, P.S. (2001). A new look at IHS-like image fusion methods. *Inf. Fusion*, 2, 177–186.
- Uuttera, J., Haara, A., Tokola, T., & Maltamo, M. (1998). Determination of the spatial distribution of trees from digital aerial photographs. *Forest Ecology Management*, 110, 275–282.
- Vincet, L., Soille, P. (1991). Watersheds in Digital Spaces: An Efficient Algorithm Based on Immersion Simulations. *IEEE Trans. Pat. Anal. Machine Intell.* 583-598.
- Vrabel, J., (1996). Multispectral Imagery Band Sharpening Study. *Photogrammetric Engineering & Remote Sensing*, 62(9), 1075-1083.
- Wald L., Ranchin T., & Mangolini M. (1997). Fusion of satellite images of different spatial resolutions-Assessing the quality of resulting images *Photogrammetric Engineering & Remote Sensing*, 63(6), 691-699.
- Wald L., (1999). Some terms of reference in data fusion. *IEEE Transactions on Geoscience and Remote Sensing* , 37 (3), 1190–1193.
- Wald, L., (2002). *Data Fusion: Definitions and Architectures: Fusion of Images of Different Spatial Resolutions*. Presses de l'Ecole, Ecole des Mines de Paris, Paris, France, ISBN 291176238X, 9782911762383, 198 pages.

References

- Walsworth, N., & King, D.J. (1998). Comparison of two tree apex. delineation techniques *International Forum on Automated Interpretation of High Resolution Digital Imagery for Forestry, Natural Resources Canada*, Canadian Forest Service, Victoria, British Columbia, 93 -104.
- Walsworth, N., & King, D.J. (1999). Image modelling of forest changes associated with acid mine drainage. *Computers and Geosciences*, 25(5), 567-580.
- Wang, L., Gong, P., & Biging, G.S. (2004). Individual tree-crown delineation and treetop detection in high-spatial-resolution imagery. *Photogrammetric Engineering and Remote Sensing*, 70(3), 351–358.
- Wang, Z., & Bovik, A.C. (2002). A Universal Image Quality Index. *IEEE Signal Processing Letters*, 9(3), 81-84.
- Warner, T.A., Yeol Lee, J., & McGraw, J.B. (1998). Delineation and identification of individual trees in the eastern deciduous forest. In: Hill, D.A., Leckie, D.C. (Eds.), *Proceedings Automated Interpretation of High Spatial Resolution Digital Imagery for Forestry*, Victoria, B.C., 81-92.
- Warner, T. A. McGraw, J. B. Landenberger, R. (2006). Segmentation and classification of high resolution imagery for mapping individual species in a closed canopy, deciduous forest. *Science in China: Series E Technological Sciences*, Vol.49 Supp. I 128—139.
- Wei-qi, Y., & De-sheng, L. (2006). Edge detection based on directional space . *Front. Electr. Electron. Eng. China*, 2, 135–140.
- Wulder, M., Niemann, K.O., & Goodenough, D. (2000). Local Maximum Filtering for the Extraction of Tree Locations and Basal Area from High Spatial Resolution Imagery. *Remote Sensing of Environment*, 73, 103–114.
- Wulder, M.A., & Franklin, S.E. (2003). *Remote Sensing of Forest Environments: Concepts and Case Studies*. Springer, ISBN 1402074050, 9781402074059, 519 pages.
- Wulder, M.A., White, J., Niemann, K.O., & Nelson, T. (2004). Comparison of airborne and satellite high spatial resolution data for the identification of individual trees with local maxima filtering. *International Journal of Remote Sensing*, 25(11), 2225–2232.
- Wulder, M.A., Ortlepp, S.M., White, J.C., & Coops, N.C. (2008). Impact of sun-surface-sensor geometry upon multi-temporal high spatial resolution satellite imagery. *Canadian Journal of Remote Sensing*: 34(5) 455-461
- Xiao and Ceulemans, (2004) C.W. Xiao and R. Ceulemans, Allometric relationships for below- and aboveground biomass of young Scots pines, *Forest Ecology and Management* 3, 177–186.
- Yocky, D.A., (1996). Multiresolution wavelet decomposition image merger of Landsat thematic mapper and SPOT panchromatic data, *Photogrammetric Engineering & Remote Sensing* 62 (9), 1067–1074.
- Zagalikis, G. Cameron, A.D. and Miller, D.R. (2005).The application of digital photogrammetry and image analysis techniques to derive tree and stand characteristics. *Canadian Journal of Remote sensing*, 35, 1224–1237.
- Zhang, Y. (2002). Problems in the fusion of commercial high-resolution satellite images as well as Landsat 7 images and Initial solutions. *International Archives of Photogrammetry and Remote Sensing (IAPRS)*, Volume 34, Part 4, ISPRS, CIG, SDH Joint International Symposium on "GeoSpatial Theory, Processing and Applications", Ottawa, Canada, July 8-12, 2002.
- Zhang, Y. (2004). Highlight Article: Understanding Image Fusion. *Photogrammetric Engineering & Remote Sensing*, 70(6), 657-661.

References

Zhou, J., Civco, D.L., & Silander, J.A. (1998). A wavelet transform method to merge Landsat TM and SPOT panchromatic data. *International Journal of Remote Sensing*, 19(4), 743-757.

Zobeiry M., & Dalaki, A. (1997). *Fundamental of aerial photo interpretation with application to natural resources*. University of Tehran, Faculty of Natural Resources, Tehran University Publication: 323 pages. (in Persian)

CURRICULUM VITAE

Personal Data

Date / Place of birth	05 May 1974 / Shiraz, Iran
Nationality	Iranian
Gender / Marital Status	Male / Single

Education

- 2005-2010 PhD in Forestry-Remote Sensing and GIS,
Georg-August-University Göttingen, Burckhardt-Institute, Chair of
Forest Inventory and Remote Sensing
- 1999-2001 M.Sc. in Forestry-Remote Sensing and GIS,
Thesis title: “Determination of the most suitable method for natural
resources mapping (1:250000) using satellite data in Dasht-e
Arzhan region.”
University of Tehran, Faculty of Natural Resources, Department of
Forestry and Forest Economy.
- 1992-1996 B.Sc. in Forestry and Forest Economics,
University of Gilan, Faculty of Natural Resources, Department of
Forestry.

Professional Work Experience

- 2001-2003 Senior Research Associate, Team leader of Geomatics
Group, Bandar Abbas Natural Resources Head
Organization, Hormozgan, Iran.

Project Manager, Engineering and Evaluation Bureau, Forest,
Range & Watershed Management Organization (FRWO), Tehran,
Iran.
- 2000 - 2001 Chief scientist at the Geomatics group in the Department of the
Environment, Bureau of Habitats & Protected Areas, Tehran, Iran.

